POLITECNICO DI TORINO

M.Sc. PETROLEUM AND MINING ENGINEERING

Master Degree Thesis

Data Transform for EM Sounding Direct Interpretation

Candidate:

Oscar Iván Calderón Hernández

Supervisors:

PhD. Laura Valentina Socco (PoliTO)

PhD. Evert Slob (TU Delft)

Turin, October 2021

"The important thing is not to stop questioning. Curiosity has its own reason for existing. One cannot help but be in awe when he contemplates the mysteries of eternity, of life, of the marvelous structure of reality. It is enough if one tries merely to comprehend a little of this mystery every day. Never lose a holy curiosity."

Albert Einstein

Acknowledgments

To the Polytechnic of Turin, for the opportunity to study a master's degree and for the opportunity to grow in my professional career.

To ENI Mexico and the ENI Project, for the opportunity to study in Italy, for all the friends I met and for all the experiences I had the opportunity to live.

To my supervisors, Prof. Socco, Prof. Evert, Karim, and Dieter, thank you for all the patience, for your advice, for the opportunity to work with you. I am truly grateful for the experience, it was amazing to work with you and I really hope to have the opportunity to keep working together.

To my mother, for all the love and support, I cannot express my gratitude with words, I love you mom.

To Steph, for all the love, for all the patience, for everything I've learned with you, for all the amazing histories we have made so far and for all the stories we will make from now on, for being my support during this journey. You showed me another view of the world and thanks to you I've been able to learn so many things, that it would take me forever to write them down. Thanks for everything my love.

To my family, for all its support along this amazing journey, without it for sure I wouldn't be here.

To Tom, for all the support, for all the incredible histories, and even for mocking me in the astronomy courses, it was incredibly fun. You made me a better person and I cannot thank you enough for that.

To Eric, Geri, Illias, and Emmanuel, being with you during this master was amazing.

To my dearest friends, for being there for me, for allowing me to get this far, for helping me to grow and to improve. Without you, all of this would have been a dream.

Abstract

The Magneto-Telluric method (MT) uses natural electromagnetic fields to investigate the conductivity structure of the Earth, however, as in any geophysical method, usually, an inversion process is required in order to generate a view of the structure which causes the data that has been retrieved, this process might be computationally expensive and very time consuming.

The main goal of this work is to assess if it is possible to determine a polynomial function to directly relate MT measurements to a resistivity model and hence to attribute the measured resistivity to a specific point in depth using several constraints. To do it a first depth approximation is obtained using theoretical relationships proposed in literature, this first resistivity model is compared to the real resistivity model present in the site assuming that information from an exploratory well is at hand. The difference in depth (Δz) for a given resistivity point between models is obtained and this difference is modeled using a polynomial regression. The polynomial analysis aims to model the Δz difference for a given resistivity value providing us a mathematical expression that describes the difference between real and theoretical behavior as a function of the electrical properties in the subsurface.

In literature, rescaling techniques for some geophysical prospecting methods are proposed to obtain accurate models that describe the geological settings present in the subsurface using simple mathematical expressions derived from sites in which surface measurements along with well data were compared. This mathematical expressions can be used to describe sites surrounding the well in which the geological settings are slightly different from the well. In this work it is proposed to use the mathematical expression derived from the regression analysis used to model the Δz behavior as a rescaling tool to retrieve accurate geological models for sites nearby the exploration well.

The applicability of the method was tested in two synthetic scenarios aiming to simulate the characterization phase of a field of interest in which only one exploratory well was drilled. The method was also tested in a real scenario in which the goal was to monitor the difference in the resistivity of the target layer due to water injection on a geothermal field.

Overall further research is needed to determine the actual limits of the proposed rescaling process, as a first step, the method seems promising especially for identifying resistivity variations in shallow targets.

Contents

List of Figures

List of Tables

List of Symbols

Symbol	Description	SI Units
$\mathbf{D}$	Electric displacement	C/m^2
$\mathbf{B}$	Magnetic induction	T
$\mathbf{E}$	Electric field	V/m
$\mathbf{H}$	Magnetic field	A/m
$\mathbf{J}$	Electric current density	A/m^2
ρ_e	Electric charge density	C/m^3
ϵ	Dielectric permitivity	F/m
μ	Magnetic permeability	H/m
f	Frequency	Hz
ω	Angular frequency	rad/s
σ	Electric conductivity	S/m
z	Depth	m
μ_0	Magnetic permeability in the void	H/m
Z	Electric impedance	m/s
T	Period	s
σ_a	Apparent conductivity	$1/(\Omega/m)$
ρ_a	Apparent resistivity	Ωm
S_c	Cumulative Conductance	S
ρ_c	Cumulative resistivity	Ωm^2
h	Thickness	m

Chapter 1

Introduction

1.1 Background to the Electromagnetic Method

Geophysical prospecting methods are used to obtain information about the physical properties of the subsurface of the Earth that are not available from geological observations. Electromagnetic methods (EM) for the exploration of the subsurface have been widely used since the early 20th century to map the electromagnetic properties of the materials in the subsurface (Nabighian, 1991).

Electromagnetic methods include a variety of techniques, survey methods, applications and interpretation procedures, however, each technique is based on the measurement of one or more electric or magnetic field components. The measured fields are a response of the electrical properties of the materials in the subsurface. A detailed analysis will provide an approximation of the electrical properties of the materials and their location in the subsurface.

Applications of EM methods can be at any scale, from searching coins in beach sands up to a magnetotelluric survey to detect hydrocarbons in a sandy formation 3 km bellow the bottom of the ocean (Swift Jr, 1988). Over the past years, EM techniques initially developed for deeper applications such as mining, hydrocarbon exploration or crustal studies have been scaled for shallow objectives such as environmental studies or geotechnical investigations (Pellerin, 2002). In general, the reliability and applicability of electromagnetic methods is well known.

1.2 Justification

The Magneto-Telluric method (MT) uses natural electromagnetic fields to investigate the conductivity structure of the Earth knowing that the electromagnetic waves will penetrate into the Earth up to a depth given as a function of the frequency of the wave and the electrical properties of the rocks (Niblett and Sayn-Wittgenstein, 1960). However, as in any geophysical method, usually an inversion process is required to generate a view of the structure which causes the data that has been retrieved. This process might be computationally expensive and very time consuming, for this reason how to improve the inversion techniques is a topic of active research.

Over the last years new techniques are being researched in order directly estimate relevant geological models of the subsurface without using an inversion process by obtaining relationships between the data obtained by geophysical surveys and the data obtained in one place by well logging, core analysis or other techniques in which the actual physical properties of the rocks present in the subsurface are measured. This approach has proved to be useful to retrieve geological models that can describe properly the geological settings present in the subsurface and in some instances the relationships obtained can be applied to rescale the data in areas in which only surface measurements have been acquired.

Florio (2018) proposed a simple method to obtain the depth of the basement using gravity or pseudogravity measurements based on a linear iterative rescaling approach. The approach takes into consideration that the gravity measurements can be related to a certain depth using a polynomial regression, in the case of a constant density contrast the relationship will be linear and in the case of a variable density contrast the relationship can be approximated using a polynomial.

Socco et al. (2017) proposed a new technique to obtain the direct estimation of time-average S-wave velocity models from Surface Waves Dispersion Curves without the need to invert the data. Their proposed method requires the knowledge of one 1D S-Wave velocity model along the seismic line together with relevant Dispersion Curves to estimate a relationship between the surface waves wavelength and the investigation depth on the time-average velocity model. This wavelength-depth relationship is then used to estimate all the other time-average S-wave velocity models along the line directly from the dispersion curves by means of a data transformation.

Considering that this approach has been proved for gravity measurements and seismic data it can be supposed that the same approach could work for other geophysical prospecting techniques such as EM methods.

1.3 Description of this work

The main goal of this work is to assess if it is possible to obtain a polynomial function that can be used to correct the misfit between the theoretical depth-apparent resistivity model obtained by MT surveys and the real depth-resistivity model present in the subsurface using additional information (provided by exploratory wells for example) as constrains.

Using the apparent resistivity measured by a MT survey an approximate depth can be obtained by theoretical relationships that have been proposed in previous works (Gómez-Treviño, 1996), this first depth-apparent resistivity model can be used as starting point for the generation of a geological model that represents the settings present at the subsurface. However, this first approximated model deviate from the real depth-resistivity model by a given factor. The behavior of the misfit between models will be modeled by a polynomial expression.

Once the polynomial expression is obtained it will be used to correct the misfit between the first model obtained by the MT measurements and the model obtained by the exploratory well. The polynomial will be also used to directly obtain geoelectrical models in zones with similar geological settings than the ones present at the exploratory well. All of this will be performed for 1D resistivity models.

The applicability of the method will be tested in two scenarios. One aims to approximate the depth using apparent electrical properties measured in the vicinity of where the real data was acquired, and the second scenario aims to monitor the variation in resistivity of a particular layer for geothermal purposes.

This work aims to provide a tool to generate a first depth-resistivity model that represents the real geological settings present in the subsurface with low computational cost and with high time efficiency.

1.4 Layout of this thesis

The theoretical background is described in Chapter 2. The Mt method is summarized briefly describing the theoretical framework in which the method is based, some acquisition tools and a brief description of what is measured and how to process the data acquired. Additionally the regression analysis theory is also described in chapter 2, including the regression tools used in this work and an explanation of the least squares method.

The methodology of this work is described in Chapter 3. Starting from MT measurements the process to obtain a first depth-apparent resistivity model is described; and the difference between this first model and the real model present at the subsurface was modeled using a polynomial regression. To see if the approach proposed by Socco et al. (2017) and Florio (2018) can be used in MT surveys the polynomial expression obtained was used to directly convert MT measurements to geolectrical 1D models.

Chapter 4 includes all the results derived from this workflow with a detailed description of what has been discovered, what are the limitations of the proposed method and in which cases this methodology provided the best results.

In Chapter 5 all the conclusions obtained from this work are stated, and foreseeable further developments of this work are proposed.

Chapter 2

Theoretical Background

The theoretical framework used in this thesis can be divided into two main categories, the first theoretical framework describes the theory in which the Magnetotelluric method (MT) is based and the second one describes the theory for regression analysis.

The MT method is a passive geophysical prospecting method that utilizes naturally occurring electromagnetic waves that travel through the Earth's subsurface to image the electrical properties of the subsurface. The MT method can be derived from Maxwell's equations considering particular cases, once the measurements are performed, they can be processed to generate useful data that describes the electrical settings of the subsurface.

Regression analysis is a predictive modelling technique in which a defined relationship between an independent variable x and a dependent variable y is established. The relationships obtained can be used to describe and predict phenomenon of interest under certain circumstances.

2.1 The Magnetotelluric Method

The megnetotelluric method (MT) is an electromagnetic geophysical exploration technique that uses natural electromagnetic fields to investigate the electrical conductivity of the Earth, from the near surface to the transition zone and beyond (Chave and Jones, 2012). The behavior of electric and magnetic fields can be fully described by the Maxwell equations, which can be expressed in the International System of Units as

$$\nabla \cdot \mathbf{D} = \rho_e, \tag{2.1a}$$

$$\nabla \cdot \mathbf{B} = 0, \tag{2.1b}$$

$$\nabla \times \mathbf{E} = -\frac{\partial \mathbf{B}}{\partial t}, \tag{2.1c}$$

$$\nabla \times \mathbf{H} = \mathbf{J} + \frac{\partial \mathbf{D}}{\partial t}. \tag{2.1d}$$

Where $\mathbf{D}$ is the electric displacement, ρ_e is the electric charge density, $\mathbf{B}$ is the magnetic induction, $\mathbf{E}$ is the electric field, $\mathbf{H}$ is the magnetic field and $\mathbf{J}$ is the electric current density. The electric and magnetic fields developed in a medium are connected to the electromagnetic properties of the medium though their constitutive relationships as follows

$$\mathbf{D} = \epsilon \mathbf{E}, \tag{2.2a}$$

$$\mathbf{B} = \mu \mathbf{H}, \tag{2.2b}$$

$$\mathbf{J} = -\sigma \mathbf{E}. \tag{2.2c}$$

Where ϵ (F/m) is the dielectric permitivity, μ (H/m) is the magnetic permeability and σ (S/m) is the electrical conductivity. In this work isotropic media will be assumed, hence these quantities are scalar values. Using the constitutive relationships the Maxwell equations can be rewritten as

$$\nabla \cdot \mathbf{E} = \frac{\rho_e}{\epsilon}, \tag{2.3a}$$

$$\nabla \cdot \mathbf{B} = 0, \tag{2.3b}$$

$$\nabla \times \mathbf{E} = -\frac{\partial \mathbf{B}}{\partial t}, \tag{2.3c}$$

$$\nabla \times \mathbf{B} = \mu\sigma\mathbf{E} + \mu\epsilon\frac{\partial \mathbf{E}}{\partial t}. \tag{2.3d}$$

Assuming a time dependency $e^{i\omega t}$ for $\mathbf{B}$ (where $\omega = 2\pi f$ is the angular frequency), the non-existence of current sources in the subsurface, no free charges in a homogeneous halfspace and in a layered 1D Earth and quasi-static conditions (the propagation of electromagnetic waves is a diffusive process) (Martí i Castells, 2006), the diffusion equations for the electromagnetic fields can be written as

$$(\nabla^2 - \boldsymbol{k}^2)\mathbf{B} = 0, \tag{2.4a}$$

$$(\nabla^2 - \boldsymbol{k}^2)\mathbf{E} = 0. \tag{2.4b}$$

Where $\boldsymbol{k}^2 = i\omega\mu\sigma$ is the propagation constant in m^{-1}. For a coordinate system x, y and z where z increases downwards, equations 2.4a and 2.4b are also depth dependent (Thiel, 2008). The solution for the diffusion equations in this case becomes

$$\mathbf{B} = \mathbf{B}_0 e^{-\boldsymbol{i}\boldsymbol{k}\boldsymbol{z}} + \mathbf{B}_1 e^{\boldsymbol{i}\boldsymbol{k}\boldsymbol{z}}, \tag{2.5a}$$

$$\mathbf{E} = \mathbf{E}_0 e^{-\boldsymbol{i}\boldsymbol{k}\boldsymbol{z}} + \mathbf{E}_1 e^{\boldsymbol{i}\boldsymbol{k}\boldsymbol{z}}. \tag{2.5b}$$

The fields **B** and **E** vanish when $z \to \infty$, for this reason $\mathbf{B}_1 = \mathbf{E}_1 = 0$. For this reason equations 2.6a and 2.6b can be simplified to:

$$\mathbf{B} = \mathbf{B}_0 e^{-\boldsymbol{i}\boldsymbol{k}\boldsymbol{z}} = \mathbf{B}_0 e^{-ivz} e^{-vz}, \tag{2.6a}$$

$$\mathbf{E} = \mathbf{E}_0 e^{-\boldsymbol{i}\boldsymbol{k}\boldsymbol{z}} = \mathbf{E}_0 e^{-ivz} e^{-vz}. \tag{2.6b}$$

Where

$$\boldsymbol{k} = (1+i)\sqrt{\frac{\omega\mu\sigma}{2}} = (1+i)v. \tag{2.7}$$

Equations 2.6a and 2.6b illustrates how the electromagnetic fields varies in a sinusoidal form with depth within the term e^{-ivz}, but also shows a depth dependent attenuation due to the e^{-vz} term (Loewenthal and Landisman, 1973). The inverse of the real part of $\boldsymbol{k}$ is known as skin depth or penetration depth δ

$$\delta = \sqrt{\frac{2}{\mu\omega\sigma}}. \tag{2.8}$$

However, since the magnetic permeability μ is almost constant in the Earth (Vozoff, 1991), equation 2.8 can be approximated as

$$\delta \approx 500\sqrt{T\rho_a}. \tag{2.9}$$

Where $\rho_a = 1/\sigma_a$ (Ωm) is the apparent resistivity and $T = 2\pi/\omega$ (s) is the period. Equation 2.9 shows that the penetration depth depends only from the conductivity of the overlying material and the period used.

2.1.1 Apparent Resistivity

The input of the MT method will be the natural magnetic field (**B**) traveling downward in the z direction inducing a perpendicular electric field (**E**) that does not have a z component ($E_z = 0$). The plane-wave assumptions states that the magnetic field only has horizontal components due to the distance from the source, this assumption also implies that ($B_z = 0$).

Expanding the curl operation in equation 2.3c shows the following relationship

$$\frac{\partial E_z}{\partial y} - \frac{\partial E_y}{\partial z} = \frac{\partial E_y}{\partial z} = i\omega B_x, \tag{2.10a}$$

$$\frac{\partial E_x}{\partial z} - \frac{\partial E_z}{\partial x} = \frac{\partial E_x}{\partial z} = -i\omega B_y, \tag{2.10b}$$

$$\frac{\partial E_y}{\partial x} - \frac{\partial E_x}{\partial y} = -i\omega B_z = 0. \tag{2.10c}$$

For a uniform Earth the ratio between electric and magnetic field (E_y, B_x) measured at the surface at a specific period is known as electrical impedance Z (m/s) and can be defined by

$$Z(\omega) = \frac{E_{x0}}{H_{y0}} = \frac{\omega\mu}{\boldsymbol{k}} = \frac{2\pi\mu}{T\boldsymbol{k}} = (1+i)\sqrt{\frac{2\pi\mu}{2T\sigma}} \tag{2.11}$$

Where $H_{y0} = B_{y0}/\mu$. To obtain the apparent conductivity measured at a period T the equation 2.11 can be reordered as

$$\sigma_a(T) = \frac{2\pi\mu_0}{T|Z_{xy}|^2}. \tag{2.12}$$

The apparent resistivity can be obtained directly by

$$\rho_a(T) = \frac{T|Z_{xy}|^2}{2\pi\mu_0}. \tag{2.13}$$

The relation between σ_a to a penetration depth z was derived by Niblett and Sayn-Wittgenstein (1960) providing the following relationship

$$\sigma_a(T) = \frac{2\pi\mu_0}{T}\left[\int_0^h \sigma(z)dz.\right]^2 \tag{2.14}$$

Where:

$$h = \sqrt{\frac{T}{2\pi\mu_0\sigma_a(T)}} \tag{2.15}$$

Equation 2.14 represents and average conductance times a transverse resistivity which is constant along depth.

Gómez-Treviño (1996) proposed that the average conductivity between two points can be calculated by

$$\overline{\sigma}(z_1, z_2) = \frac{1}{z_2 - z_1} \int_{z_1}^{z_2} \sigma(z) dz. \tag{2.16}$$

It is also stated that the average conductivity for a $T_2 > T_1$ can be computed directly using the following relationship

$$\overline{\sigma}(z_1, z_2) = \sqrt{\sigma_a(T_2)\sigma_a(T_1)} \frac{1 - XY}{Y - X}. \tag{2.17}$$

Where $X = \sqrt{T_1/T_2}$ and $Y = \sqrt{\sigma_a(T_1)/\sigma_a(T_2)}$ and where the depths are given by

$$z_n = \sqrt{\frac{T_n}{2\pi\mu_0\sigma_a(T_n)}}. \tag{2.18}$$

In the case when $z_2 \to z_1$ the solution of equation 2.17 will reduce to the solution of the equation 2.14.

The maximum depth at which a buried halfspace can be detected at a particular period depends mainly on the conductivity contrast and the accuracy of the recording and processing system. Spies (1989) mentions that the analysis of the real and imaginary parts of the impedance shows that a reasonable estimate for the depth of investigation for MT is taken to be 1.5 skin depths or

$$DOI(z) = 1.5\sqrt{\frac{2}{\sigma\mu_0\omega}} = 700\sqrt{T\rho_a} \tag{2.19}$$

However, this approach only takes into consideration a single layer; in a multilayered Earth the concept of integrate or cumulative conductance needs to be introduced. Figure 2.1 shows the graphical representation of a layered Earth.

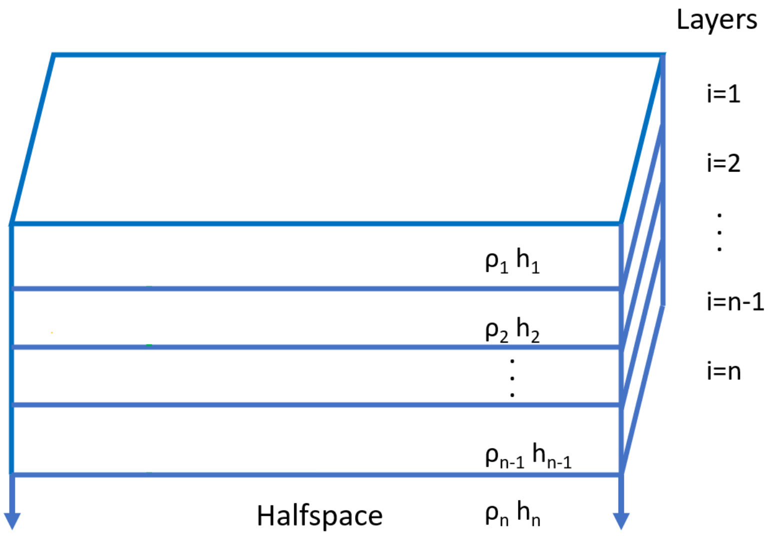

FIGURE 2.1: Graphical representation of a layered Earth in which each layer has its own electrical properties. For a layered Earth the response measured at the surface will depend on the electrical properties of all the layers present at the site.

Price (1949) introduces the term cumulative conductance $S_c(z)$ to determine the investigation depth in a layered Earth as

$$S_c(z) = \int_0^z \sigma(z)dz. \tag{2.20}$$

The previous term represents how the conductance increases along z considering the conductance and thickness of each layer. According to Spies (1989) equation 2.20 can be used to obtain the effective conductivity up to the n^{th} layer as follows

$$\sigma_{avg}(z) = \frac{\sum_{i=1}^{n} \sigma_i(z)(z_i - z_{i-1})}{z_n}. \tag{2.21}$$

2.1.2 MT Surveys

The MT method utilizes naturally occurring, broadband electromagnetic waves over the Earth's surface to image subsurface resistivity structure. A simple layout of the measuring system an equipment used in a MT survey is displayed in Figure ??

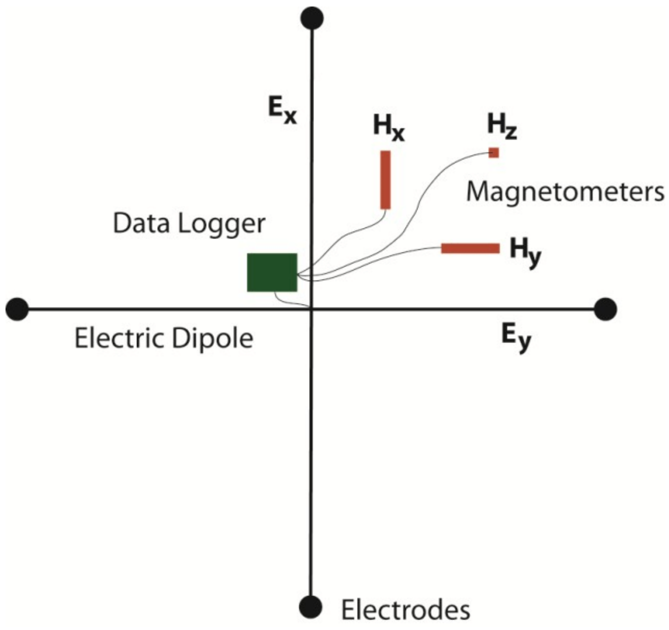

FIGURE 2.2: Graphical representation of a MT field setup in which electrical dipoles are used to measure both E x and E y field components. Induction coil magnetometers are used to measure H_x , H_y , and H_z field components. A data logger represents the station location (Comeau, 2015).

The method measures variations of the electric and magnetic fields recorded at the surface over hours or days depending on the objective to characterize. The magnetometers are used to record the variation over time of the Earth magnetic field while the electrodes are used to measure the variation of the Earth electric field.

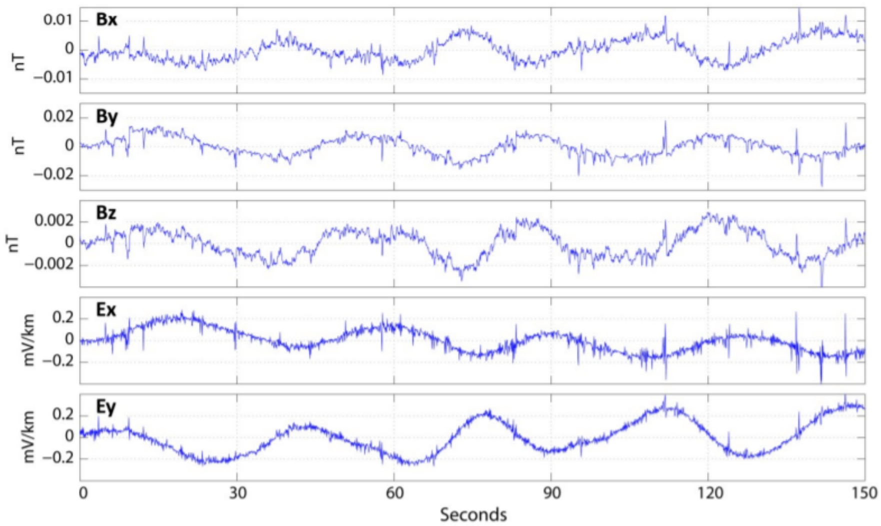

FIGURE 2.3: Time series for 5 channels of MT data. E_x and E_y are two orthogonal components of the electric field while H_x , H_y , and H_z are the three components of the magnetic field. Image taken from (Comeau, 2015).

Using the electric and magnetic fields measured over a period of time it is possible to obtain the apparent resistivity measured at the surface by

$$\rho_a(T) = \frac{T|\frac{E_x}{H_y}|^2}{2\pi\mu_0}. \tag{2.22}$$

Using equation 2.22 an example of the apparent resistivity measured by a MT survey is reported in Figure 2.4

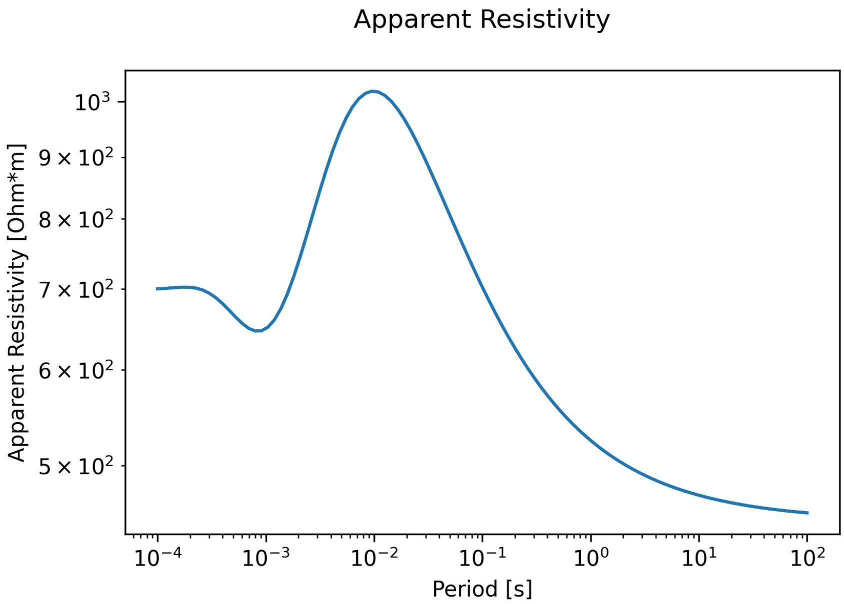

FIGURE 2.4: Apparent resistivity obtained from a MT survey using equation 2.22. The apparent resistivity measured at the surface contains information of the geological settings present at the subsurface.

The apparent resistivity measured at the surface contains information of the layers present at the subsurface and their electrical properties, however, the apparent resistivity does not represent an accurate description of the reality. To obtain the model of the subsurface that generates the apparent resistivity measured at the surface an inversion process is performed in which an initial electrical model is proposed and by an iterative process corrects the electrical model. The inversion process is finished when the electrical model is able to recreate the apparent resistivity measurements present in the data.

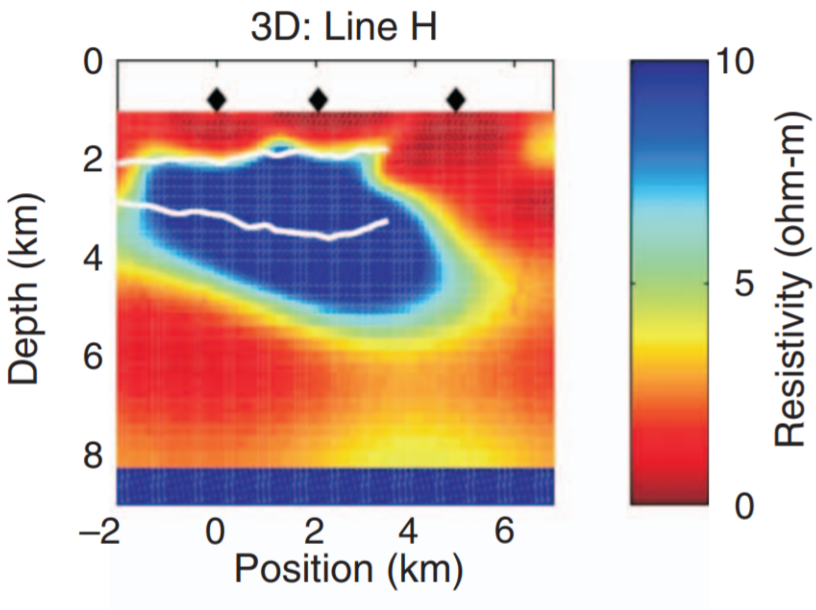

FIGURE 2.5: Example of the results of an inversion process for a MT survey in the Gemini prospect, Gulf of Mexico. Image taken from (Zhdanov et al., 2011)

Figure 2.5 shows an example of the geological profile retrieved by an inversion process from a MT survey.

2.1.3 Applications of the MT Method

The MT method is a powerful tool that can be used for different purposes, from shallow studies such as freshwater reservoir characterization up to deeper applications like mantle studies. Overall the MT method can be used for multiple studies, some examples of the applicability of the method will be described.

The MT method can be applied for the characterization of shallow targets for environmental purposes. One example is a MT survey performed at the Horonobe coastal area in Hokkaido, Japan, the goal of the study was to characterize a shallow layer containing freshwater along the coast. The inversion of the acquired data revealed a sedimentary layer containing freshwater, the layer extends horizontally several kilometers. In this survey the MT method was used to identify the groundwater distributions in coastal areas (Ueda et al., 2014).

For hydrocarbon exploration the MT method can be used to image structures that could host potential reservoirs and source rocks. In certain cases, they may also give evidence for direct indication of the presence of hydrocarbons (Unsworth, 2005). Figure 2.6 shows how a MT survey can be assumed as a smoother version of a resistivity log.

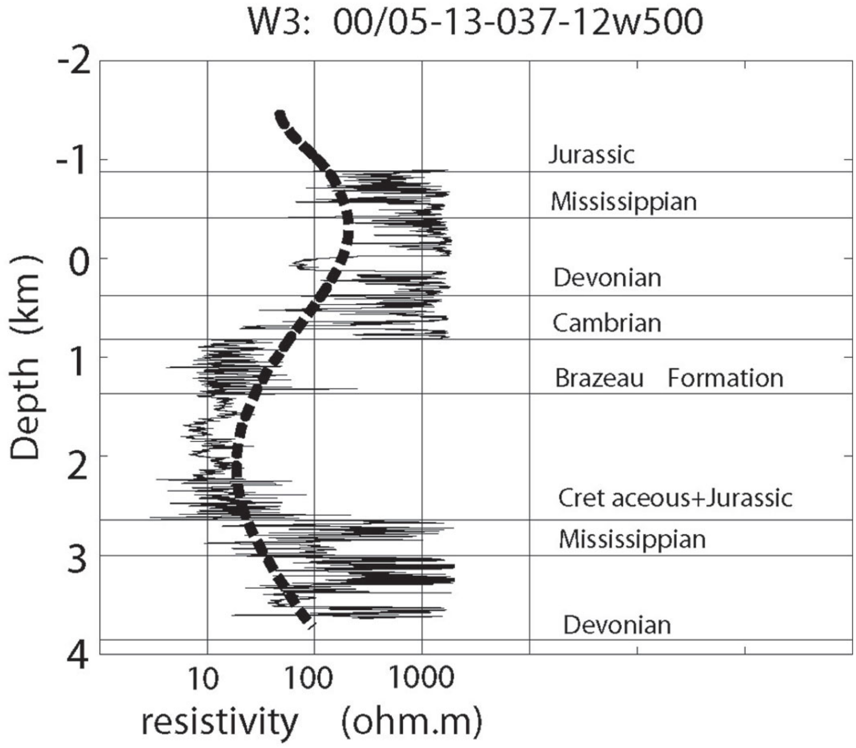

FIGURE 2.6: Comparison of resistivity derived from the MT data with a resistivity log. The resistivity-depth profile derived with the MT data is smoother than that measured in the well because MT uses long wavelength signals that average small scale features. Image taken from (Unsworth, 2005)

Currently the investigation related to the EM method is focused in different areas. New techniques for joint inversion of electromagnetic data with other geophysical methods are currently being explored, integrating electromagnetic data with other observations can improve the quality of the resulting geological model providing a more accurate characterization of the subsurface (Moorkamp, 2017).

New methods to improve the inversion problem for EM methods are also being studied. In general, the goal of these new techniques is to decrease the uncertainty of the inverted model and the real data without increasing the time invested in the inversion process or without increasing the computational power needed to perform the inversion process (Ren and Kalscheuer, 2020).

2.2 Regression Analysis

Regression analysis is a predictive modelling technique in which a defined relationship between an independent variable x and a dependent variable y is established. Most precisely, regression analysis is to find a mathematical expression $f()$ capable of explaining the y values in terms of x as $y = f(x)$.

In this work the linear and polynomial regressions will be applied.

2.2.1 Linear Regression

Linear regression is a branch of regression analysis techniques in which a linear approach is used to model the relationship between the independent variable x and the dependent variable y. The main assumption of linear regression is that the value of the dependent variable y changes at a constant rate as the value of the independent variable x increases or decreases. The mathematical expression for this relationship can be defined as:

$$\mathcal{E}(y_i) = \beta_0 + \beta_1 x_i \tag{2.23}$$

Where $\mathcal{E}(y_i)$ is the expected value y_i for the input x_i. However, in reality there is a deviation between an observation and the theoretical value, this deviation is taking into consideration by adding a random error ϵ to the linear relationship, which leads to:

$$y_i = \beta_0 + \beta_1 x_i + \epsilon_i \tag{2.24}$$

2.2.2 Least Squares Estimation

The linear relationship 2.25 contains two unknown parameters β_0 and β_1 which have to be estimated from the data. To obtain the unknown parameters the method of least squares can be used.
The method proposes that the sum of the square differences between any given value observed y_i and the value estimated from the straight line is a minimum, also the estimated line satisfies the sum of the residuals equals 0. Additionally the line estimated by least squares satisfies that when $x = \overline{x}$ the value for $y = \overline{y}$ intercept the estimated line (Gupta, 2019). The least squares can be defined as:

$$S(\beta_0, \beta_1) = \sum_{i=1}^{n} (y_i - \beta_0 - \beta_i x_i)^2 \tag{2.25}$$

The solution to the least squares method must satisfy:

$$\frac{\partial S}{\partial \beta_j} = -2 \sum_{i=1}^{n} (y_i - \hat{\beta}_0 - \hat{\beta}_i x_i) = 0 \tag{2.26}$$

Using equations 2.25 and 2.26 the solutions to the least square method can be defined as:

$$\hat{\beta}_0 = \overline{y} - \hat{\beta}_1 \overline{x} \tag{2.27}$$

And

$$\hat{\beta}_1 = \frac{\displaystyle\sum_{i=1}^{n} y_i x_i - \frac{\left(\displaystyle\sum_{i=1}^{n} y_i\right)\left(\displaystyle\sum_{i=1}^{n} x_i\right)}{n}}{\displaystyle\sum_{i=1}^{n} x_i^2 - \frac{\left(\displaystyle\sum_{i=1}^{n} x_i\right)^2}{n}} \tag{2.28}$$

Where:

$$\overline{y} = \frac{1}{n} \sum_{i=1}^{n} y_i \quad and \quad \overline{x} = \frac{1}{n} \sum_{i=1}^{n} x_i$$

Therefore $\hat{\beta}_0$ and $\hat{\beta}_1$ are the least square estimators of the intercept and the slope respectively (Van Huffel and Vandewalle, 1991).

2.2.3 Polynomial Regression

In situations in which the relationship between x and y is nonlinear the behavior can be approximated by using a higher degree polynomial over the range of the independent variable x. The $k_{th} - order$ polynomial model for one variable can be defined as:

$$\mathcal{E}(y_i) = \beta_0 + \beta_1 x_i + \beta_2 x_i^2 + ... + \beta_k x_i^k + \epsilon \tag{2.29}$$

Polynomial regressions can be solved as a multiple linear regression model, which implies that the method previously defined can be used to obtain the k_{th} unknowns Rawlings et al. (2001).
There are several aspects when fitting a polynomial expression in one variable. Some of these aspects are:

- Order of the model

  - The order of the polynomial should be the lowest possible.

- Model building strategy
  - The degree of the polynomial should be increased until the diminishing of the error between polynomials is non significant.

- Extrapolation
  - the extrapolation limits for the polynomial should be carefully determined. Polynomial models may generate data that not corresponds to the real behavior of the phenomenon for values of x outside the range in which the polynomial was created.

For this work polynomial regressions will be used to model the nonlinear behavior of the electromagnetic data.

2.2.4 Piecewise Polynomial Fitting (Splines)

Polynomial functions can be used to approximate the behavior of non linear data, however there are cases in which a low order polynomial is not useful when trying to approximate the data and a high order polynomial does not improve the approximation either. This might be due to the fact that the data behave differently depending on the range of x, to approximate the data in complex scenarios the splines functions were proposed (Montgomery et al., 2021).

Spline functions are a set of low order polynomials connected in a particular point in the curve to be modeled. The approach is to divide the range of x in a number of segments and to fit a low degree polynomial on each segment. The point in which two polynomials are going to be connected is called a knot.

The function to be modeled by an spline approximation requires to be continuous in all the range of x and to have $k-1$ continuous derivatives in order to ensure that the knots will connect between each other (Gupta, 2019).

Splines are piecewise polynomials of order k, in this work cubic splines ($k = 3$) have been used. A cubic spline with h knots can be written as:

$$E(y) = S(x) = \sum_{j=0}^{3} \beta_0 x^j + \sum_{i=1}^{h} \beta_1 (x - t_i)_+^3 \tag{2.30}$$

Where:

$$(x - t_i)_+ \begin{cases} (x - t_i), & \text{if } (x - t_i) > 0 \\ 0, & \text{if } (x - t_i) \leq 0 \end{cases}$$

Assuming the position of the knots to be known equation 2.30 can be solved by the least square method seen in Section 2.2.2.

Chapter 3

Methodology

This work aims to find a mathematical expression that can be used to transform apparent measurements of a MT survey into resistivity values to generate a rescaled geological model that represents the geological properties present in the subsurface.

Starting from field measurements and assuming information from a exploratory well, the apparent resistivity measured by the MT survey at the surface is processed to approximate the data as close as possible to the data measured from the well.

From the processed apparent resistivity data a polynomial regression is used to model and correct the differences between the apparent measurements and the log values. Once the apparent resistivity is corrected a resistivity model is derived from the data and is compared to the actual resistivity model of the subsurface.

3.1 General Overview

This work aims to find a mathematical expression that can transform apparent resistivity measurements from a MT survey into resistivity values that resembles the electrical settings present at the subsurface. Figure 3.1 shows a graphical representation of the steps followed to obtain the expression needed to correct the apparent resistivity data by means of a polynomial regression.

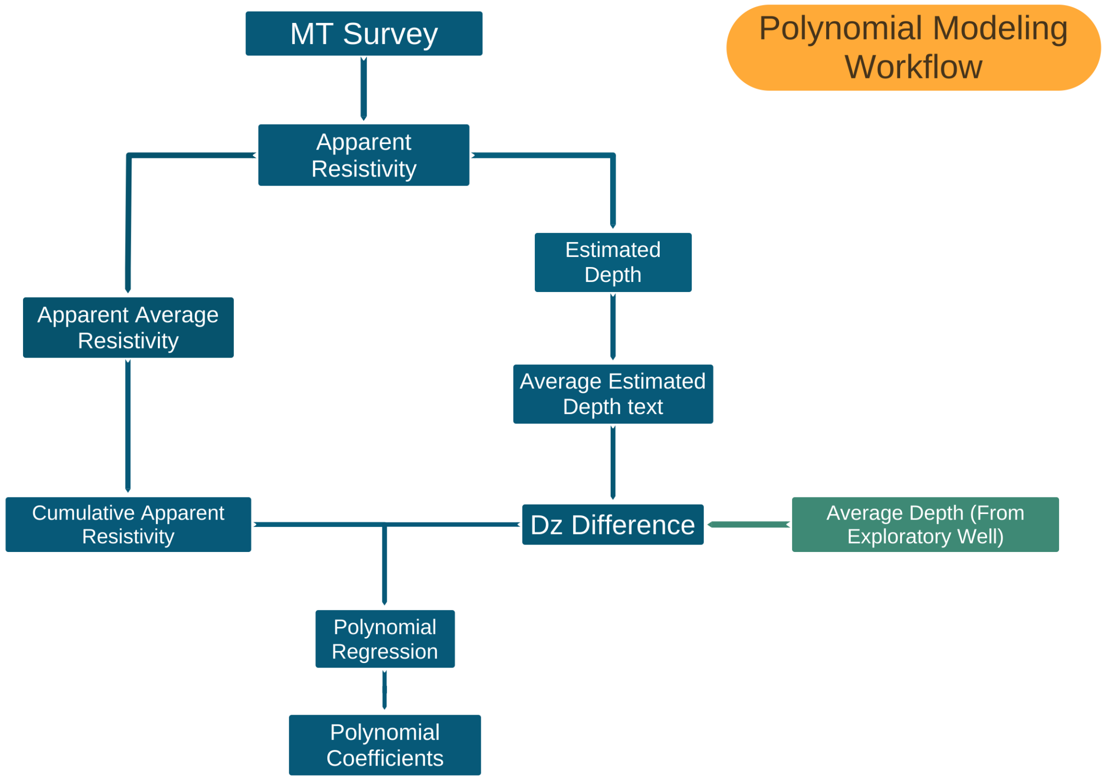

Figure 3.1: Workflow for the polynomial modeling process. The apparent resistivity data will be approximated to the data from a exploratory well using different approaches, once the apparent resistivity data is improved a polynomial regression is used to model and correct the existing differences between the apparent measurements and the measurements from the well.

Starting from the apparent resistivity measurements equation 2.18 is used to obtain a first depth-apparent resistivity model that can be compared to the geological settings in the subsurface. However this first approximation is not close to the measurements from the resistivity logs and can be improved.

The average resistivity proposed by Gómez-Treviño (1996) is used as a way to improve the depth-apparent resistivity relationship; this approximation proved to be closer to the log values, however in this representation the misfit between the measured apparent resistivity and the resistivity values cannot be modeled by a polynomial expression. For this reason in this work it is proposed to used the cumulative values for the average apparent resistivity.

The cumulative apparent resistivity is compared with the cumulative resistivity, and the behavior of the differences between the apparent data and the log values is modeled by a polynomial regression, the expression then is used to correct the cumulative apparent resistivity data and a resistivity model is retrieved.

In this work the methodology described above will be applied for apparent resistivity and apparent conductivity measurements to compare the behavior of the methodology and to see if there are any differences overall.

3.2 Apparent Conductivity and Apparent Resistivity

To simulate the data acquired in a MT survey a resistivity model was proposed. The characteristics of the geological settings of the subsurface are reported in Table 3.1 and in Figure 3.2.

TABLE 3.1: Resistivity and Conductivity model parameters.

Resistivity [Ohm*m]	**Conductivity [Ohm/m]**	**Thickness of the Layer [m]**
750	$1.3 \text{x} 10^{-3}$	500
2500	$4 \text{x} 10^{-4}$	800
450	$2.2 \text{x} 10^{-3}$	Half Space

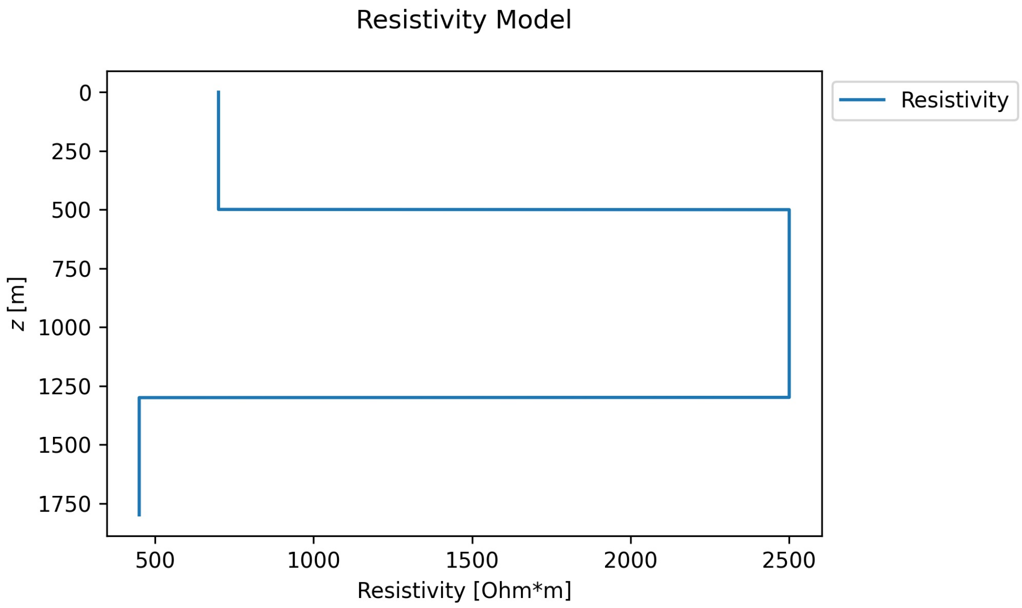

FIGURE 3.2: Resistivity Model

The measurements from the MT survey represent an apparent resistivity curve that is function of the period of the electromagnetic waves propagating through the Earth. The apparent electrical responses corresponding to the geological model presented in Figure 3.2 are reported in Figures 3.3(a) and 3.3(b)

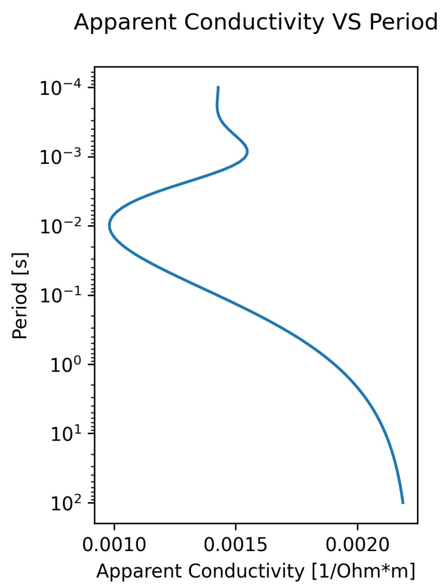

(a) Apparent Conductivity.

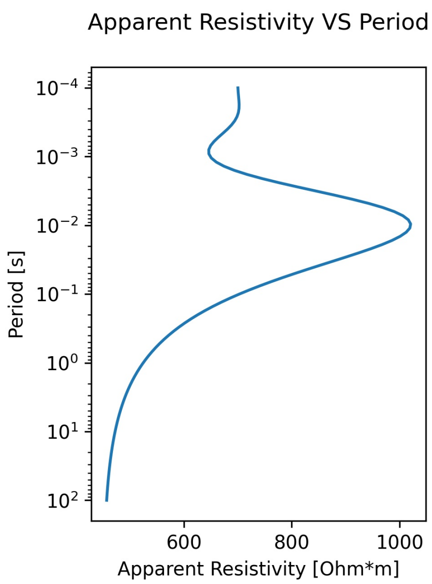

(b) Apparent Resistivity.

FIGURE 3.3: Apparent conductivity and apparent resistivity.

This first result represents the electrical properties of the rocks present in the subsurface, however, this estimation cannot be related to a location in depth, for this reason a depth estimation for the electrical measurements is needed.

3.3 Calculated Apparent Depth

The apparent resistivity measured by the MT survey is a function of the period of the signal used to characterize the subsurface. To generate a apparent depth-apparent resistivity model equation 2.18 can be used to obtain an estimation of a point in depth as a function of an apparent resistivity value for a period T. Gómez-Treviño (1996) states that the apparent location in depth for an apparent electrical measurement can be calculated by means of

$$z_a(T) = \sqrt{\frac{T}{2\pi\mu_0\sigma_a(T)}}. \tag{3.1}$$

Figure 3.4 reports the apparent depth estimation for a period T.

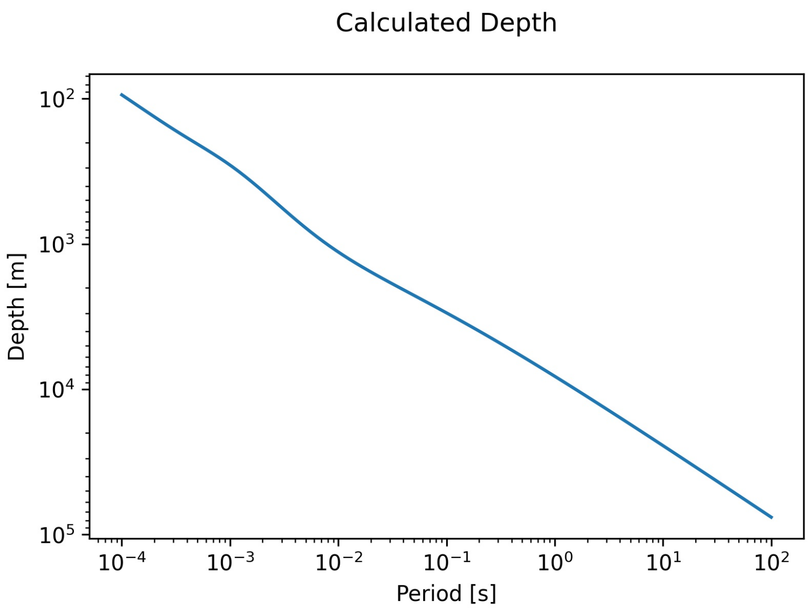

FIGURE 3.4: Calculated apparent depth as a function of the apparent resistivity for a given period T using equation 2.18.

Figure 3.4 shows that for small periods the depth estimation is shallower than for longer periods, this implies that the apparent resistivity measured for short periods corresponds to shallower points in the subsurface, whereas apparent resistivity values obtained for longer periods should be located at higher depths. Using the apparent depths previously derived, a first approximated model is obtained using the apparent resistivity values measured in the MT survey and the depths calculated by means of equation 3.1. However, compared to Figure 3.5(a) it can be seen that the model obtained is not an accurate representation of the local properties of the subsurface.

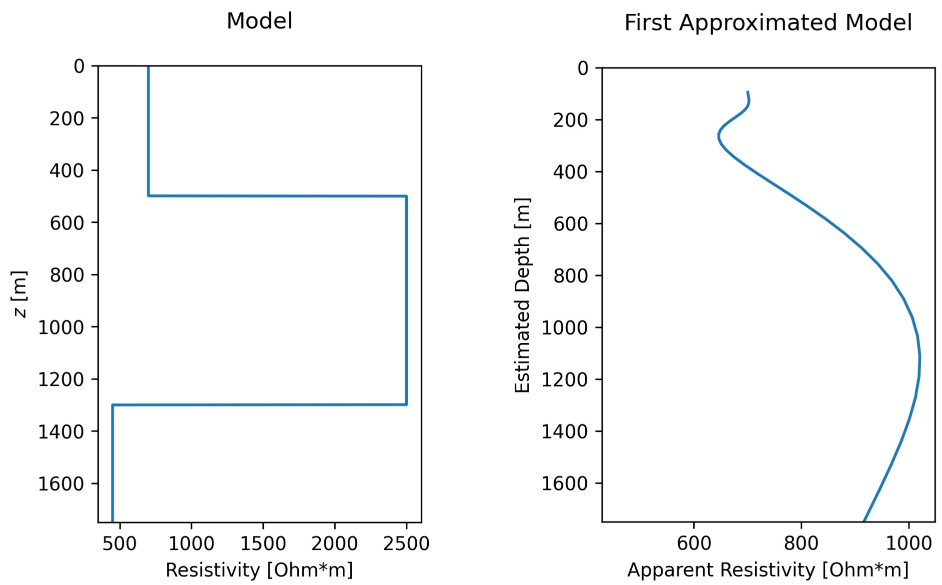

(a) Local resistivity model as a function of depth

(b) First approximated calculated apparent depth - apparent resistivity

FIGURE 3.5: Comparison between the local resistivity as a function of depth measured in the exploratory well vs the first approximated model using the apparent resistivity measurements and the calculated apparent depth.

This first model cannot represent the reality of the subsurface, for this reason in this work another step is proposed to obtain a more reliable apparent resistivity model.

3.4 Average Apparent Electrical Properties and Average Apparent Depth

The first approximated model shown in Figure 3.5(b) is not a fully accurate representation of the resistivity values and their location in depth. For this reason it is proposed to obtain the average apparent resistivity (Gómez-Treviño, 1996) to see if the model shown in Figure 3.5(b) can be improved.

The average apparent resistivity proposed by Gómez-Treviño (1996) is an average resistivity representative of the electrical properties of the subsurface along the depth interval between two apparent resistivity measurements. However, since we are obtaining an average apparent resistivity that corresponds to an interval between measurements its location in depth should be an average point too, for this reason the average electrical resistivity will be related to an average apparent depth by means of:

$$\overline{z_a}(z_{i+1}, z_i) = \frac{z_{a(i+1)}(\rho_a(T_i+1)) + z_{a(i)}(\rho_a(T_i))}{2} \tag{3.2}$$

Once the average apparent electrical properties and the average apparent depth were obtained, the hypothesis that it could help to improve the model obtained was tested. A comparison between the average apparent properties, the local electrical properties of the subsurface shown in Figure 3.2 and the first model obtained is reported in Figure 3.5(b) provided the following results

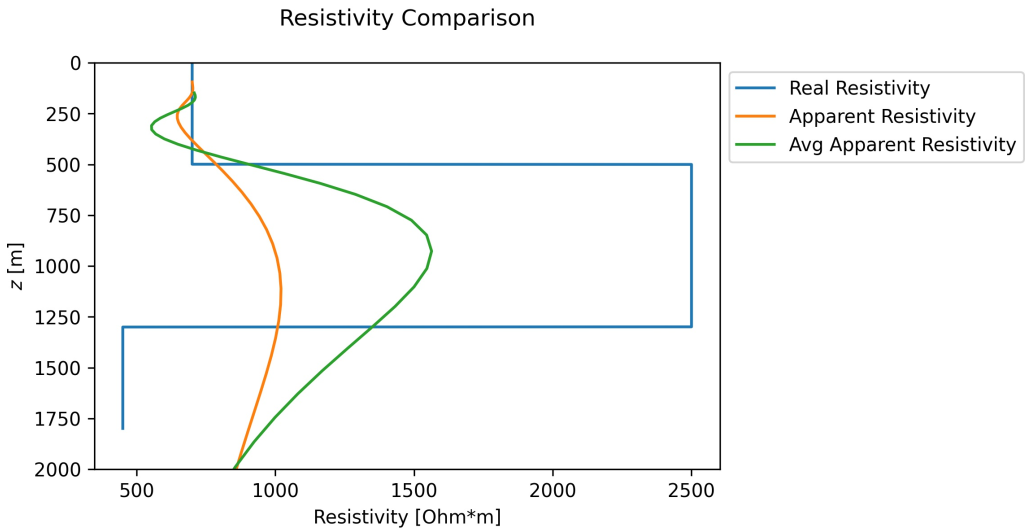

FIGURE 3.6: Comparison between the local resistivity as a function of depth measured by resistivity logs(blue), the model obtained by using the apparent resistivity as a function of the apparent depth (orange) and the model obtained by using the average apparent resistivity as a function of an average apparent depth (green). At first glance it seems that the average apparent resistivity as a function of average apparent depth is closer to the real geological model.

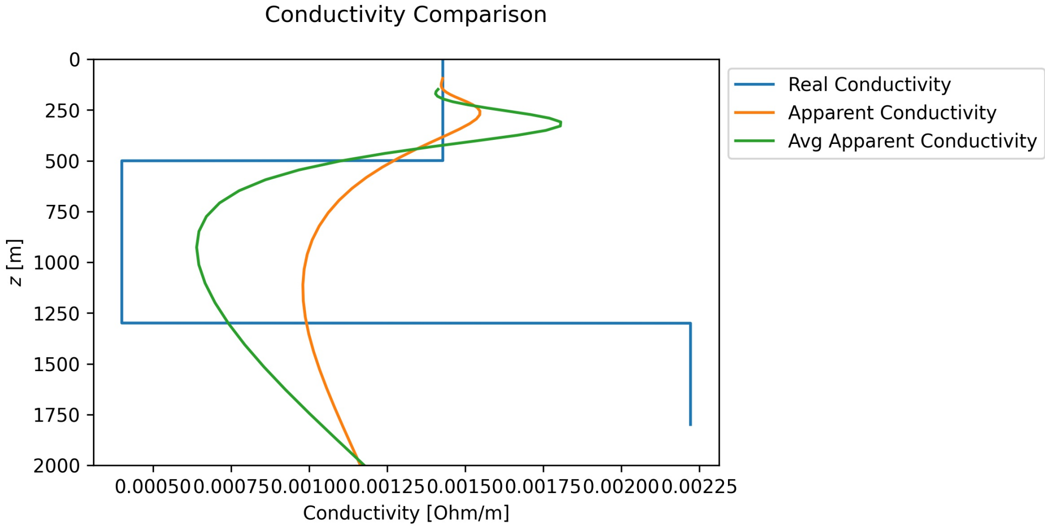

FIGURE 3.7: Comparison between the local conductivity as a function of depth derived from the resistivity logs (blue), the model obtained by using the apparent conductivity as a function of the apparent depth (orange) and the model obtained by using the average apparent conductivity as a function of an average apparent depth (green). For the conductivity it also seems that the average apparent conductivity model is closer to the geological settings present in the subsurface.

At first glance it seems that the model obtained using average apparent values is closer to the local geological setting present in the subsurface. To confirm this hypothesis the numerical error between the model obtained by the resistivity logs and the apparent models was obtained. First the total error between estimations was calculated by means of

$$E_{Total} = \sum_{i=1}^{n} = \left| \frac{z(\rho) - z(\rho_a)}{z(\rho)} \right| \times 100 \qquad For\ \rho \approx \rho_a. \tag{3.3}$$

Where $z(\rho)$ is the depth value for a given resistivity point measured by the resistivity logs. The average error was obtained by means of

$$E_{Avg} = \frac{1}{n} \sum_{i=1}^{n} = \left| \frac{z(\rho) - z(\rho_a)}{z(\rho)} \right| \times 100 \qquad For\ \rho \approx \rho_a \tag{3.4}$$

The results of the total error and the average error between models is reported in Tables 3.3 and 3.2

TABLE 3.2: Total error between real and apparent electrical model compared to the total error between real and average apparent electrical model. The error comparison was performed to confirm the hypothesis that the average apparent electrical model is closer to the local electrical model measured in the subsurface.

Total Error %	
Apparent Resistivity	**Apparent Conductivity**
2030	6039
Average Apparent Resistivity	**Average Apparent Conductivity**
2015	1822

TABLE 3.3: Average error between real and apparent electrical model compared to the average error between real and average apparent electrical model.

Average Error %	
Apparent Resistivity	**Apparent Conductivity**
45	140
Average Apparent Resistivity	**Average Apparent Conductivity**
43	42

It can be seen in the Figures 3.6 and 3.7 and in Tables 3.2 and 3.3 that the average values for the apparent electrical properties are closer to the geological settings present in the subsurface shown in Figure 3.2. Based on the previous results, the model obtained by the average apparent electrical properties and average apparent depth will be used as a starting point to determine if it is possible to correct the differences between apparent measurements and local measurements by means of a mathematical expression to obtain an accurate representation of the subsurface by only using apparent measurements performed in the surface.

However, for the current representation of the data a given apparent resistivity value can be related with two or more points in depth, which cannot be modeled by a polynomial expression. For this reason it is proposed to use the cumulative average electrical properties as a representation of the data in which for a given cumulative value there is only one point in depth in correspondence.

3.5 Cumulative Apparent Conductivity and Cumulative Apparent Resistivity

In this thesis it is proposed to use the cumulative apparent electrical properties as a representation of the data that can be used to obtain a polynomial expression able to correct the differences between apparent and local measurements .

The cumulative resistivity can be defined as the integrated total resistivity from the surface up to a certain point in depth z. To calculate the cumulative electrical properties for discrete data equation 3.9 will be used for cumulative conductivity or conductance as

$$S_c(T) = \sum_{0}^{n} \overline{\sigma_i}(T) h_i. \tag{3.5}$$

For cumulative resistivity as

$$\rho_c(T) = \sum_{i=0}^{n} \overline{\rho_i}(T) h_i. \tag{3.6}$$

Where n is the number of layers and h is the thickness of the the n_{th} layer.

The curves for the integrated electrical properties can provide information of the layers present in the subsurface in similar way as the apparent electrical curves seen previously, but the main advantage is that for one value of cumulative resistivity it has only one corresponding depth value.

Using equations 3.5 and 3.6 the cumulative apparent electrical properties can be obtained for each period in the same way the apparent electrical properties are function of the period. To obtain a cumulative apparent resistivity vs depth each cumulative value was related to its point of average apparent depth for a period T and an average apparent depth-cumulative apparent property model can be obtained similarly as the models shown in Figures 3.6 and 3.7.

The cumulative models obtained for cumulative apparent resistivity and cumulative apparent conductance are reported in Figures 3.8 and 3.9 respectively.

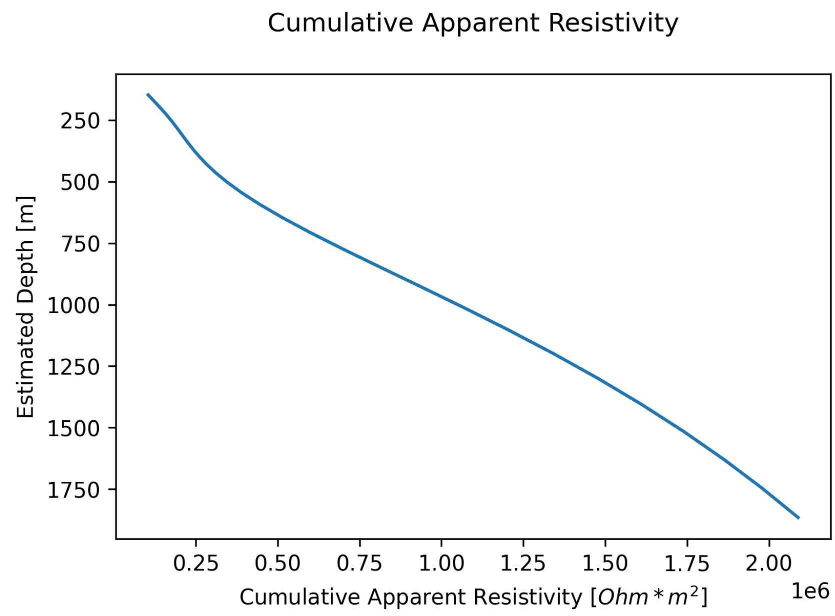

FIGURE 3.8: Average apparent depth-cumulative apparent resistivity model obtained by integrating the apparent average resistivity shown in Figure 3.6.

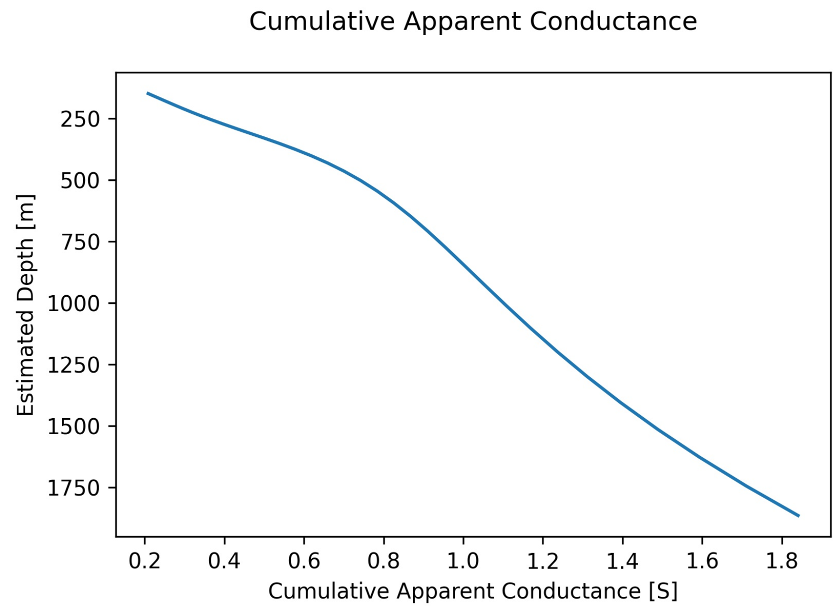

FIGURE 3.9: Average apparent depth-cumulative apparent conductivity model obtained by integrating the apparent average conductivity shown in Figure 3.7.

The models shown in Figures 3.8 and 3.9 were compared to the cumulative models obtained by using the data coming from the resistivity logs. The comparison between cumulative models is reported in Figures 3.10 and 3.11.

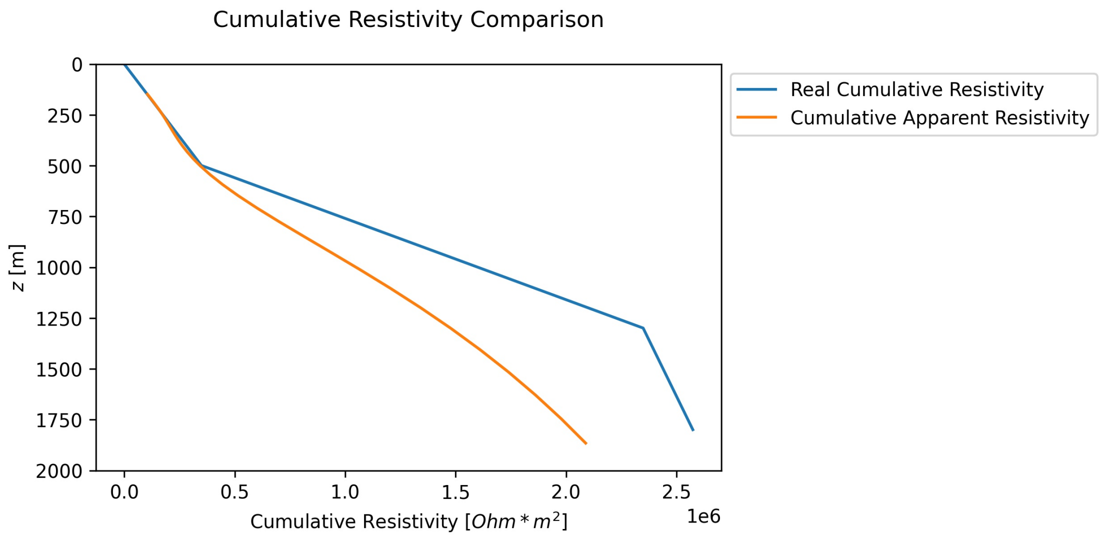

FIGURE 3.10: Comparison between the cumulative resistivity model generated using the measurements from a resistivity log (blue) and cumulative apparent resistivity model generated using MT measurements (orange).

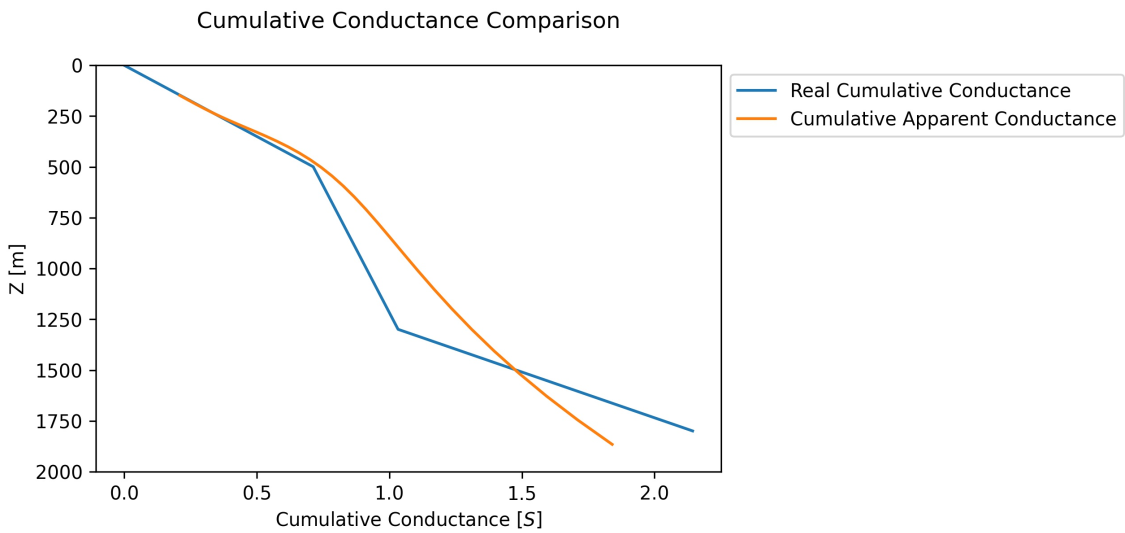

FIGURE 3.11: Comparison between the cumulative conductivity model generated using the measurements from a resistivity log (blue) and cumulative apparent conductivity model generated using MT measurements (orange)

Figures 3.10 and 3.11 shown that there is a difference in depth (Δz) for the cumulative apparent resistivity measured from a MT survey and the local cumulative resistivity measured from resistivity logs. This means that for a certain cumulative property there is a Δz between the real location in depth and the location obtained using the apparent measurements.

3.6 Δz Difference Between Local and Apparent Cumulative Measurements

Based on the previous analysis it can be concluded that the cumulative apparent electrical properties deviate from the cumulative properties measured using resistivity logs in their location in depth. The z difference identifies the correction that must be applied to the apparent depth for a specific cumulative apparent resistivity value to transform it into a cumulative resistivity. The Δz difference was computed for a given value of the cumulative electrical property by means of

$$\Delta z = z - z_a \qquad When\ S \approx S_a. \tag{3.7}$$

The results of this Δz difference between cumulative apparent measurements and cumulative values are reported in Figures 3.12 and 3.13

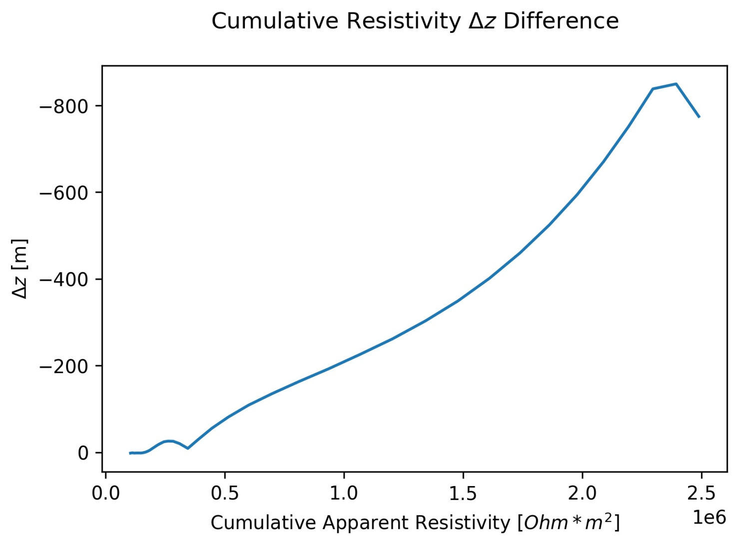

FIGURE 3.12: Δz difference for cumulative apparent resistivity. The curve represents the misfit in meters between the value in depth calculated for a cumulative apparent resistivity value and the value in depth for a cumulative resistivity value.

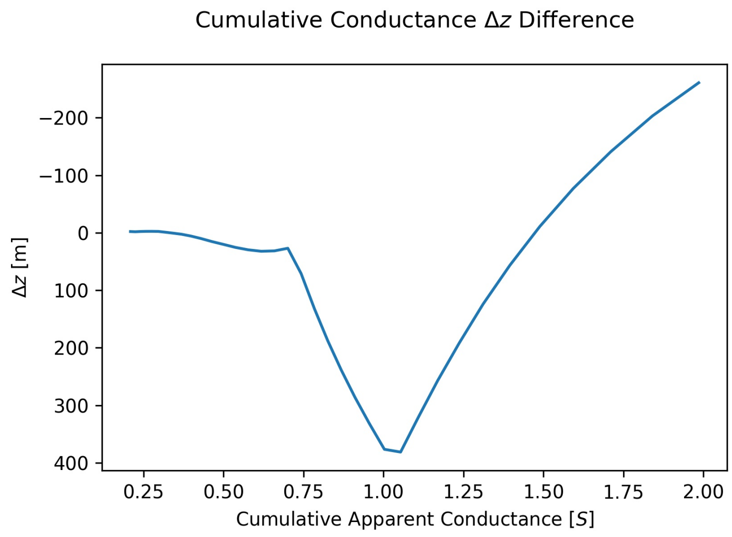

FIGURE 3.13: Δz difference for cumulative apparent conductivity. The curve represents the misfit in meters between the value in depth calculated for a cumulative apparent conductivity value and the value in depth for a cumulative conductivity value.

Considering the behavior of the Δz difference it is proposed to use a polynomial regression to model the Δz difference and correct the apparent values measured from a MT survey to obtain a rescaled geological model that describes the settings present in the subsurface.

3.7 Polynomial Regression

In this work it is proposed to generate a polynomial expression that will work as a filter in the sense that it will be used to obtain a mathematical expression able to correct the Δz difference between cumulative apparent and cumulative values.
The polynomial expression will have the following structure

$$\Delta z_i(\rho_c) = \beta_0 + \beta_1 x_i^1 + ... + \beta_n x_i^n. \tag{3.8}$$

Where x is the cumulative electrical property.

Rawlings et al. (2001) mentions that the degree of a polynomial used to model a phenomenon should be kept as low as possible, for this reason, the root mean squared error (RMSE) was used. To determine the degree of the polynomial to be used, a search was performed along the first 20 polynomials, the range of polynomials that provided the lowest RMSE were selected and compared between each other by means of

$$Improvement = \frac{RMSE_{i-1} - RMSEi}{RMSE_{i-1}} \times 100. \tag{3.9}$$

Where i is the degree of the polynomial. The degree of the polynomial is determined when the improvement between regressions is less than 10 %. If the condition is satisfied the polynomial with the lower degree is used, otherwise, the polynomial with the lower RMSE is used.

Figures 3.12 and 3.13 shown that the range of variation for the cumulative apparent resistivity is in an order of magnitude of 1×10^6 and for the cumulative apparent conductivity is in an order of magnitude of 1×10^1. For this reason it was concluded that the curve behavior and the regression analysis should be performed to two different representations of the data. The analysis was performed in a linear representation and for the second case the logarithmic representation of the data was studied.

3.7.1 Polynomial Regression for linear data

The first regression analysis was performed to the original Δz difference without any modification. The results of the regression are reported in Figures 3.14 and 3.15

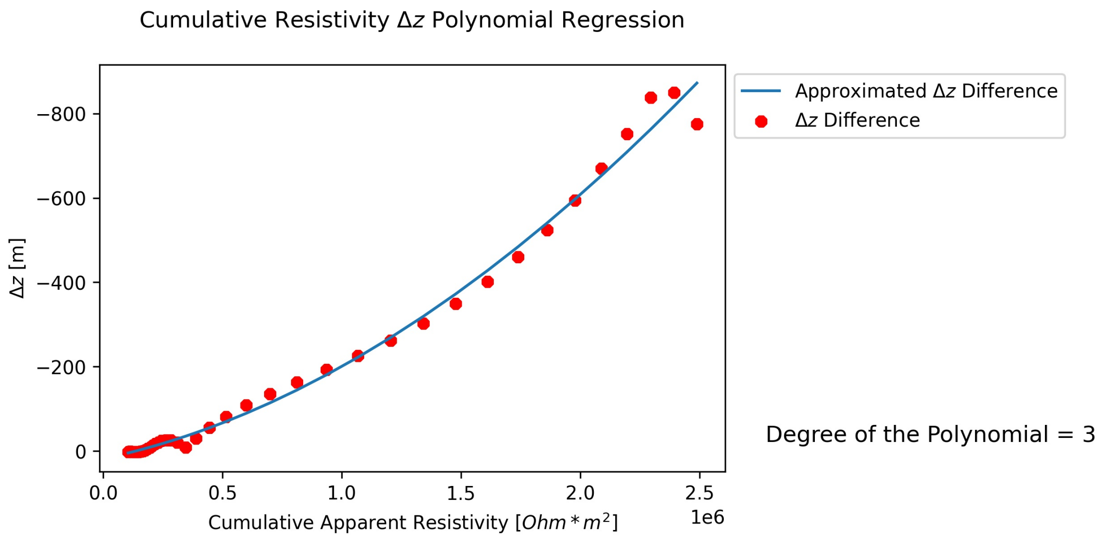

FIGURE 3.14: Polynomial regression modeling of the ΔZ difference using a 3 degree polynomial for the cumulative apparent resistivity

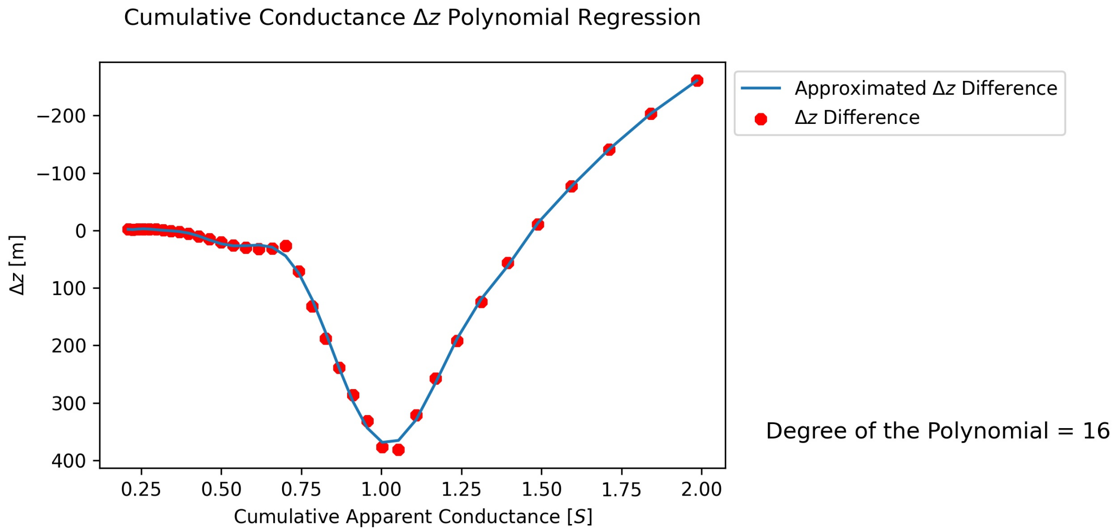

FIGURE 3.15: Polynomial regression modeling of the ΔZ difference using a 6 degree polynomial for the cumulative apparent conductance

It can be seen on Figure 3.14 that the polynomial regression of the linear representation of the Δz difference for the cumulative resistivity is not able to describe the subtle changes of the Δz difference. For this reason the regression analysis for the logarithmic representation of the data was implemented.

3.7.2 Polynomial Regression for the logarithmic representation of the data

For the logarithmic regression analysis the log_{10} of the Δz and the cumulative apparent property was obtained and in this representation of the data the regression was performed.The results of the polynomial regression analysis are reported in Figures 3.16 and 3.17.

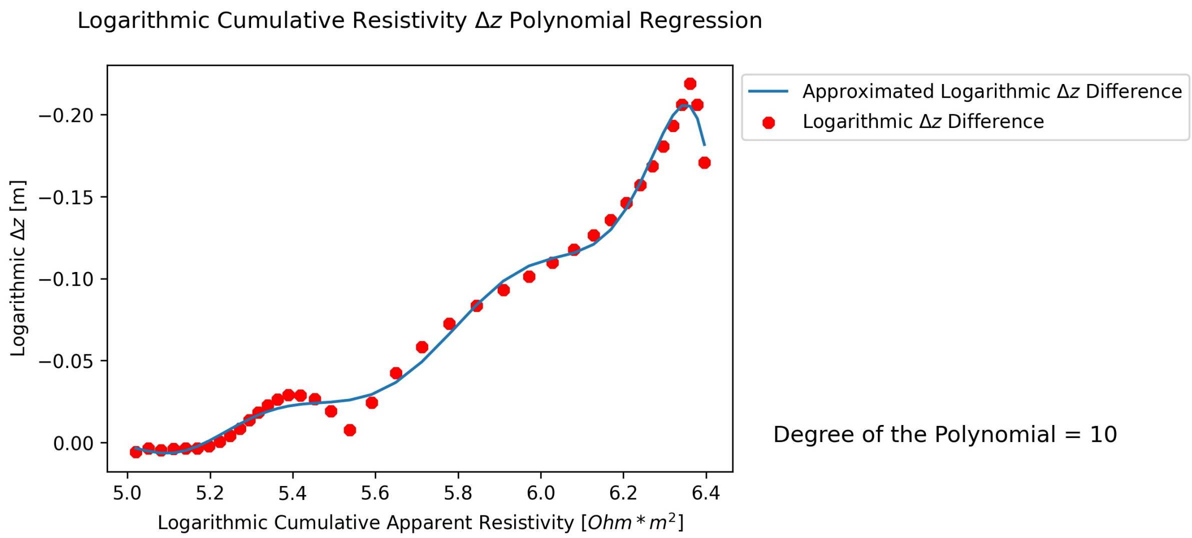

FIGURE 3.16: Polynomial regression modeling of the logarithmic representation of the ΔZ difference using a 10 degree polynomial for the cumulative apparent resistivity

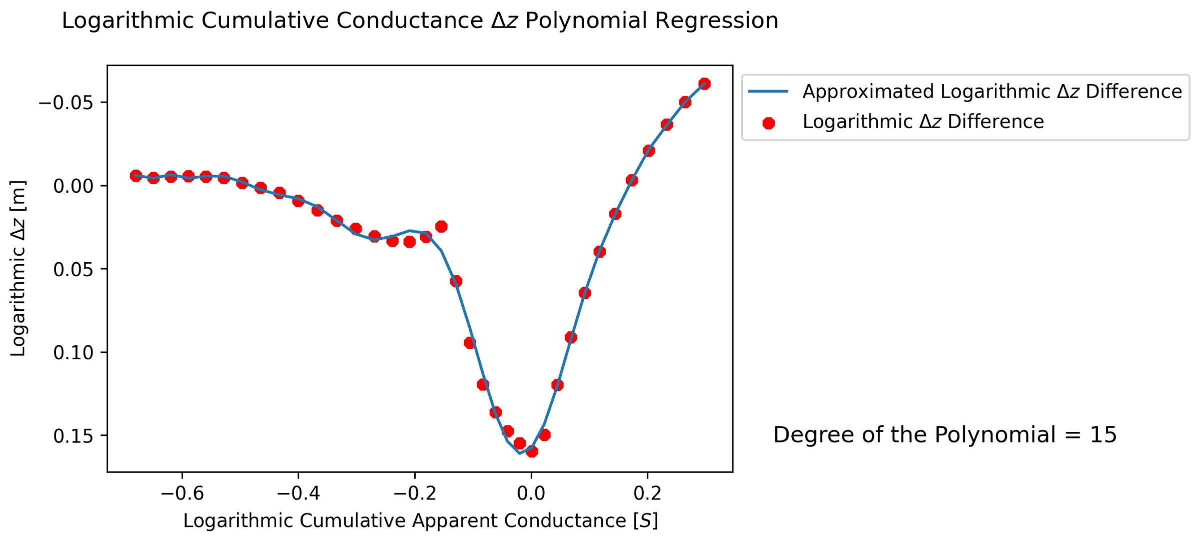

FIGURE 3.17: Polynomial regression modeling of the logarithmic representation of the ΔZ difference using a 15 degree polynomial for the cumulative apparent conductance

Based on the results of polynomial regressions presented in Figures 3.16 and 3.17 it can be seen that even though the logarithmic representation of the data could be modeled in a more accurate way, there are still some parts of the Δz difference that the polynomial regression cannot fully describe, based on this a another approach was applied.

3.7.3 Cubic Spline Interpolation

The analysis of the results of polynomial regressions presented in Figures 3.16 and 3.17 lead to the conclusion that the polynomial regression could be improved even more, considering this, a cubic spline interpolation was proposed. The cubic splines divide the Δz curve into smaller segments, where each segment is modeled by a cubic polynomial expression, this approximation is used to model points in the curve where sudden changes appear, which cannot be modeled by a simple polynomial regression.

To obtain the best spline curve the number of knots was increased until a good fitting of the Δz difference was obtained, the results of the cubic spline interpolation are reported in Figures 3.18 and 3.19:

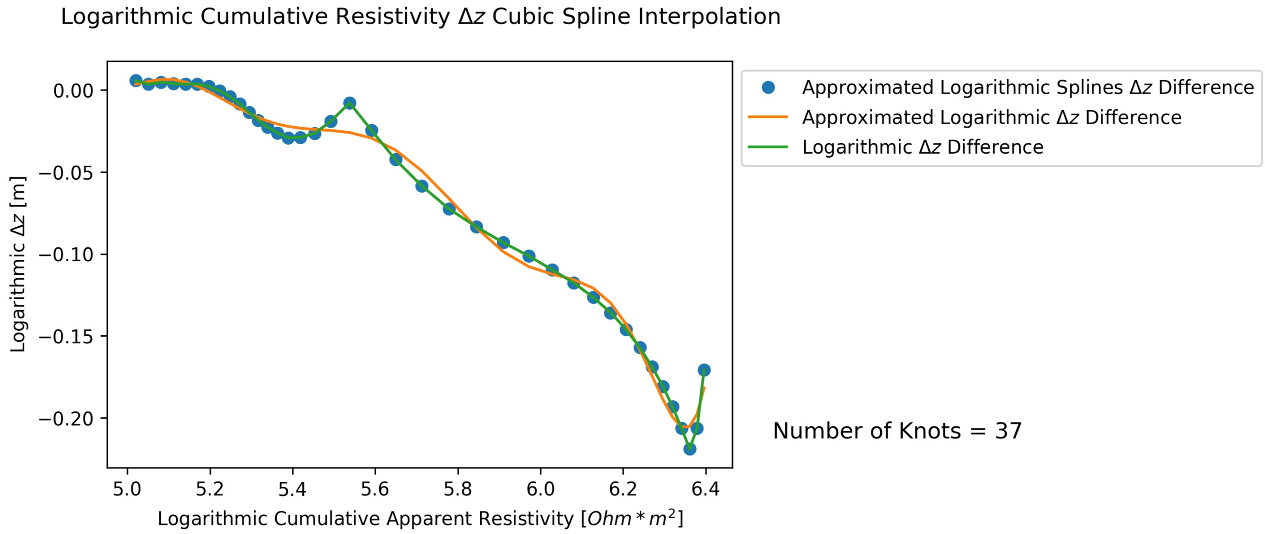

FIGURE 3.18: Cubic spline interpolation of the logarithmic representation of the ΔZ difference for the cumulative apparent resistivity

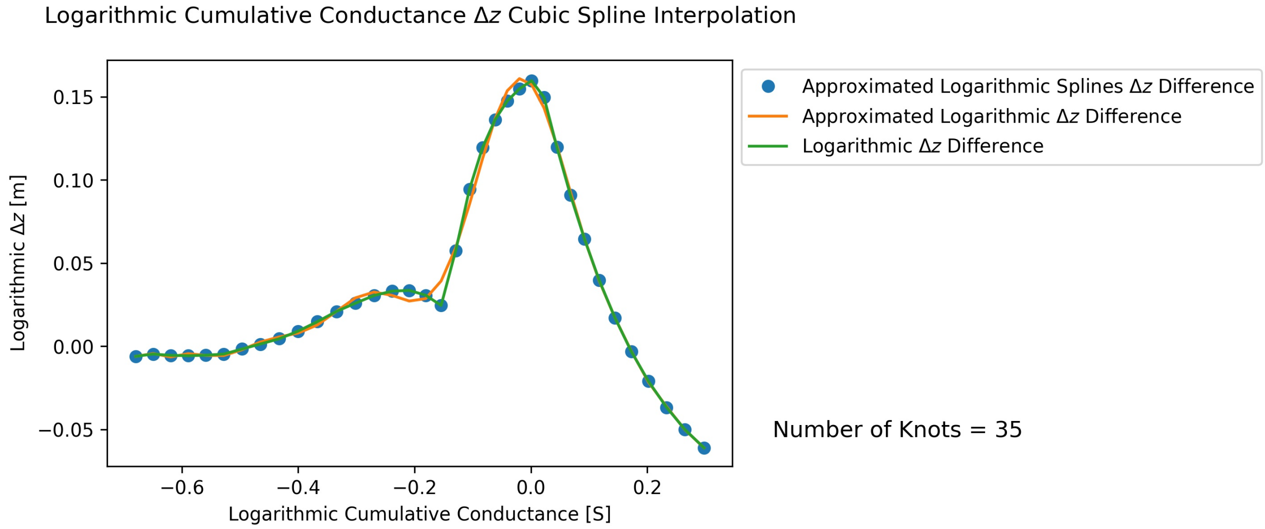

FIGURE 3.19: Cubic spline interpolation of the logarithmic representation of the ΔZ difference for the cumulative apparent conductance

Figures 3.18 and 3.19 shows that the cubic spline interpolation approximates the behavior of the Δz difference in a more accurate way compared to the behavior modeled by the logarithmic representation of the data.

3.7.4 Validation of the polynomials

To determine if the process used to determine the degree of the polynomial expression to be used mentioned in Chapter 3.7 provided the best approximation of the Δz difference a validation phase was performed. In this validation process different degrees for polynomial and different number of knots were used to generate different models for the Δz difference, then each model was used to generate the Δz difference and each approximation was compared to the real Δz difference.

The error between approximations was then compared, the results of the comparisons are reported in Tables 3.4 and 3.5.

TABLE 3.4: Cumulative resistivity error comparison between different polynomial approximations.

Cumulative Resistivity Polynomial Regression Analysis

Type of Data	**Degree / Knots Used**	**Cumulative Error %**	**Avg. Error %**
Proposed Methodology			
Linear	3	68	1.7
Logarithmic	10	40	1.07
Spline	37	0.28	0.007
Different Approximations			
Linear	6	269	6.9
Logarithmic	7	53	1.3
Spline	23	3.3	0.08
Different Approximations			
Linear	9	486	12
Logarithmic	13	44.2	1.13
Spline	14	34	0.9
Different Approximations			
Linear	15	781	20
Logarithmic	18	45	1.14
Spline	8	64	1.6

Table 3.5: Cumulative conductivity error comparison between different polynomial approximations.

Cumulative Conductivity Polynomial Regression Analysis

Type of Data	**Degree / Knots Used**	**Cumulative Error %**	**Avg. Error %**
	Proposed Methodology		
Linear	16	20.3	0.6
Logarithmic	15	19.4	0.55
Spline	35	0.34	0.009
	Different Approximations		
Linear	10	44	1.2
Logarithmic	10	56.1	1.5
Spline	8	193	5.3
	Different Approximations		
Linear	13	31.07	1.8
Logarithmic	12	39	1.0
Spline	20	3.2	0.09
	Different Approximations		
Linear	19	29	1.8
Logarithmic	18	20.4	0.6
Spline	13	31.01	0.9

Tables 3.4 and 3.5 confirmed that the process used to determine the degree of the polynomial expression to be used provided the best approximation to the Δz difference. The polynomial generated were used to obtained the Δz difference for the cumulative apparent resistivity and the cumulative apparent conductivity.

3.8 Depth Rescaling

The main proposition of this work is that the polynomial expressions previously defined can be used to correct the pseudo depth values for the existing Δz difference.

This Δz difference can be used to correct the average apparent depth value obtained for the cumulative apparent properties, which in theory will provide a depth-cumulative property model that describes the electrical settings present in the subsurface. The correction process was performed by means of

$$z_{Rescaled}(S) = z(S) + \Delta z(S) \qquad When\ S \approx S_a. \tag{3.10}$$

Once the depth is corrected a rescaled depth-cumulative apparent property model was generated, the results of this rescaled model are presented in Figures 3.20 and 3.21

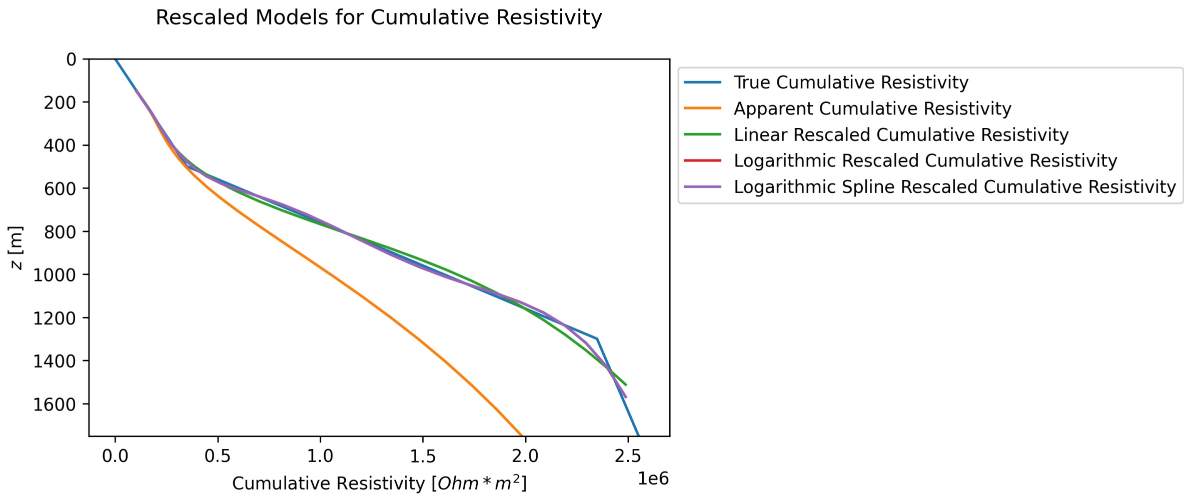

FIGURE 3.20: Rescaled cumulative resistivity models

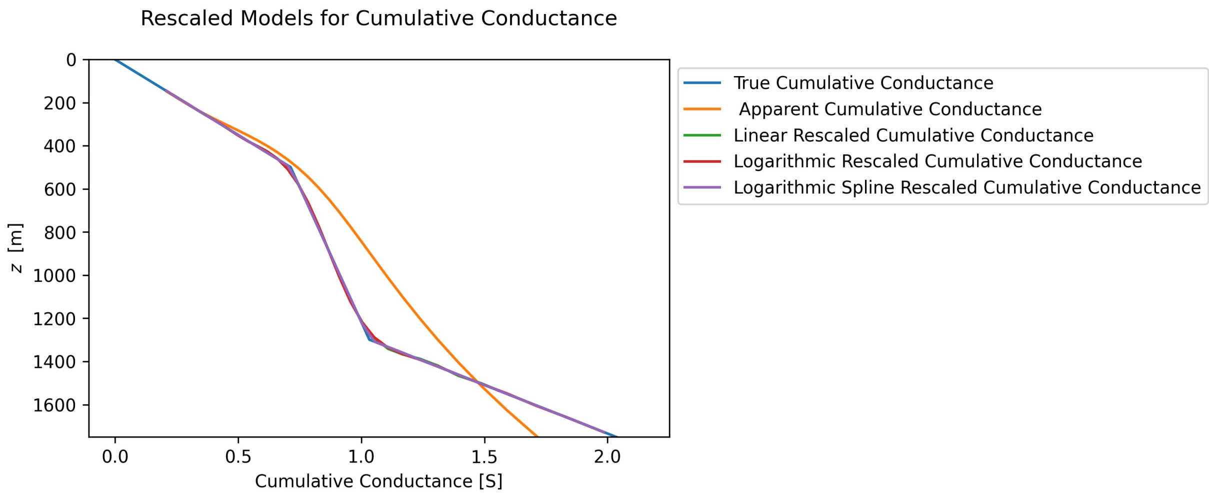

FIGURE 3.21: Rescaled cumulative conductance models

This rescaled models represent the cumulative electrical values for a certain depth in the subsurface, however, what is useful for us is not the cumulative electrical property. but the layered system present in the subsurface. For this reason to retrieve the layered system the following numerical derivative was used

$$\rho(i) = \frac{z_{Rescaled}(i+1) - z_{Rescaled}(i)}{\rho_c(i+1) - \rho_c(i)} \tag{3.11}$$

The layered systems recovered by using equation 3.11 are reported in Figures 3.22 and 3.23.

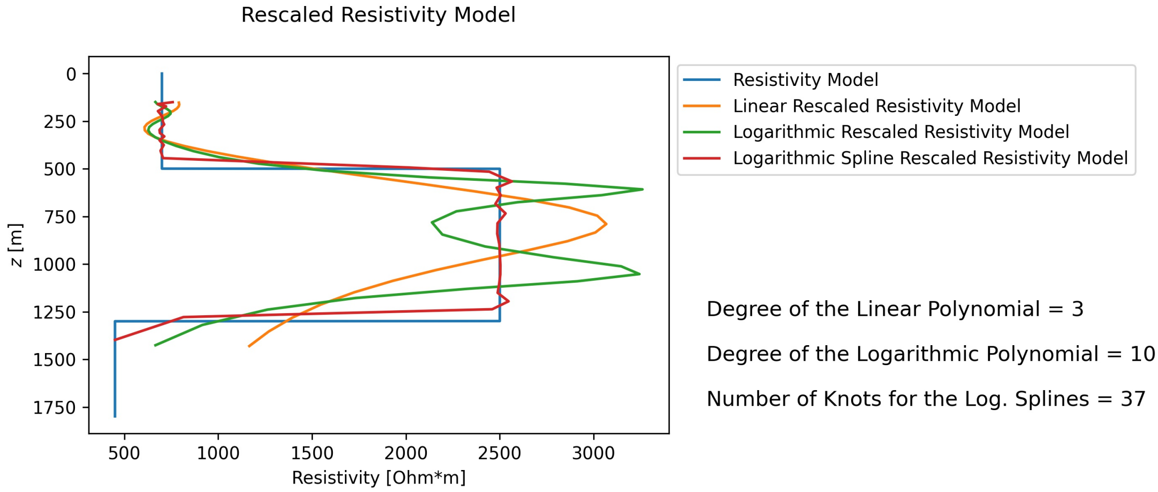

FIGURE 3.22: Rescaled resistivity models obtained by deriving the corrected cumulative resistivity models for the three different representations of the data. The model obtained by the logarithmic spline corrected data was the one that resembles the geological settings of the subsurface the most.

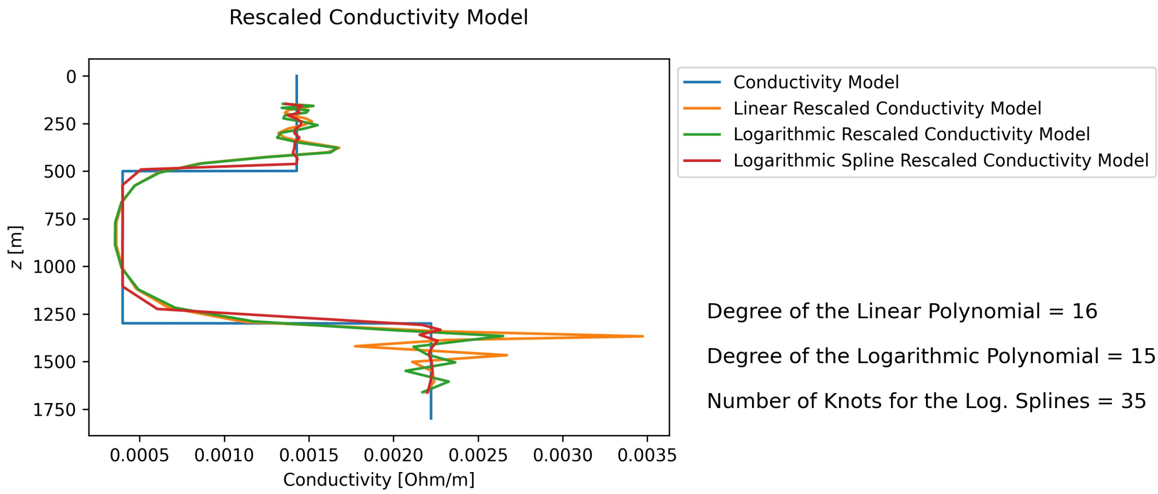

FIGURE 3.23: Rescaled conductivity models obtained by deriving the corrected cumulative conductivity models for the three different representations of the data. Similarly to the resistivity rescaled model, the model obtained by the logarithmic spline corrected data was the one that resembles the geological settings of the subsurface the most.

The error between the resistivity model and the rescaled model for each polynomial expression was computed by means of equations 3.3 and 3.4. The error for the rescaled models are reported in Table 3.6.

Table 3.6: Total and average error comparison for each polynomial used in the rescaling process of the resistivity model.

Rescaled Model Total Error %		
Linear Polynomial	**Logarithmic Polynomial**	**Cubic Splines Polynomial**
1493	741	437
Rescaled Model Average Error %		
Linear Polynomial	**Logarithmic Polynomial**	**Cubic Splines Polynomial**
35	18	11

Based on Figures 3.22 and 3.23 and in Table 3.6 the proposed method is able to retrieve the layered system present in the subsurface using apparent measurements from a MT survey and data from an exploratory well that allow us to correct the apparent measurements. The cubic splines interpolation provided the best approximation of the three polynomials used, however, all of the polynomials provided a good rescaled resistivity model.

One question that arises is if the polynomial expressions generated using exploratory data can be used to correct apparent measurements from nearby zones to the exploratory well in which only apparent measurements have been conducted. In theory, the area surrounding the exploratory well should have similar geological settings, however, some parameters might differ, for example the resistivity of the target layer might be different, also the depth at which the target layer can be found or the thickness of the target layer can be slightly different. For this reason, the polynomial expression generated by means of the exploratory data will be used to rescale apparent measurements originated from a different layered systems that present small variations compared to the geological settings found in the exploratory well to test if the proposed method can be applied as a more general rescaling tool.

Chapter 4

Results

The goal of this work is to obtain a polynomial expression that can be used to directly transform cumulative apparent measurements from Mt surveys into cumulative values. The methodology to obtain the mentioned mathematical expression has been described in detail in Chapter 3.

However, for the polynomial expression to be of practical use it should be able to transform cumulative apparent measurements into cumulative measurements from zones in which the geological settings are slightly different from the ones used to create this expression. To test if the polynomials obtained can perform this task, small perturbations will be applied to different resistivity models (two synthetic models and one real case) modifying resistivity, thickness and location of the target layer.

The rescaled geological models obtained will be compared with the expected geological models to determine if the proposed method can perform the expected rescaling process. In this chapter only the most representative cases for the testing phase will be displayed.

4.1 Testing Phase

The proposition of this work is to determine the relationship between apparent measurements form a MT survey and local data from an exploratory well (like resistivity logs) by means of a polynomial expression. To make this of practical use the polynomial expression derived will be used to retrieve the layered system in areas in which only apparent measurements have been conducted and the geological model is unknown. For the testing phase it is assumed that the areas nearby where the polynomial was estimated will have mild variations in the geological settings with respect the ones at the exploratory well.

To determine if the polynomial can work as a more general rescaling tool a series of tests were performed. For each test a geological model was defined and the apparent resistivity measured at the surface was simulated using a modeling tool, then using the apparent measurements and the local measurements the polynomial expression was obtained following the steps seen in Chapter 3, after that the model is perturbed and apparent measurements are obtained, finally using the polynomial previously retrieved the apparent data coming from the disturbed model is rescaled to directly obtain a geological. If the rescaled model is similar enough compared to the disturbed model then it can be said that the proposed methodology can be used as a rescaling tool.

The proposed method was tested in two different geological settings and for each layered system a disturbed model was generated varying one of the following parameters.

- Resistivity of the target layer.
  - From -100 % up to 100 % Difference in 10 % Intervals
- Thickness of the target layer.
  - From -100 % up to 50 % Difference in 10 % Intervals
- Position of the target layer.
  - From -50 % up to 100 % Difference in 10 % Intervals

Additionally a real case for monitoring purposes was included. The goal of the real case was to monitor the variation in resistivity in a specific layer due to the injection of water in a geothermal field.

For sake of simplicity only the more significant rescaled resistivity models are presented in this work, there is an online repository that contains all the results derived from the testing phase, the link to access the repository is provided at the end of this work.

4.2 3 Layers High Contrast Resistivity Model

The first reference model was the one reported in Figure 3.2. This model is a 3 layer system with a high resistivity layer in the middle, the properties of the model are reported in Table 4.1

Table 4.1: Electrical parameters for the 3 layer reference model.

Resistivity [Ohm*m]	**Conductivity [Ohm/m]**	**Thickness of the Layer [m]**
750	1.3x10^{-3}	500
2500	4x10^{-4}	800
450	2.2x10^{-3}	Half Space

The results of the polynomial rescaling process for the reference model are displayed in Figures 3.22 and 3.23. The testing phase used the three polynomials retrieved for the three representations of the data as described in Chapter 3, one for the data without any modification, one for the logarithmic representation for the data and the one obtained using cubic splines for the logarithmic representation of the data.

4.2.1 Resistivity Variation

The first test was performed by applying resistivity variations to the reference model. The perturbations applied are reported in Table 4.2.

Table 4.2: Resistivity perturbations applied to the target layer of the 3 layer model.

Resistivity Perturbations		
Original Value	**Disturbed Value**	**Difference %**
2500 [Ohm*m]	1250 [Ohm*m]	-50%
	3750 [Ohm*m]	50%

The results for the resistivity perturbation are displayed in Figures 4.1 and 4.2 respectively. Each figure display the results using the three polynomials obtained and in each figure is displayed the original layer model (blue line), the rescaled original model (dashed blue line), the disturbed model that is unknown (orange line) and the rescaled disturbed model retrieved (dashed orange line). Figure 4.1 shows the results of the testing phase for a resistivity perturbation of -50%.

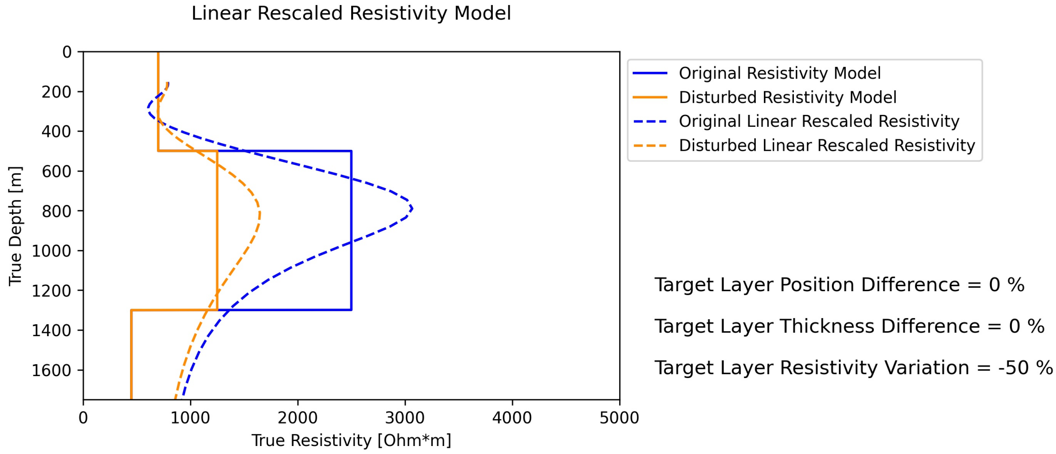

(a) Rescaled model for a 3 layer system with -50 % resistivity variation compared with the original model using the polynomial expression obtained without applying any change to the apparent data.

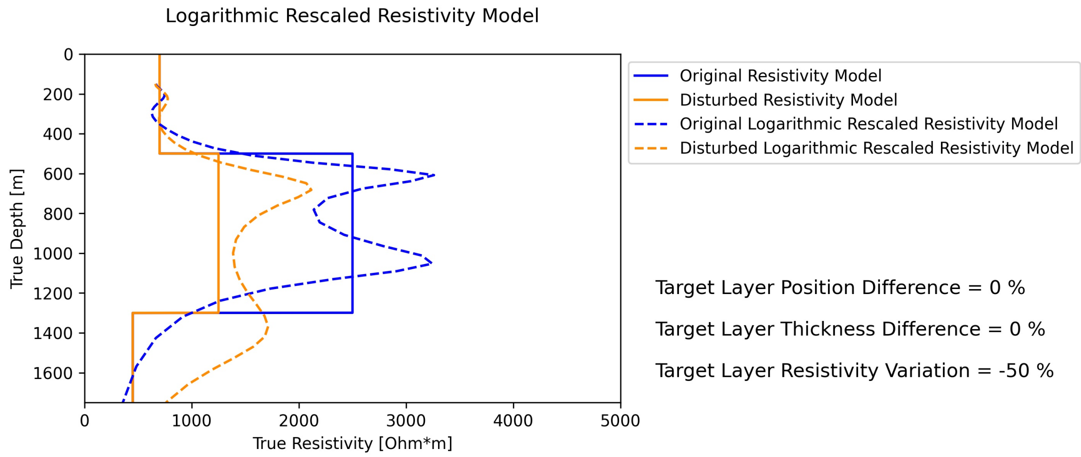

(b) Rescaled model for a 3 layer system with -50 % resistivity variation compared with the original model using the polynomial expression obtained for the logarithmic representation of the data.

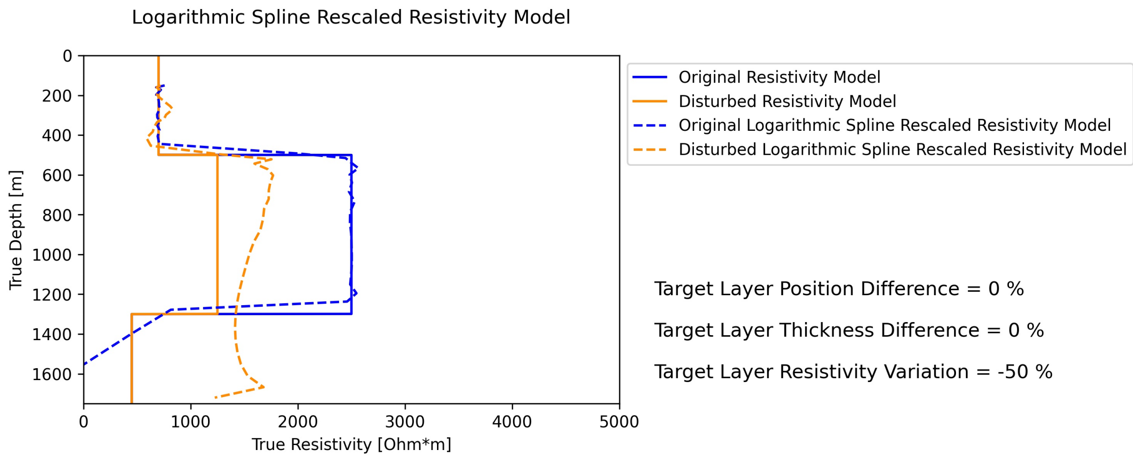

(c) Rescaled model for a 3 layer system with -50 % resistivity variation compared with the original model using the polynomial expression obtained by using cubic splines for the logarithmic representation of the data.

FIGURE 4.1: Comparison between the three rescaling process using different polynomials for a -50% variation in the resistivity of the target layer of the 3 layer system.

To compare the quality of each rescaled model the total error and the average error were obtained using Equations 3.3 and 3.4 respectively. Table 4.3 shows the error comparison between the polynomials used to obtained the rescaled model for a resistivity variation of -50 %.

TABLE 4.3: Total and average error comparison for each polynomial used in the rescaling process for the -50% resistivity 3 layer disturbed model.

Rescaled Model Total Error %		
Linear Polynomial	**Logarithmic Polynomial**	**Cubic Splines Polynomial**
1537	2353	2549
Rescaled Model Average Error %		
Linear Polynomial	**Logarithmic Polynomial**	**Cubic Splines Polynomial**
38	54	59

Figure 4.2 shows the results of the testing phase for a resistivity perturbation of 50%.

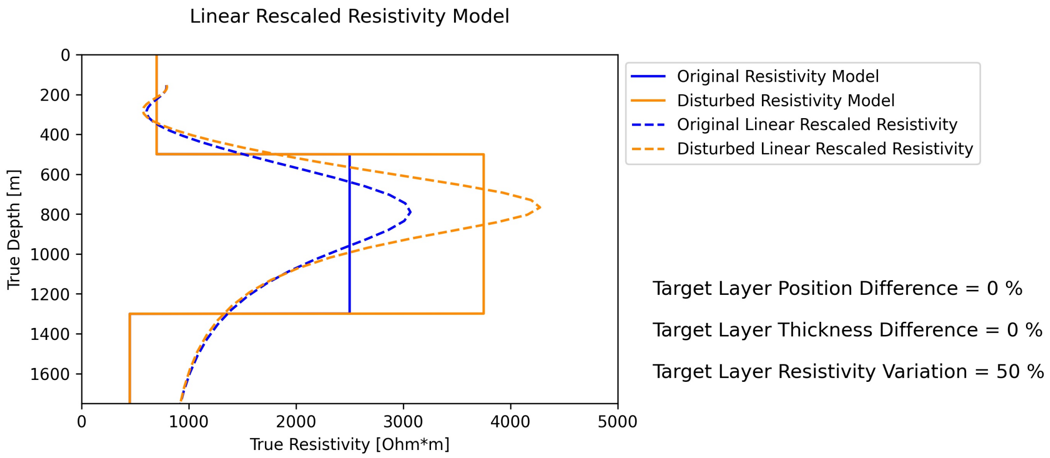

(a) Rescaled model for a 3 layer system with 50 % resistivity variation compared with the original model using the polynomial expression obtained without applying any change to the apparent data.

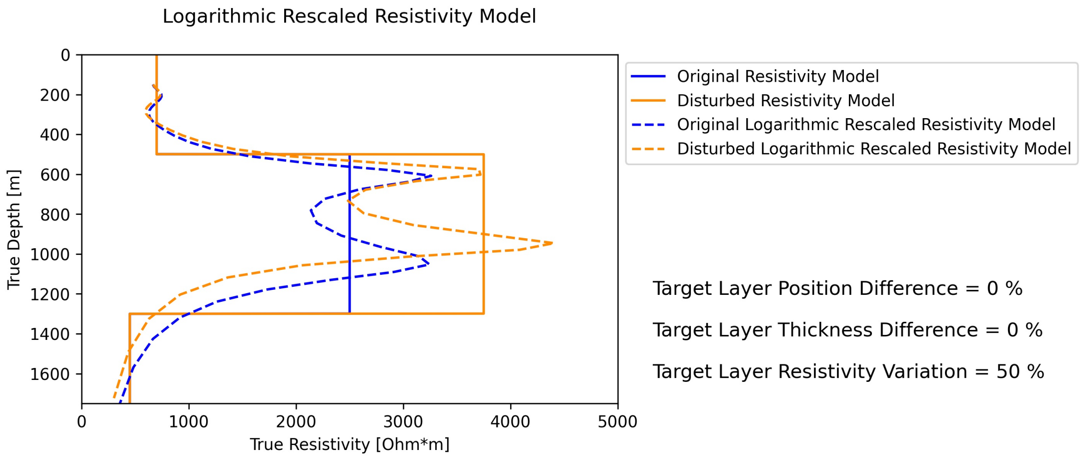

(b) Rescaled model for a 3 layer system with 50 % resistivity variation compared with the original model using the polynomial expression obtained for the logarithmic representation of the data.

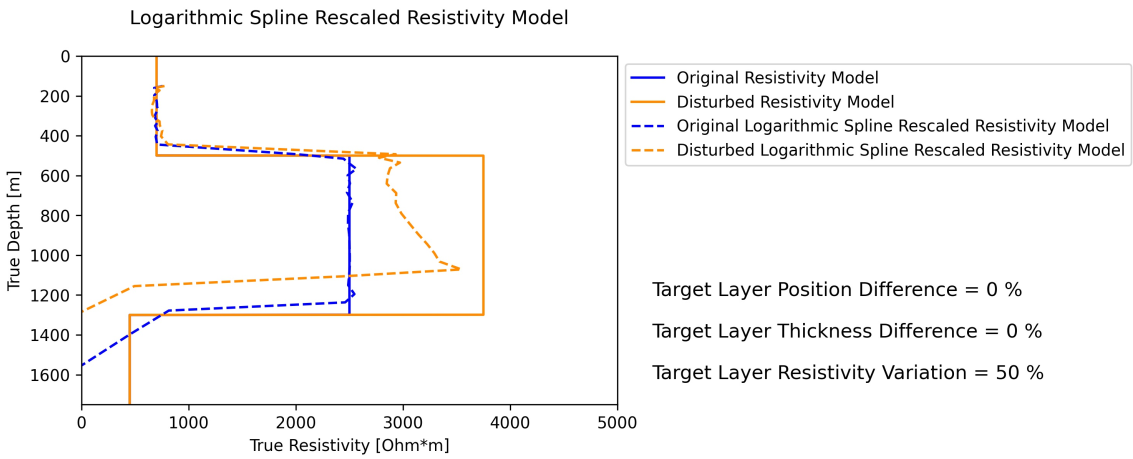

(c) Rescaled model for a 3 layer system with -50 % resistivity variation compared with the original model using the polynomial expression obtained by using cubic splines for the logarithmic representation of the data.

FIGURE 4.2: Comparison between the three rescaling process using different polynomials for a 50% variation in the resistivity of of the target layer of the 3 layer system.

Table 4.4 shows the error comparison between the polynomials used to obtained the rescaled model for a resistivity variation of 50 %.

TABLE 4.4: Total and average error comparison for each polynomial used in the rescaling process for the 50% resistivity 3 layer disturbed model.

Rescaled Model Total Error %		
Linear Polynomial	**Logarithmic Polynomial**	**Cubic Splines Polynomial**
1883	921	992
Rescaled Model Average Error %		
Linear Polynomial	**Logarithmic Polynomial**	**Cubic Splines Polynomial**
43	24	27

Figures 4.1 and 4.2 shows that the proposed method can track the resistivity variation up to a certain degree, however the change in rescaled resistivity is not proportional to the change in real resistivity, this implies that an increasing resistivity might be underestimated, whereas a decreasing resistivity might be overestimated. The rescaled resistivity is different from the expected resistivity for a percentage $\approx 30\%$ to overcome this outcome a more detailed study might help to determine the ratio in which the resistivity is over or under estimated to properly retrieve the resistivity values at the subsurface.

4.2.2 Thickness Variation

The second test was performed by applying thickness variations to the reference model. The perturbations applied are reported in Table 4.5.

TABLE 4.5: Thickness perturbations applied to the target layer of the 3 layer model

Thickness Perturbations		
Original Value	**Disturbed Value**	**Difference %**
800 [m]	400 [m]	-50%
	1200 [m]	50%

The results for the thickness perturbation are displayed in Figures 4.3 and 4.4 respectively. Figure 4.3 shows the results of the testing phase for a thickness perturbation of -50%.

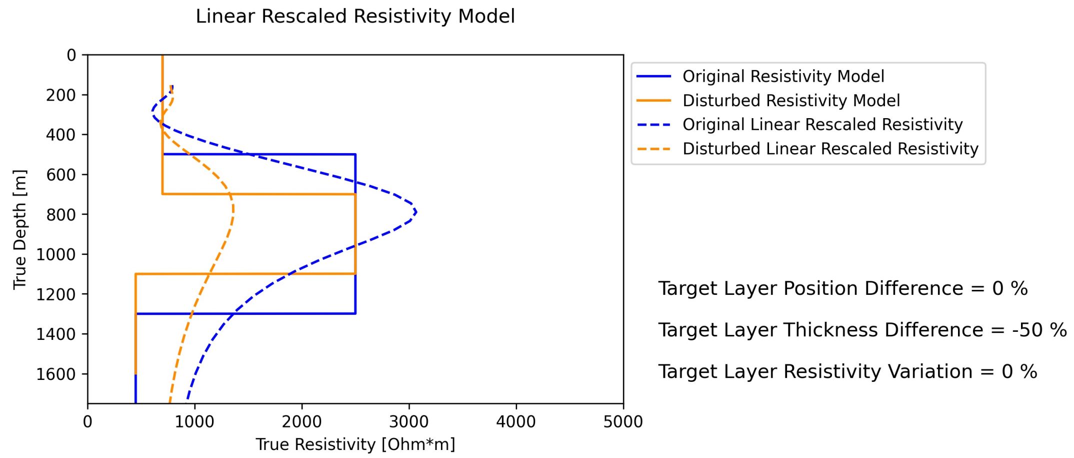

(a) Rescaled model for a 3 layer system with -50 % thickness variation compared with the original model using the polynomial expression obtained without applying any change to the apparent data.

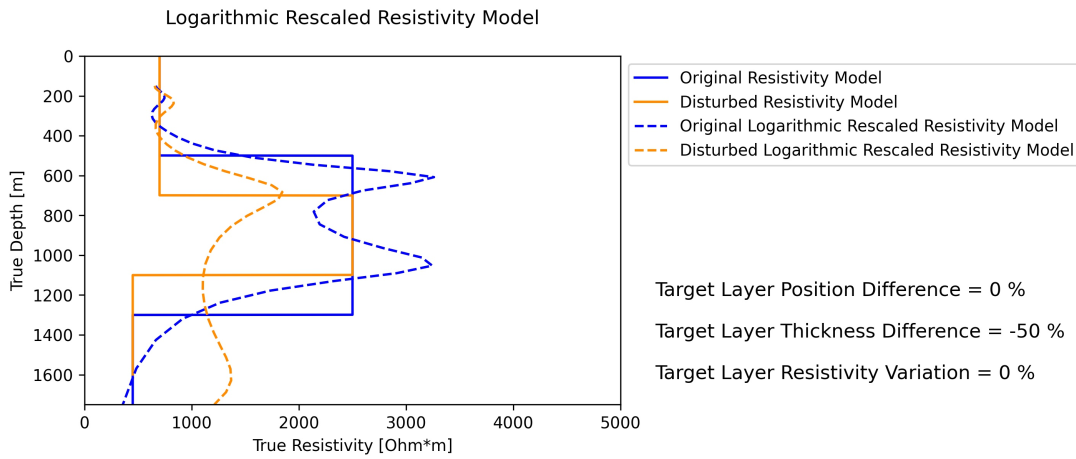

(b) Rescaled model for a 3 layer system with -50 % thickness variation compared with the original model using the polynomial expression obtained for the logarithmic representation of the data.

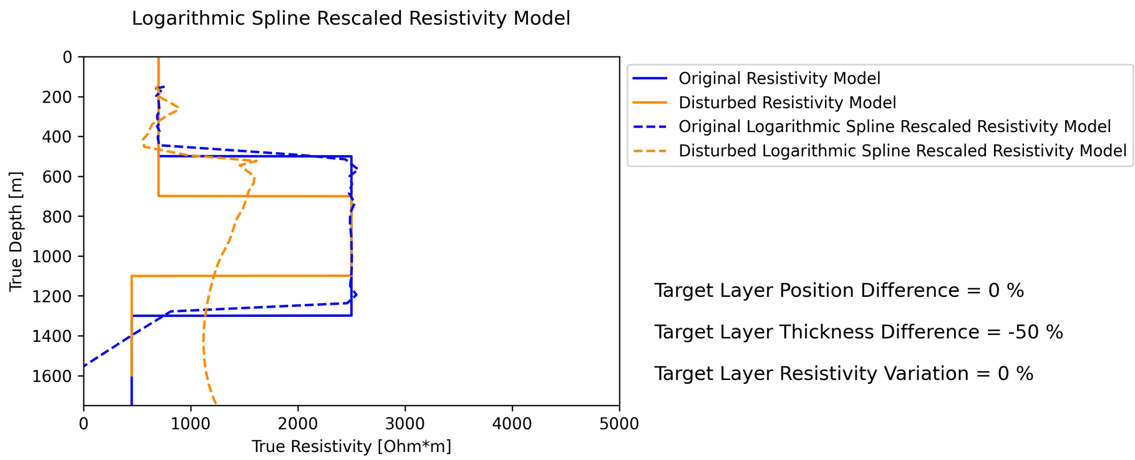

(c) Rescaled model for a 3 layer system with -50 % thickness variation compared with the original model using the polynomial expression obtained by using cubic splines for the logarithmic representation of the data.

Figure 4.3: Comparison between the three rescaling process using different polynomials for a -50% variation in the thickness of the target layer of the 3 layer system. The original layer model is represented by the blue line, the rescaled original model by dashed blue line, the disturbed model that is unknown by the orange line, and the rescaled disturbed model retrieved is represented by the dashed orange line.

Table 4.6 shows the error comparison between the polynomials used to obtained the rescaled model for a thickness variation of -50 %.

TABLE 4.6: Total and average error comparison for each polynomial used in the rescaling process for the -50% thickness 3 layer disturbed model.

Rescaled Model Total Error %		
Linear Polynomial	**Logarithmic Polynomial**	**Cubic Splines Polynomial**
1485	2359	2200
Rescaled Model Average Error %		
Linear Polynomial	**Logarithmic Polynomial**	**Cubic Splines Polynomial**
37	54	51

Figure 4.4 shows the results of the testing phase for a thickness perturbation of 50%.

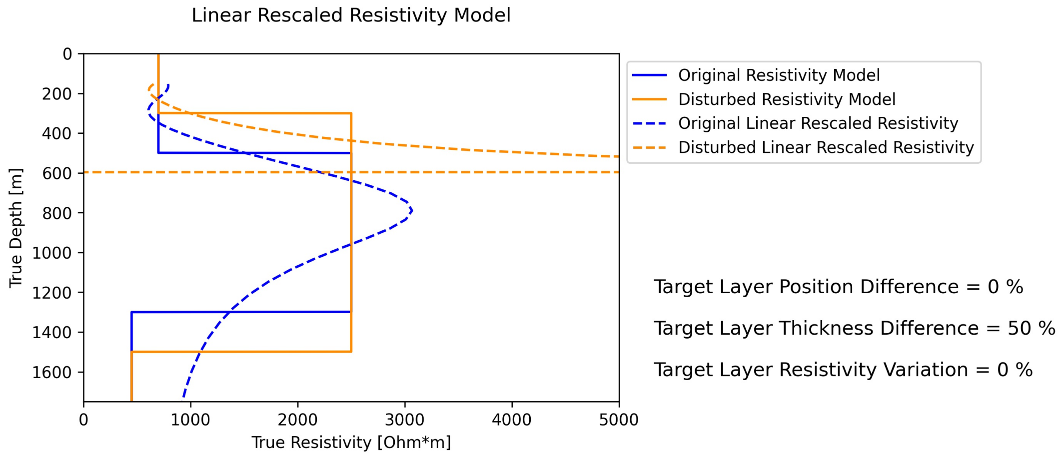

(a) Rescaled model for a 3 layer system with 50 % thickness variation compared with the original model using the polynomial expression obtained without applying any change to the apparent data.

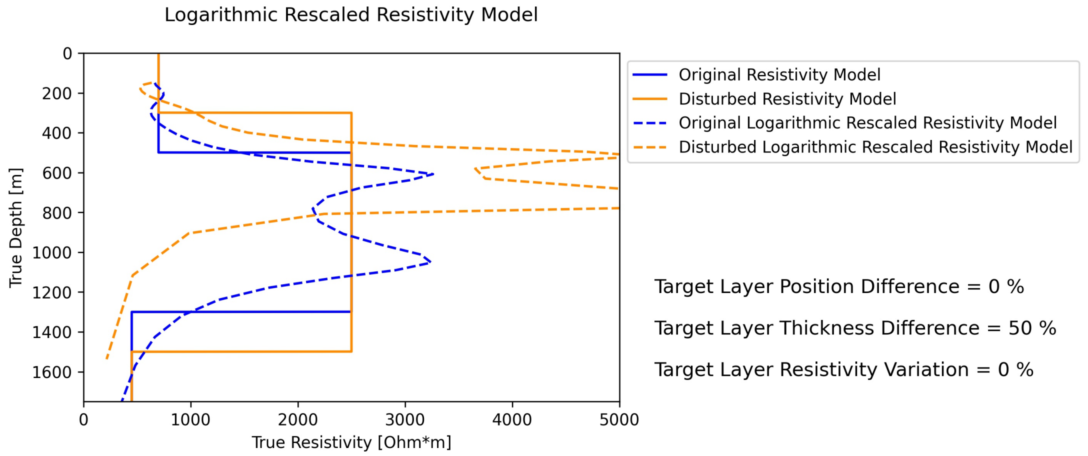

(b) Rescaled model for a 3 layer system with 50 % thickness variation compared with the original model using the polynomial expression obtained for the logarithmic representation of the data.

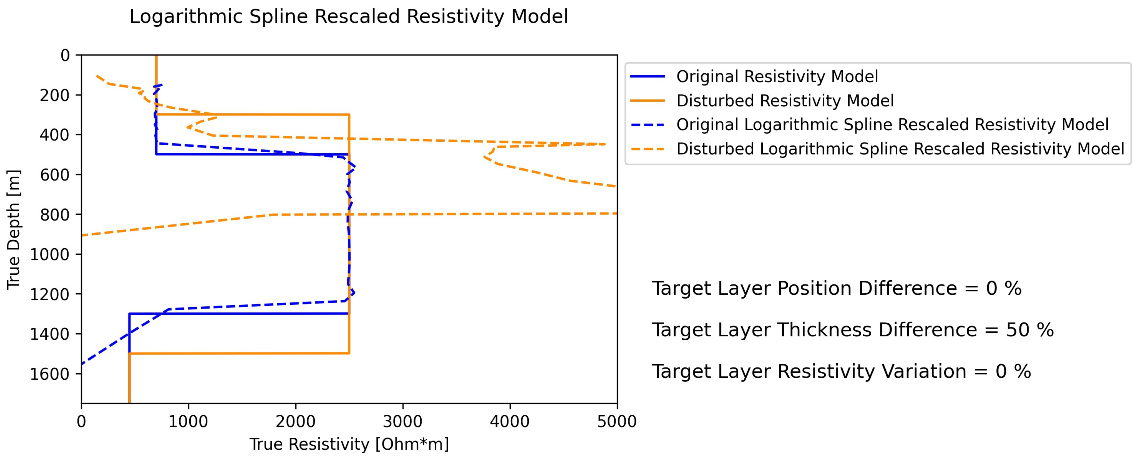

(c) Rescaled model for a 3 layer system with 50 % thickness variation compared with the original model using the polynomial expression obtained by using cubic splines for the logarithmic representation of the data.

FIGURE 4.4: Comparison between the three rescaling process using different polynomials for a 50% variation in the thickness of the target layer of the 3 layer system. The original layer model is represented by the blue line, the rescaled original model by dashed blue line, the disturbed model that is unknown by the orange line, and the rescaled disturbed model retrieved is represented by the dashed orange line.

Table 4.7 shows the error comparison between the polynomials used to obtained the rescaled model for a thickness variation of 50 %.

TABLE 4.7: Total and average error comparison for each polynomial used in the rescaling process for the 50% thickness 3 layer disturbed model.

Rescaled Model Total Error %		
Linear Polynomial	**Logarithmic Polynomial**	**Cubic Splines Polynomial**
30033	3107	3395
Rescaled Model Average Error %		
Linear Polynomial	**Logarithmic Polynomial**	**Cubic Splines Polynomial**
1001	100	117

Figures 4.3 and 4.4 shows that the proposed method cannot retrieve a change in thickness; in this case an increase of the thickness is retrieved as an increase in resistivity, and vice versa, in real applications this differences can be misleading and might lead to wrong interpretations of the subsurface.

4.2.3 Position Variation

The third test was performed by applying variations to the position of the target layer in the 3 layer model. The perturbations applied are reported in Table 4.8.

TABLE 4.8: Position perturbations of the target layer applied to the 3 layer model

Position Perturbations		
Original Value	**Disturbed Value**	**Difference %**
Located at 500 [m]	Located at 250 [m]	-50%
	Located at 750 [m]	50%

The results for the variation of the position of the target layer are displayed in Figures 4.5 and 4.6 respectively. Figure 4.5 shows the results of the testing phase for a variation of the location of the target layer by -50%.

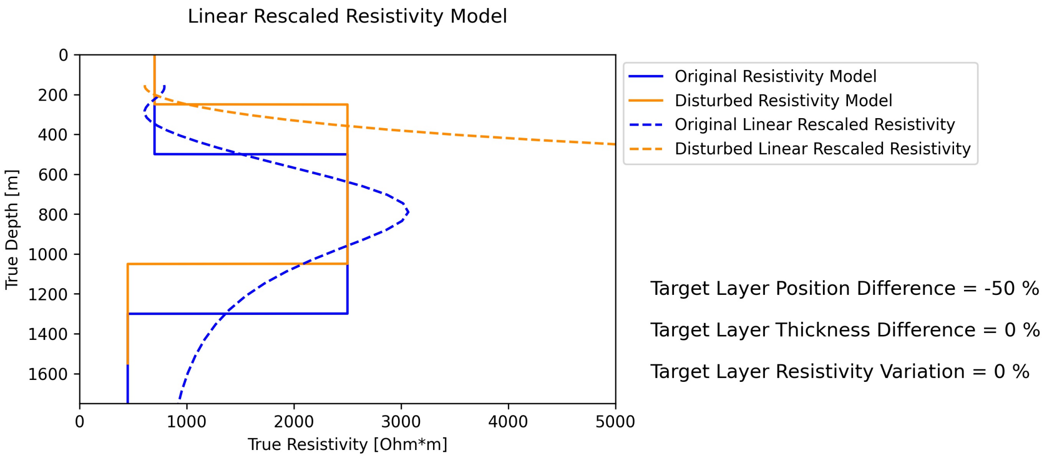

(a) Rescaled model for a 3 layer system with -50 % variation in the position of the target layer compared with the original model using the polynomial expression obtained without applying any change to the apparent data.

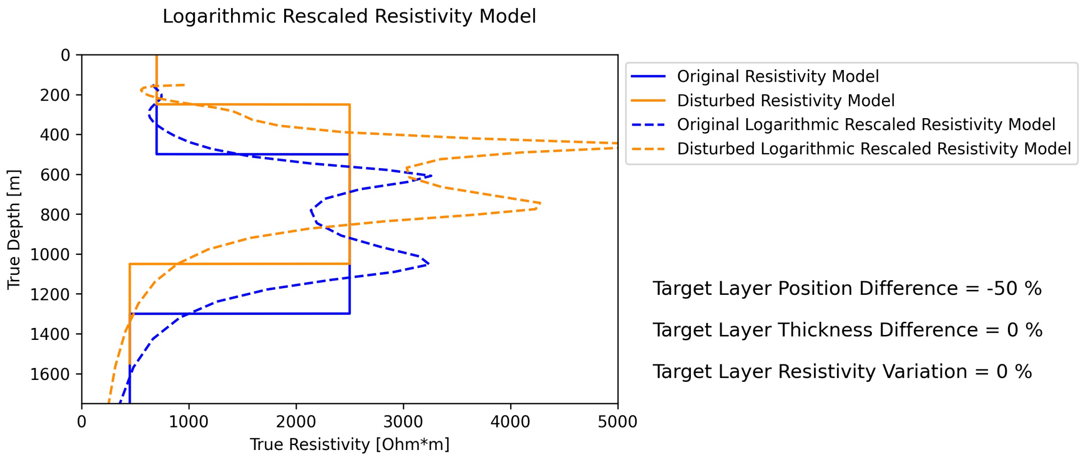

(b) Rescaled model for a 3 layer system with -50 % variation in the position of the target layer compared with the original model using the polynomial expression obtained for the logarithmic representation of the data.

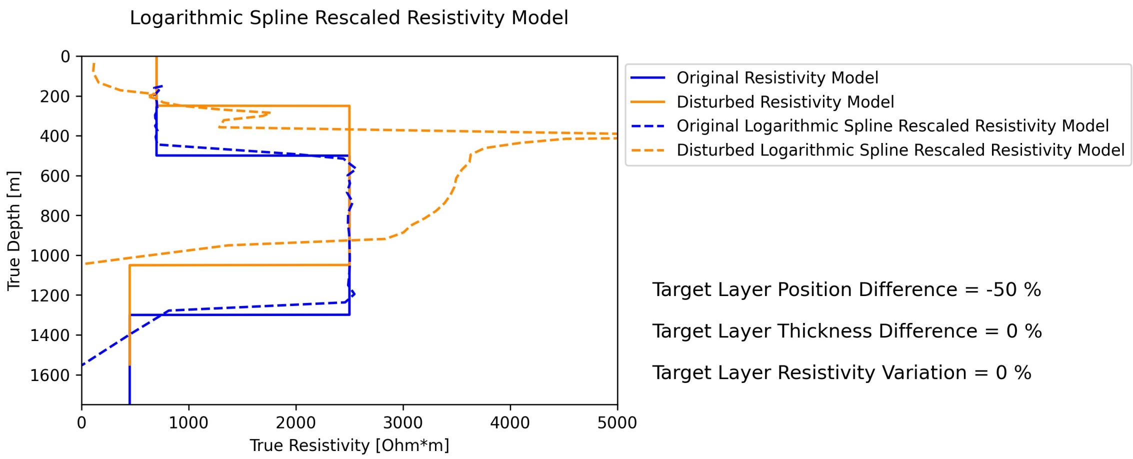

(c) Rescaled model for a 3 layer system with -50 % variation in the position of the target layer compared with the original model using the polynomial expression obtained by using cubic splines for the logarithmic representation of the data.

Figure 4.5: Comparison between the three rescaling process using different polynomials for a -50% variation in the position of the target layer of the 3 layer model. The original layer model is represented by the blue line, the rescaled original model by dashed blue line, the disturbed model that is unknown by the orange line, and the rescaled disturbed model retrieved is represented by the dashed orange line.

Table 4.9 shows the error comparison between the polynomials used to obtained the rescaled model for a position variation of the target layer by -50 %.

TABLE 4.9: Total and average error comparison for each polynomial used in the rescaling process for the variation of -50% in the position of the target layer for the 3 layer model.

Rescaled Model Total Error %		
Linear Polynomial	**Logarithmic Polynomial**	**Cubic Splines Polynomial**
4335	3932	4297
Rescaled Model Average Error %		
Linear Polynomial	**Logarithmic Polynomial**	**Cubic Splines Polynomial**
180	106	130

Figure 4.6 shows the results of the testing phase for a variation of the location of the target layer by 50%.

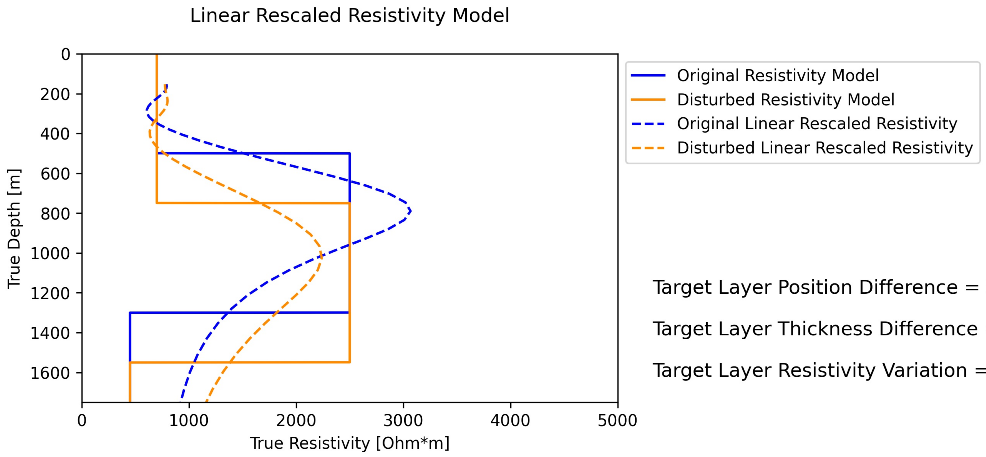

(a) Rescaled model for a 3 layer system with 50 % variation in the position of the target layer compared with the original model using the polynomial expression obtained without applying any change to the apparent data.

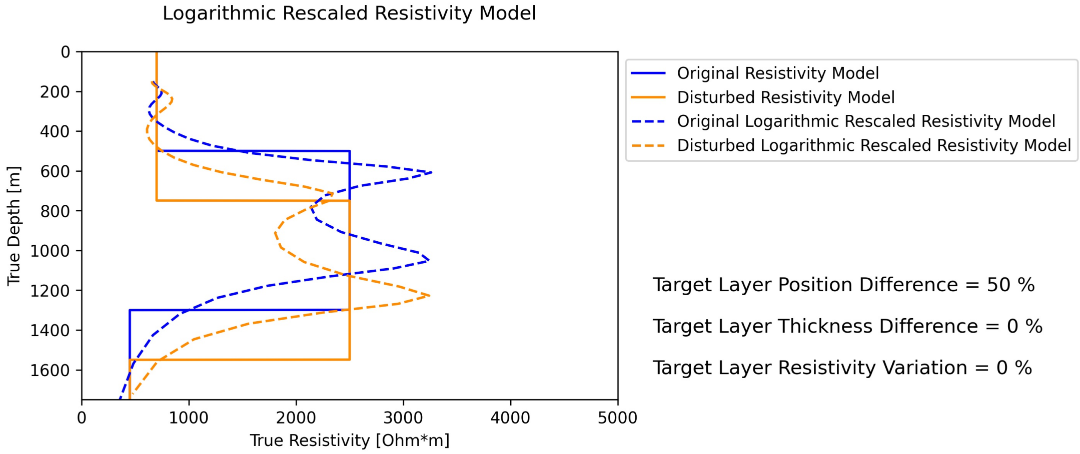

(b) Rescaled model for a 3 layer system with 50 % variation in the position of the target layer compared with the original model using the polynomial expression obtained for the logarithmic representation of the data.

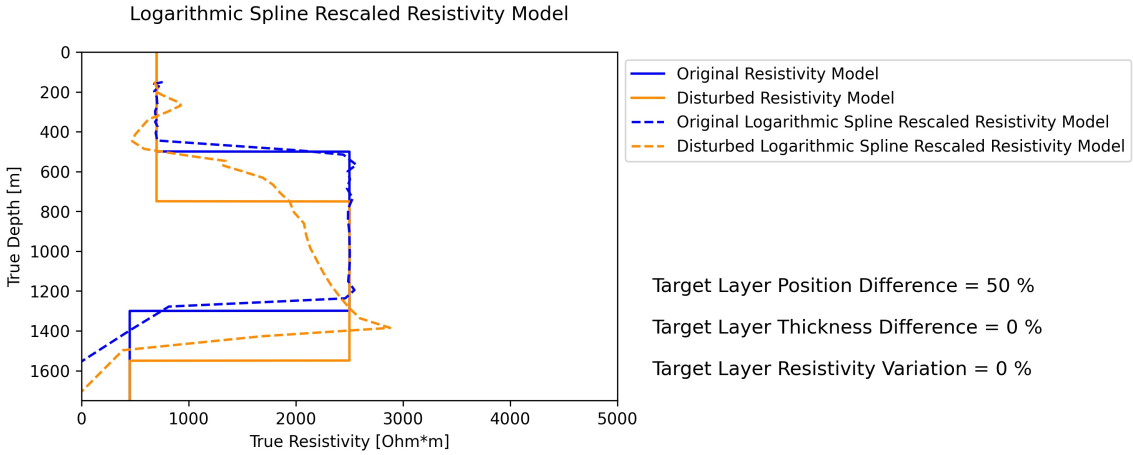

(c) Rescaled model for a 3 layer system with 50 % variation in the position of the target layer compared with the original model using the polynomial expression obtained by using cubic splines for the logarithmic representation of the data.

FIGURE 4.6: Comparison between the three rescaling process using different polynomials for a -50% variation in the position of the target layer of the 3 layer model. The original layer model is represented by the blue line, the rescaled original model by dashed blue line, the disturbed model that is unknown by the orange line, and the rescaled disturbed model retrieved is represented by the dashed orange line.

Table 4.10 shows the error comparison between the polynomials used to obtained the rescaled model for a position variation of the target layer by 50 %.

Table 4.10: Total and average error comparison for each polynomial used in the rescaling process for the variation of 50% in the position of the target layer of the 3 layer model.

Rescaled Model Total Error %		
Linear Polynomial	**Logarithmic Polynomial**	**Cubic Splines Polynomial**
1914	1513	2121
Rescaled Model Average Error %		
Linear Polynomial	**Logarithmic Polynomial**	**Cubic Splines Polynomial**
46	36	51

Figures 4.5 and 4.6 shows that the proposed method is capable of tracking the position changes in a simple scenario, this might be helpful in cases in which the target layer is varying its position along the field of study.

At first glance it seems that the proposed method is capable of rescaling changes in the resistivity and position of the target layer for a high contrast resistivity model as shown in Figure 3.2. Nonetheless, in reality usually the changes in the electrical properties of the subsurface are more subtle, for this reason, the proposes method was tested in a more realistic model in which the changes between resistivities are smoother.

4.3 Five Layer Low Contrast Resistivity Model

The model shown in Figure 3.2 is a high contrast resistivity model, however, in reality the resistivity contrast between layers tend to be more subtle, for this reason a second resistivity model was used to test the applicability of the proposed rescaling tool. The new model has 5 layers diminishing the resistivity contrast and the thickness of the layers. The parameters for this resistivity model are reported in Table 4.11 and in Figure 4.7.

Table 4.11: Low contrast resistivity and conductivity model parameters.

Resistivity [Ohm*m]	**Conductivity [Ohm/m]**	**Thickness [m]**
750	1.3x10^{-3}	500
1500	6.6x10^{-4}	300
2800	3.57x10^{-4}	300
1050	9.52x10^{-4}	300
450	2.22x10^{-3}	Half Space

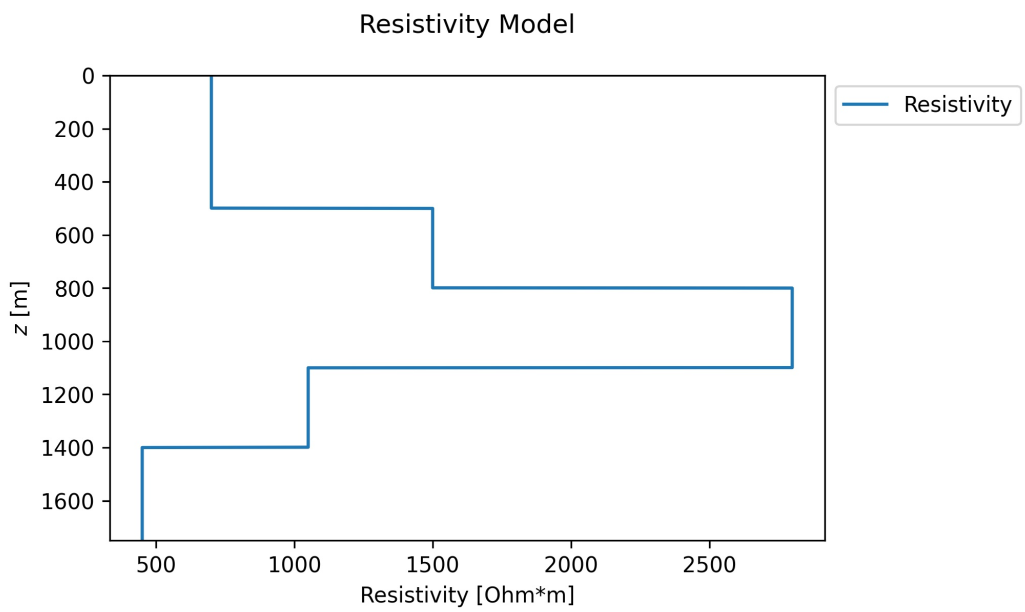

Figure 4.7: 5 layer low contrast resistivity model.

Using the model shown in Figure 4.7 apparent measurements were simulated and using the methodology described in Chapter 3 a polynomial expression able to correct the differences between apparent measurements was obtained for the representation of the data without any change, for the logarithmic representation for the data, and also a cubic spline interpolation was obtained for the logarithmic representation of the data.

Once the differences between apparent and local measurements were corrected a rescaled model was obtained by means of Equation 3.11 for each representation of the data. The rescaled models obtained are reported in Figures 4.8 and 4.9.

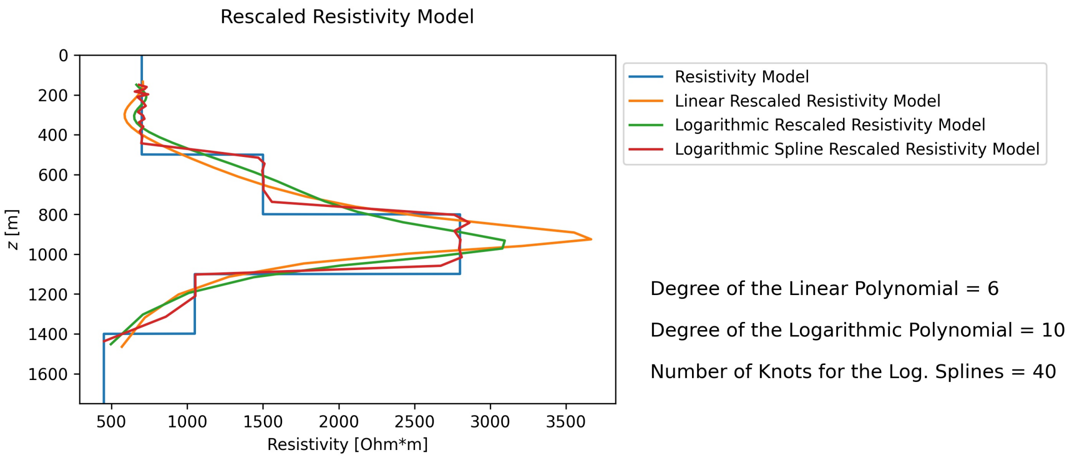

FIGURE 4.8: 5 layer rescaled resistivity models obtained by deriving the corrected cumulative resistivity models for the model shown in Figure 4.7 for the three different representations of the data. The model obtained by the logarithmic spline corrected data was the one that resembles the geological settings of the subsurface the most.

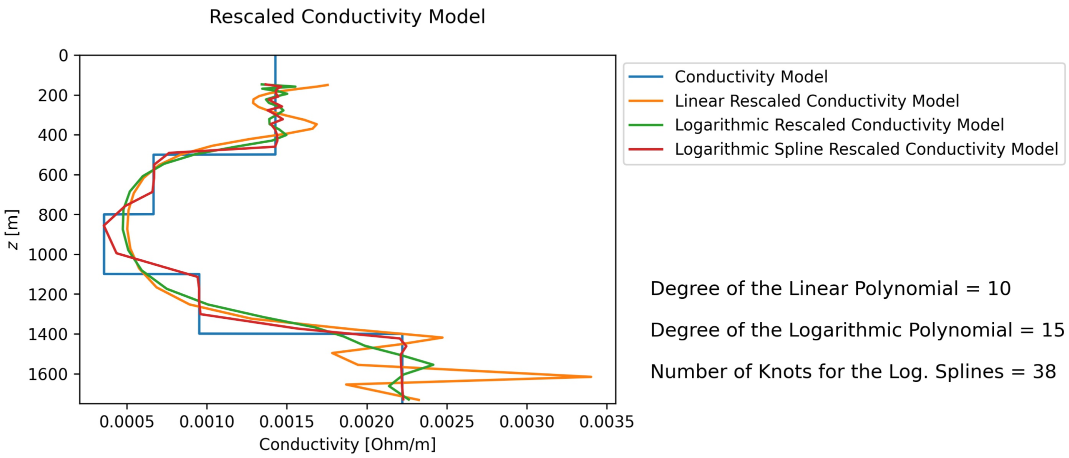

FIGURE 4.9: 5 layer rescaled conductivity models obtained by deriving the conductivity models for the for the model shown in Figure 4.7 three different representations of the data. Similarly to the resistivity rescaled model, the model obtained by the logarithmic spline corrected data was the one that resembles the geological settings of the subsurface the most.

To determine the quality of the rescaling process the total and average error between the resistivity model and the rescaled model for each polynomial expression was obtained using equations 3.3 and 3.4. The error for the rescaled models are reported in Table 3.6.

Table 4.12: Total and average error comparison for each polynomial used in the rescaling process of the resistivity model for the 5 layer system.

Rescaled Model Total Error %		
Linear Polynomial	**Logarithmic Polynomial**	**Cubic Splines Polynomial**
527	458	197
Rescaled Model Average Error %		
Linear Polynomial	**Logarithmic Polynomial**	**Cubic Splines Polynomial**
14	12	5

Similarly to the errors shown in Table 3.6 the rescaled model obtained by using the cubic spline interpolation provided the best approximation to the geological settings present in the subsurface.

Also for the resistivity model shown in Figure 4.7, the testing phases included variations to the resistivity, thickness and location of the target layer.

4.3.1 5 Layer System Resistivity Variation

The first test was performed by applying resistivity variations to the reference model shown in Figure 4.7. The perturbations applied are reported in Table 4.24.

Table 4.13: Resistivity perturbations applied to the target layer of the 5 layer model

Resistivity Perturbations		
Original Value	**Disturbed Value**	**Difference %**
2800 [Ohm*m]	1400 [Ohm*m]	-50%
	4200 [Ohm*m]	50%

The results for the resistivity perturbation are displayed in Figures 4.10 and **??** respectively. Each figure display the results using the three polynomials obtained and in each figure is displayed the original layer model (blue line), the rescaled original model (dashed blue line), the disturbed model that is unknown (orange line) and the rescaled disturbed model retrieved (dashed orange line). Figure 4.10 shows the results of the testing phase for a resistivity perturbation of -50%.

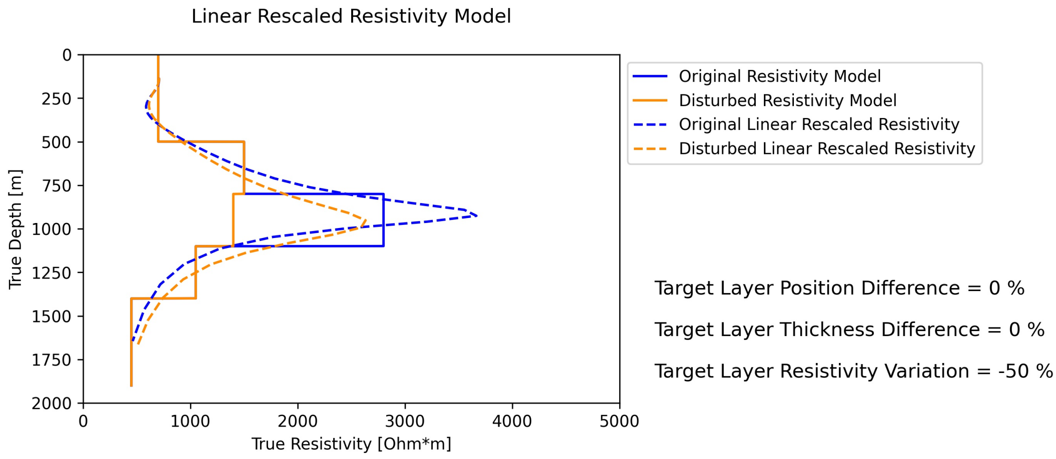

(a) Rescaled model for a 5 layer system with -50 % resistivity variation compared with the original model using the polynomial expression obtained without applying any change to the apparent data.

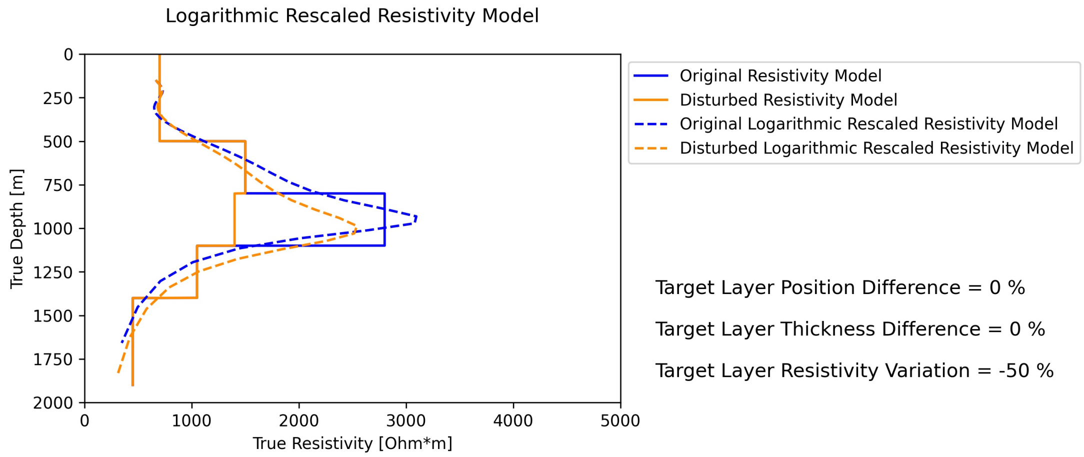

(b) Rescaled model for a 5 layer system with -50 % resistivity variation compared with the original model using the polynomial expression obtained for the logarithmic representation of the data.

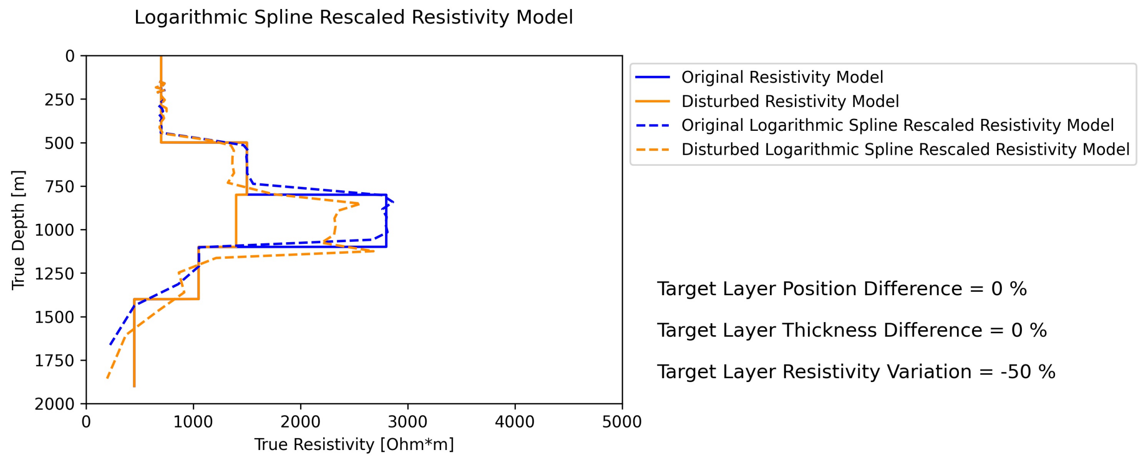

(c) Rescaled model for a 5 layer system with -50 % resistivity variation compared with the original model using the polynomial expression obtained by using cubic splines for the logarithmic representation of the data.

FIGURE 4.10: Comparison between the three rescaling process using different polynomials for a -50% variation in the resistivity of the target layer of the 5 layer resistivity model.

Table 4.14 shows the error comparison between the polynomials used to obtained the rescaled model for a resistivity variation of -50 % for the 5 layer system.

TABLE 4.14: Total and average error comparison for each polynomial used in the rescaling process for the -50% resistivity disturbed 5 layer model.

Rescaled Model Total Error %		
Linear Polynomial	**Logarithmic Polynomial**	**Cubic Splines Polynomial**
611	537	390
Rescaled Model Average Error %		
Linear Polynomial	**Logarithmic Polynomial**	**Cubic Splines Polynomial**
16	14	10

Figure 4.11 shows the results of the testing phase for a resistivity perturbation of 50%.

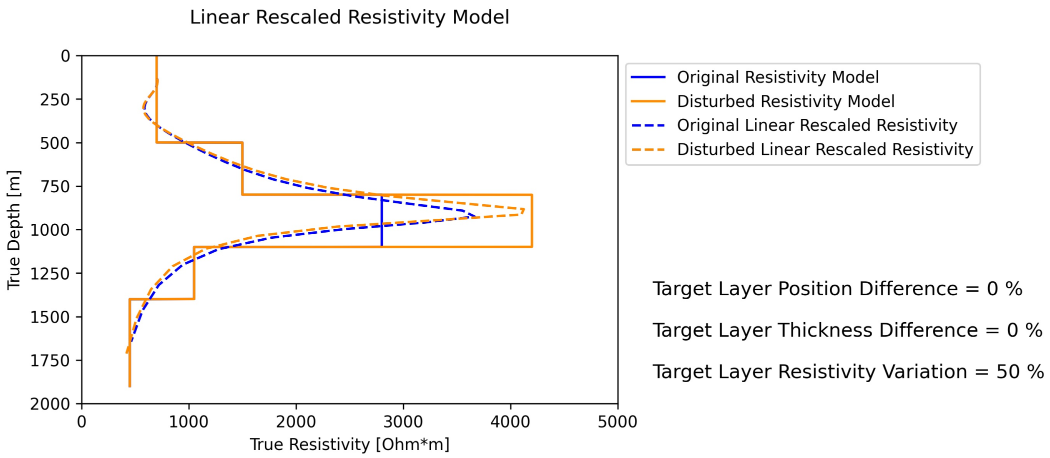

(a) Rescaled model for a 5 layer system with 50 % resistivity variation compared with the original model using the polynomial expression obtained without applying any change to the apparent data.

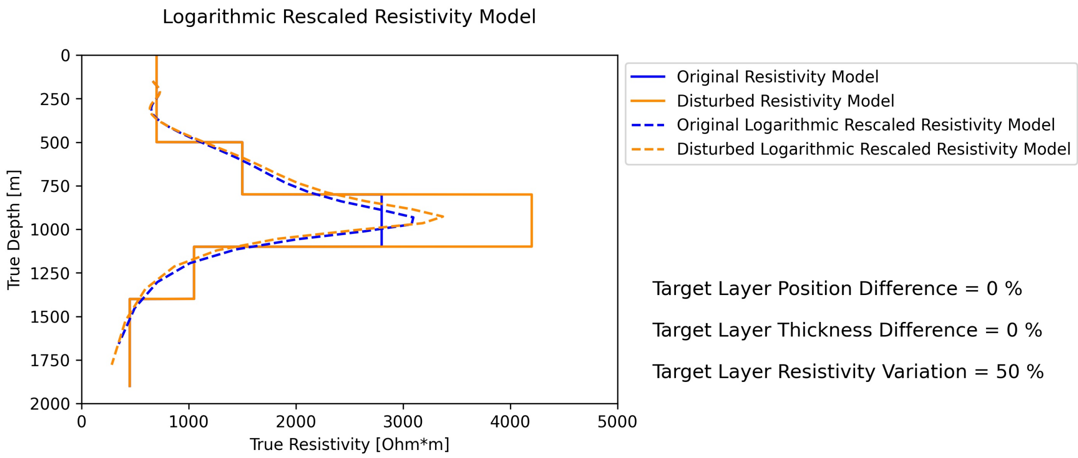

(b) Rescaled model for a 5 layer system with 50 % resistivity variation compared with the original model using the polynomial expression obtained for the logarithmic representation of the data.

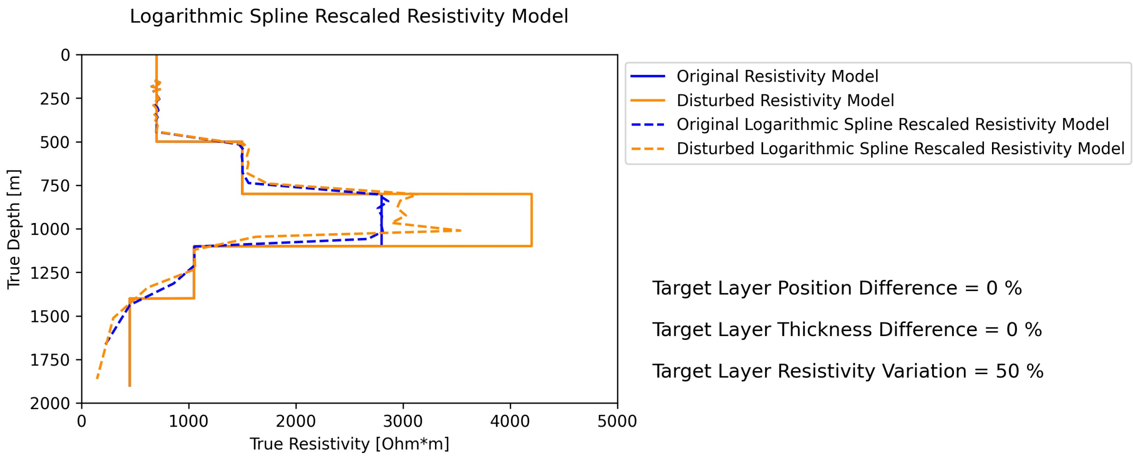

(c) Rescaled model for a 5 layer system with 50 % resistivity variation compared with the original model using the polynomial expression obtained by using cubic splines for the logarithmic representation of the data.

FIGURE 4.11: Comparison between the three rescaling process using different polynomials for a 50% variation in the resistivity of the target layer of the 5 layer model.

Table 4.15 shows the error comparison between the polynomials used to obtained the rescaled model for a resistivity variation of 50 % for the 5 layer system.

TABLE 4.15: Total and average error comparison for each polynomial used in the rescaling process for the 50% resistivity disturbed 5 layer model.

Rescaled Model Total Error %		
Linear Polynomial	**Logarithmic Polynomial**	**Cubic Splines Polynomial**
516	538	538
Rescaled Model Average Error %		
Linear Polynomial	**Logarithmic Polynomial**	**Cubic Splines Polynomial**
13	13	16

Figures 4.10 and 4.11 shows that even though the rescaled models show a resistivity variation, the rescaled resistivities are not a real representation of the actual changes in resistivity between the disturbed and the original model. This could be due to the fact that since the resistivity contrast between layers is smaller the tracking capabilities of the proposed model are reduced as well.

4.3.2 5 Layer System Thickness Variation

The second test was performed by applying thickness variations to the 5 layer model shown in Figure 4.7. The perturbations applied are reported in Table 4.16.

TABLE 4.16: Thickness perturbations applied to the target layer of the 5 layer model

Thickness Perturbations		
Original Value	**Disturbed Value**	**Difference %**
300 [m]	150 [m]	-50%
	450 [m]	50%

The results for the thickness perturbation are displayed in Figures 4.12 and 4.13. Figure 4.13 shows the results of the testing phase for a variation in the thickness of the target layer of -50% for the 5 layer system.

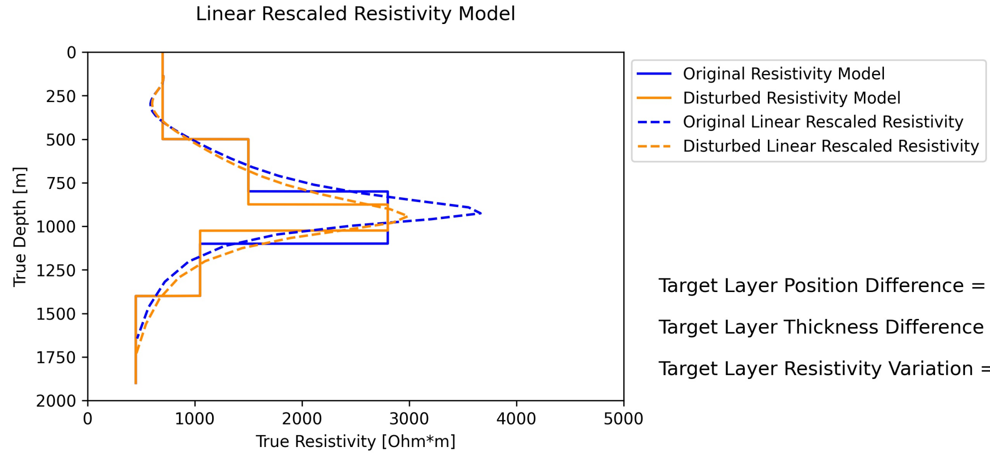

(a) Rescaled model for a 5 layer system with -50 % thickness variation compared with the original model using the polynomial expression obtained without applying any change to the apparent data.

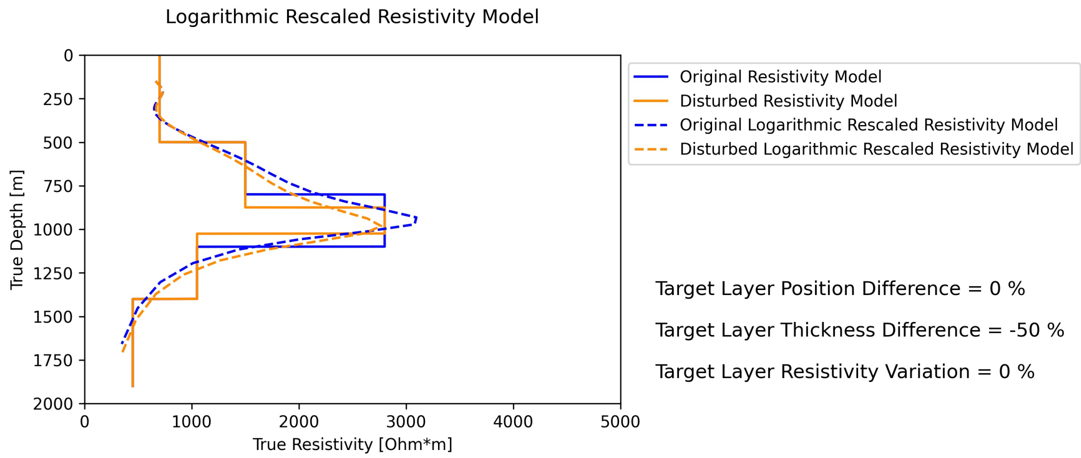

(b) Rescaled model for a 5 layer system with -50 % thickness variation compared with the original model using the polynomial expression obtained for the logarithmic representation of the data.

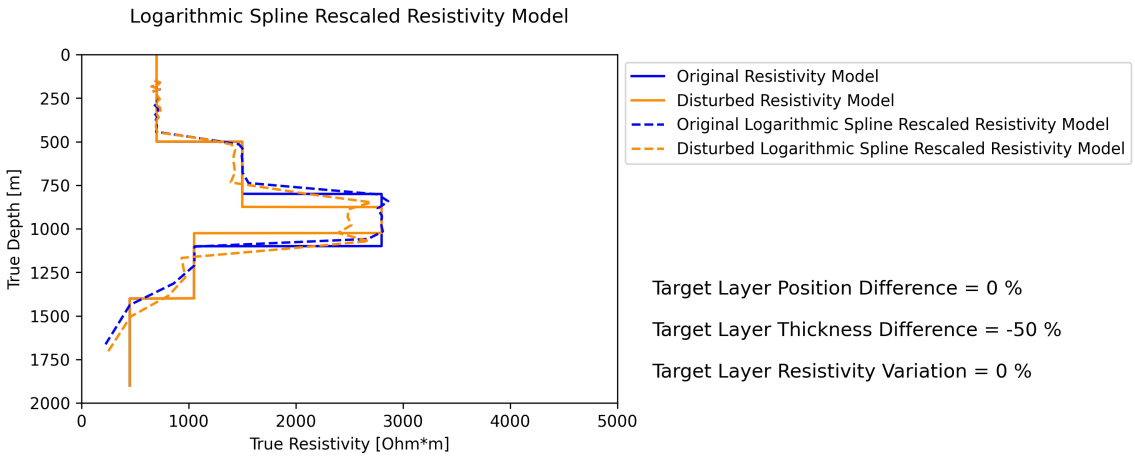

(c) Rescaled model for a 5 layer system with -50 % thickness variation compared with the original model using the polynomial expression obtained by using cubic splines for the logarithmic representation of the data.

FIGURE 4.12: Comparison between the three rescaling process using different polynomials for a -50% variation in the thickness of the target layer of the 5 layer model.

Table 4.17 shows the error comparison between the polynomials used to obtained the rescaled model for a thickness variation of -50 % for the 5 layer system.

TABLE 4.17: Total and average error comparison for each polynomial used in the rescaling process for the -50% thickness disturbed 5 layer model.

Rescaled Model Total Error %		
Linear Polynomial	**Logarithmic Polynomial**	**Cubic Splines Polynomial**
485	479	405
Rescaled Model Average Error %		
Linear Polynomial	**Logarithmic Polynomial**	**Cubic Splines Polynomial**
13	12	11

Figure 4.13 shows the results of the testing phase for a thickness perturbation of 50% of the 5 layer system.

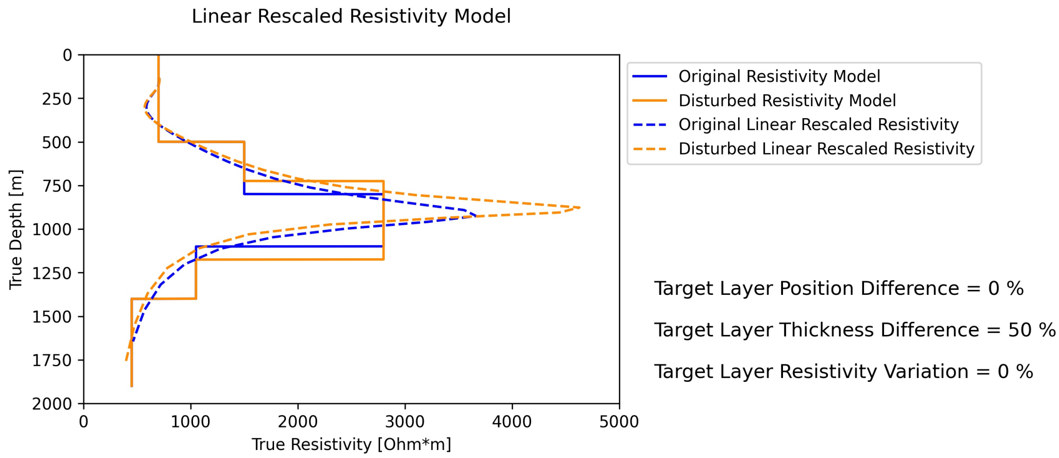

(a) Rescaled model for a 5 layer system with 50 % thickness variation compared with the original model using the polynomial expression obtained without applying any change to the apparent data.

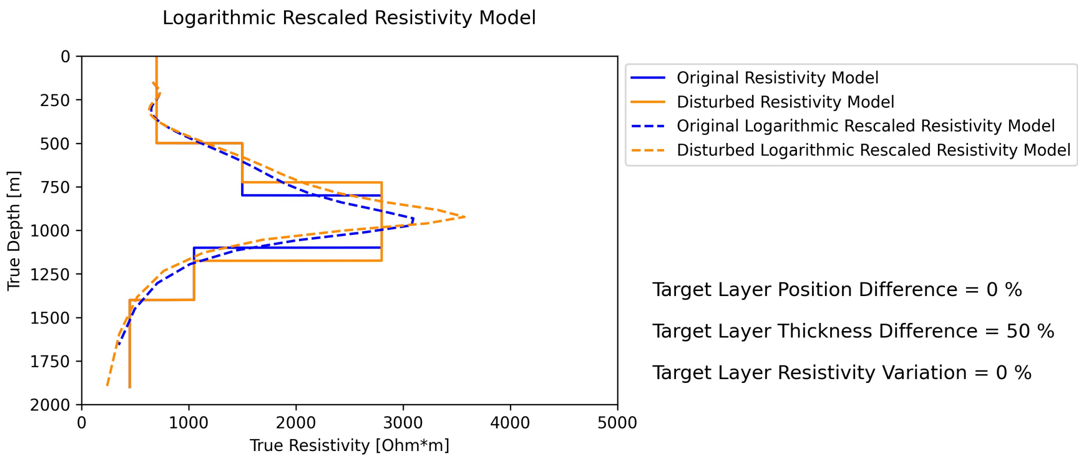

(b) Rescaled model for a 5 layer system with 50 % thickness variation compared with the original model using the polynomial expression obtained for the logarithmic representation of the data.

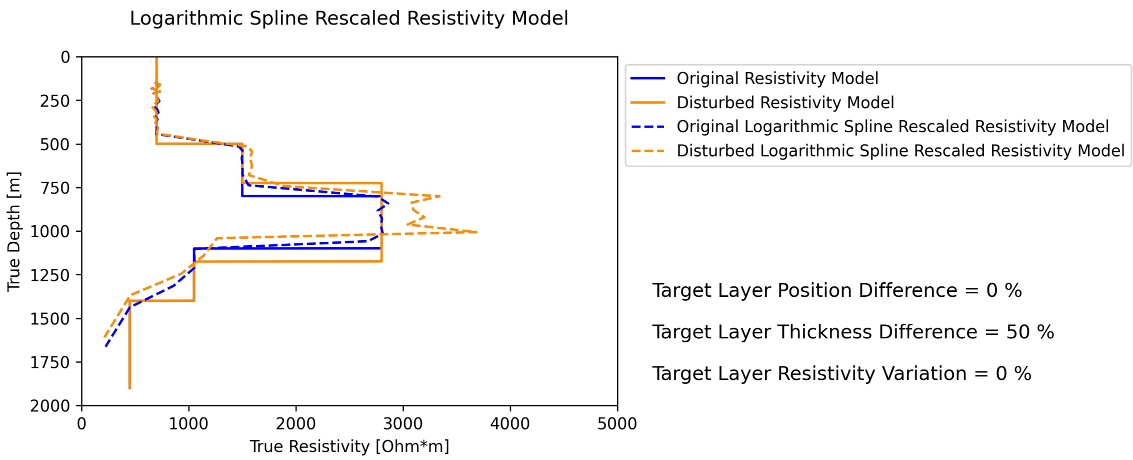

(c) Rescaled model for a 5 layer system with 50 % thickness variation compared with the original model using the polynomial expression obtained by using cubic splines for the logarithmic representation of the data.

FIGURE 4.13: Comparison between the three rescaling process using different polynomials for a 50% variation in the thickness of the target layer of the 5 layer model.

Table 4.18 shows the error comparison between the polynomials used to obtained the rescaled model for a thickness variation of 50 % for the 5 layer system.

Table 4.18: Total and average error comparison for each polynomial used in the rescaling process for the 50% thickness disturbed 5 layer model.

Rescaled Model Total Error %		
Linear Polynomial	**Logarithmic Polynomial**	**Cubic Splines Polynomial**
697	613	443
Rescaled Model Average Error %		
Linear Polynomial	**Logarithmic Polynomial**	**Cubic Splines Polynomial**
19	17	12

Figures 4.12 and 4.13 shows the same behavior seen in the thickness variation for the 3 layer system (Figures 4.3 and 4.4). This implies that thickness variations of the target layer are misinterpreted as variations in resistivity.

4.3.3 5 Layer System Position Variation

The third test was performed by applying variations to the position of the target layer in the 5 layer model. The perturbations applied are reported in Table 4.19.

Table 4.19: Position perturbations of the target layer applied to the 5 layer model

Position Perturbations		
Original Value	**Disturbed Value**	**Difference %**
Located at 800 [m]	Located at 400 [m]	-50%
	Located at 1200 [m]	50%

The results for the variation of the position of the target layer are displayed in Figures 4.14 and 4.15 respectively. Figure 4.14 shows the results of the testing phase for a variation of the location of the target layer by -50%.

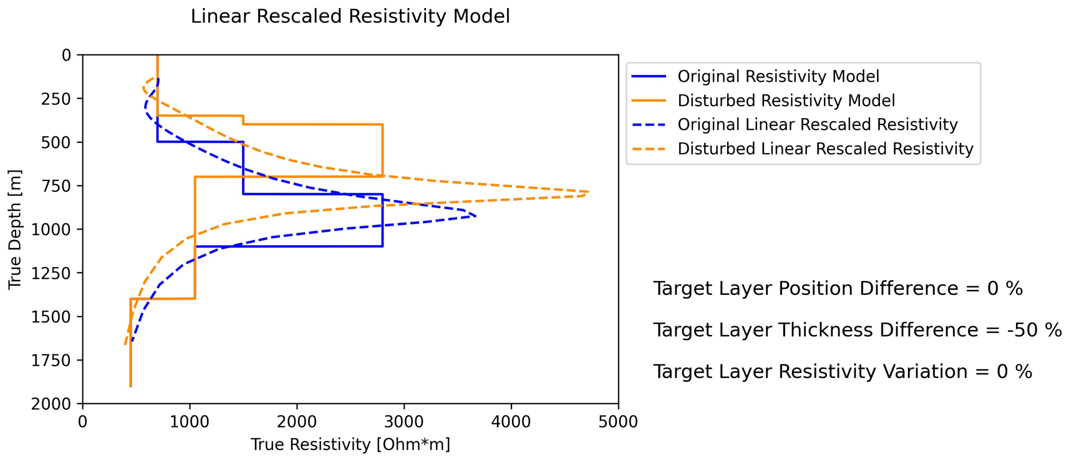

(a) Rescaled model for a 5 layer system with -50 % variation in the position of the target layer compared with the original model using the polynomial expression obtained without applying any change to the apparent data.

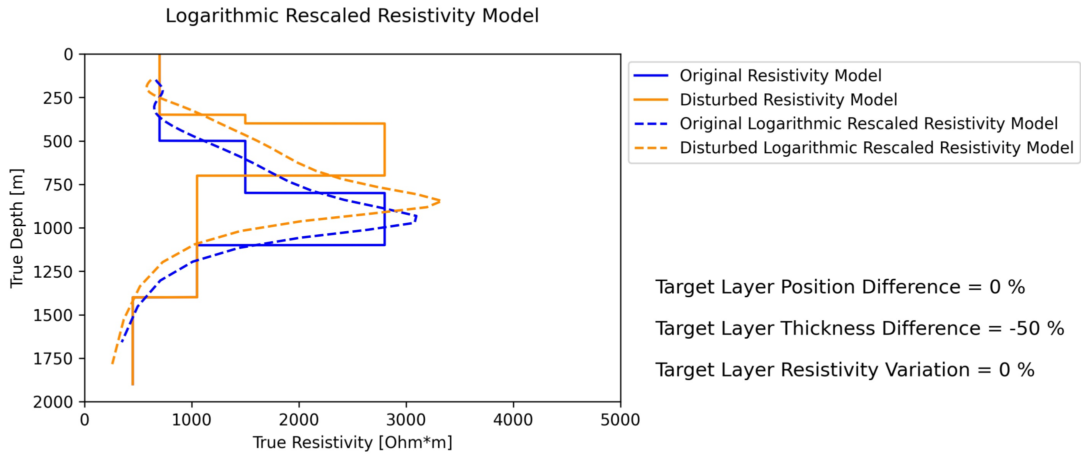

(b) Rescaled model for a 5 layer system with -50 % variation in the position of the target layer compared with the original model using the polynomial expression obtained for the logarithmic representation of the data.

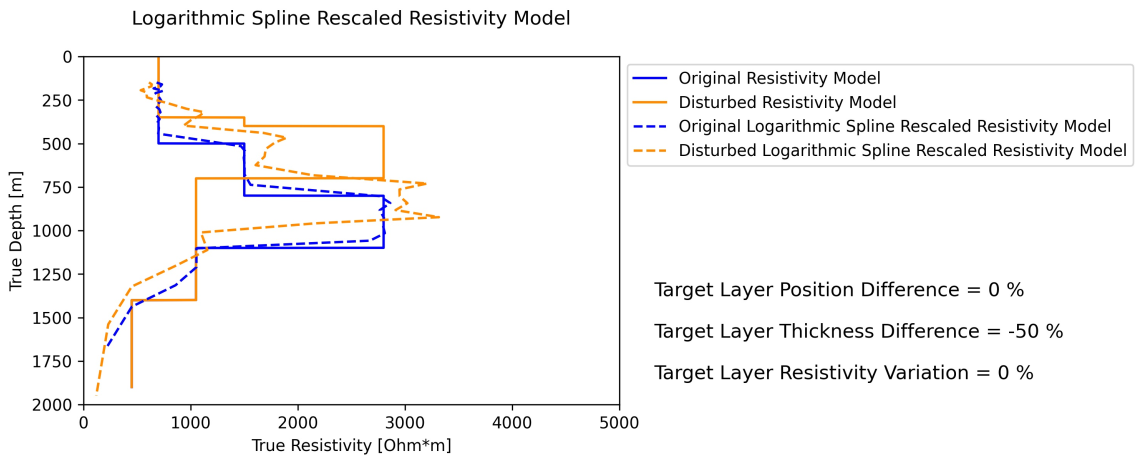

(c) Rescaled model for a 5 layer system with -50 % variation in the position of the target layer compared with the original model using the polynomial expression obtained by using cubic splines for the logarithmic representation of the data.

FIGURE 4.14: Comparison between the three rescaling process using different polynomials for a -50% variation in the position of the target layer of the 5 layer model. The original layer model is represented by the blue line, the rescaled original model by dashed blue line, the disturbed model that is unknown by the orange line, and the rescaled disturbed model retrieved is represented by the dashed orange line.

Table 4.20 shows the error comparison between the polynomials used to obtained the rescaled model for a position variation of the target layer by -50 % in the 5 layer system.

TABLE 4.20: Total and average error comparison for each polynomial used in the rescaling process for the variation of -50% in the position of the target layer of the 5 layer model.

Rescaled Model Total Error %		
Linear Polynomial	**Logarithmic Polynomial**	**Cubic Splines Polynomial**
1499	1332	1463
Rescaled Model Average Error %		
Linear Polynomial	**Logarithmic Polynomial**	**Cubic Splines Polynomial**
42	37	41

Figure 4.15 shows the results of the testing phase for a position perturbation of 50% in the target layer of the 5 layer system.

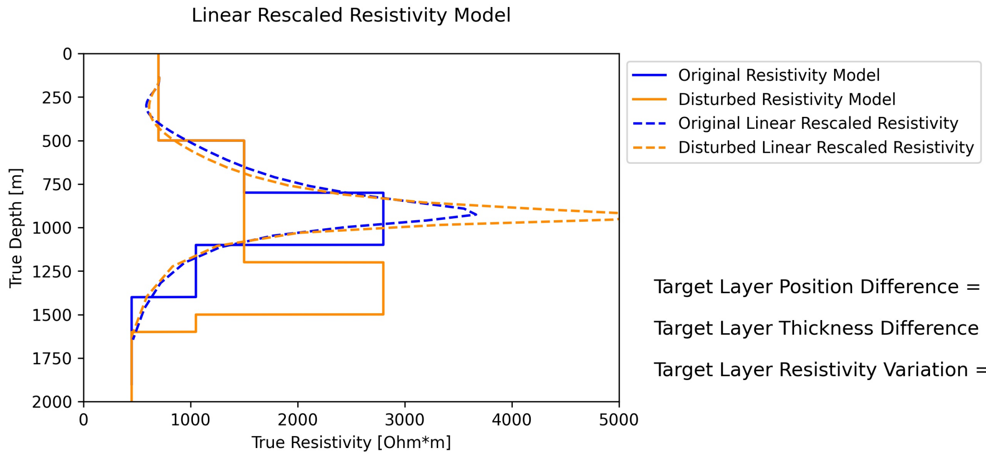

(a) Rescaled model for a 5 layer system with 50 % variation in the position of the target layer compared with the original model using the polynomial expression obtained without applying any change to the apparent data.

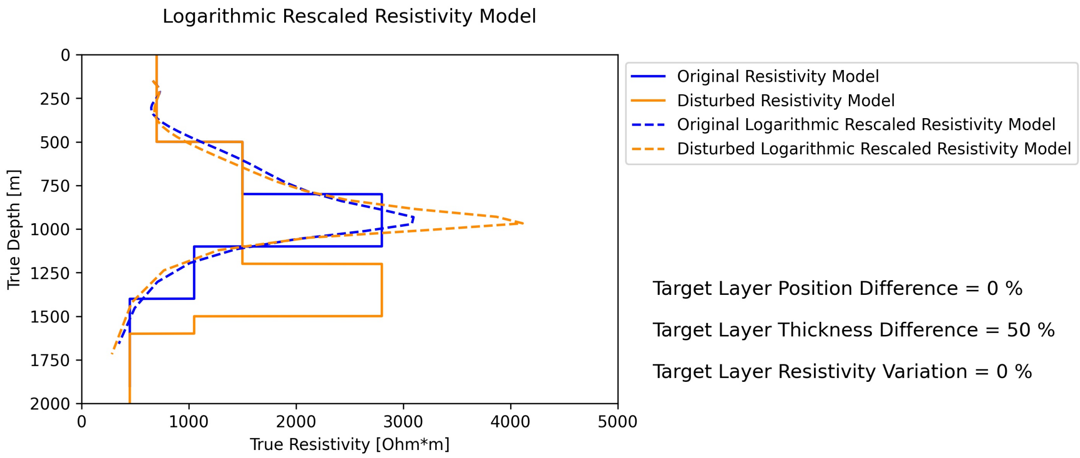

(b) Rescaled model for a 5 layer system with 50 % variation in the position of the target layer compared with the original model using the polynomial expression obtained for the logarithmic representation of the data.

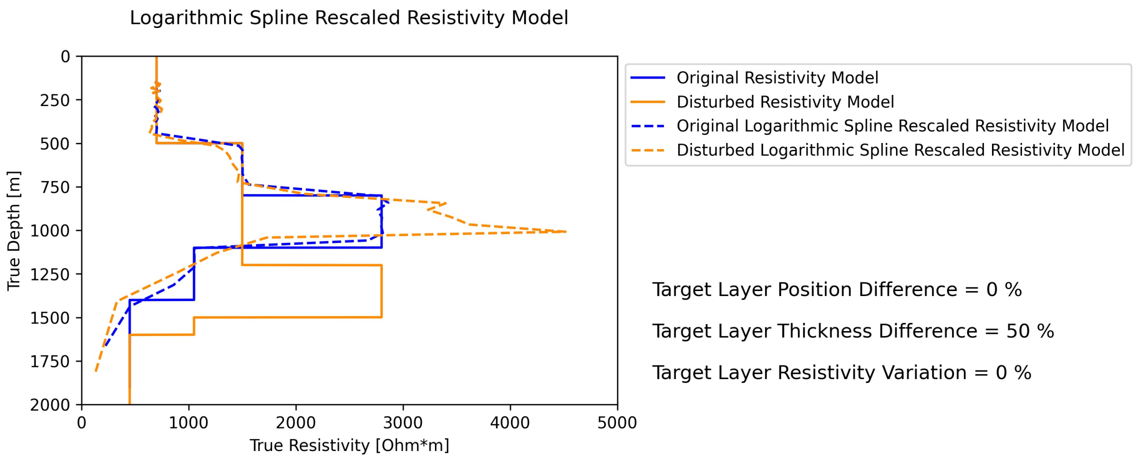

(c) Rescaled model for a 5 layer system with 50 % variation in the position of the target layer compared with the original model using the polynomial expression obtained by using cubic splines for the logarithmic representation of the data.

FIGURE 4.15: Comparison between the three rescaling process using different polynomials for a 50% variation in the position of the target layer of the 5 layer model.

Table 4.21 shows the error comparison between the polynomials used to obtained the rescaled model for a position variation of the target layer by 50 % in the 5 layer system.

TABLE 4.21: Total and average error comparison for each polynomial used in the rescaling process for the variation of 50% in the position of the target layer of the 5 layer model.

Rescaled Model Total Error %		
Linear Polynomial	**Logarithmic Polynomial**	**Cubic Splines Polynomial**
644	473	514
Rescaled Model Average Error %		
Linear Polynomial	**Logarithmic Polynomial**	**Cubic Splines Polynomial**
19	13	15

Figures 4.14 and 4.15 show a different and more complex behavior compared to the 3 layer model. In this case if the target layer is located above its original position the proposed method is capable of tracking this movement, but the rescaled movement is less than the actual movement of the target layer. Whereas,if the target layer is below its original position the proposed method cannot see it, when the movement of the target layer is below its original position the proposed method rescaled it also as a resistivity variation.

The proposed method only works for cases in which the resistivity of the target layer is the only parameter that is changing. As seen previously the proposed method struggles to accurately rescale the position or thickness of the target layer if those parameters differ from the ones from which the polynomial expression was obtained.

4.4 Delft Model

As final test the proposed rescaling tool was used in a real case. The goal for this case was to track the resistivity changes in a water bearing zone at 2300 [m] deep in the subsurface of a geothermal field in Delft, Netherlands. In the geothermal field water is being injected into the formation, for this reason is of particular interest to track how the injected water is moving through the water bearing layer, this could be tracked by means of the resistivity changes. The layered system of the geothermal field is described in Table 4.22 and in Figure 4.16.

Table 4.22: Delft case resistivity and conductivity model parameters.

Resistivity [Ohm*m]	**Conductivity [Ohm/m]**	**Thickness [m]**
3	0.33	750
5.5	0.181	500
30	0.033	750
25	0.04	300
10	0.1	200
40	0.025	Half Space

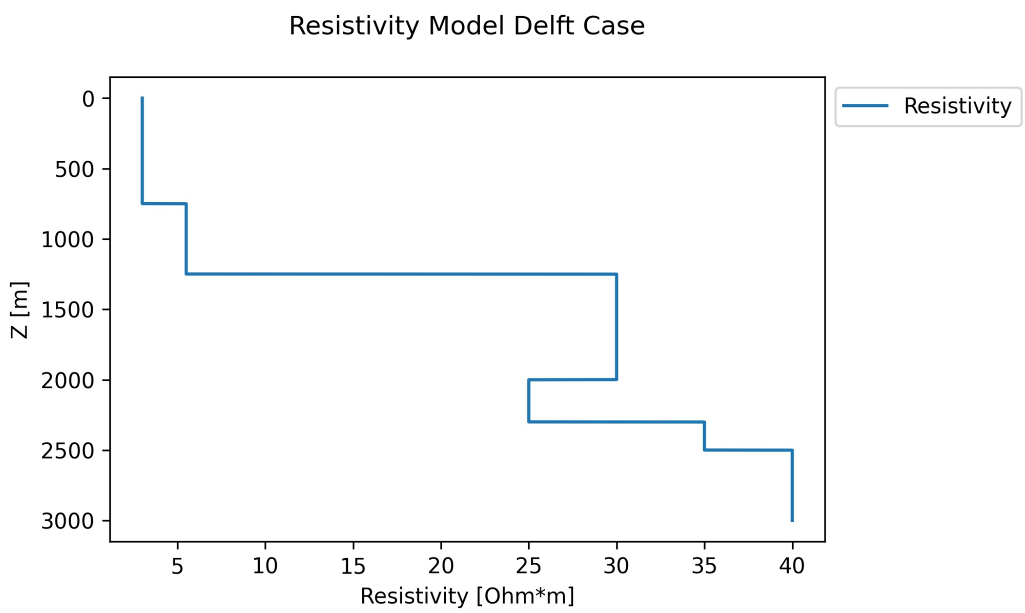

Figure 4.16: Delft resistivity model.

Using the model shown in Figure 4.16 apparent measurements were simulated and using the methodology described in Chapter 3 a polynomial expression able to correct the differences between apparent measurements was obtained for the representation of the data without any change, for the logarithmic representation for the data, and also a cubic spline interpolation was obtained for the logarithmic representation of the data.

Once the differences between apparent and local measurements were corrected a rescaled model was obtained by means of Equation 3.11 for each representation of the data. Figures 4.20 and 4.21 show the rescaled models.

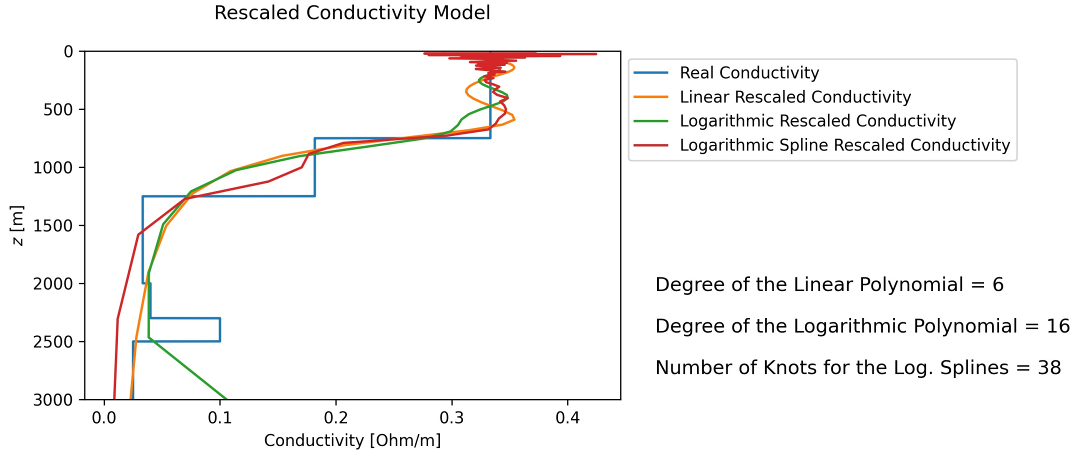

FIGURE 4.17: Rescaled resistivity models obtained by deriving the corrected cumulative resistivity models for the Delft case for the three different representations of the data. Similarly to the resistivity rescaled model.

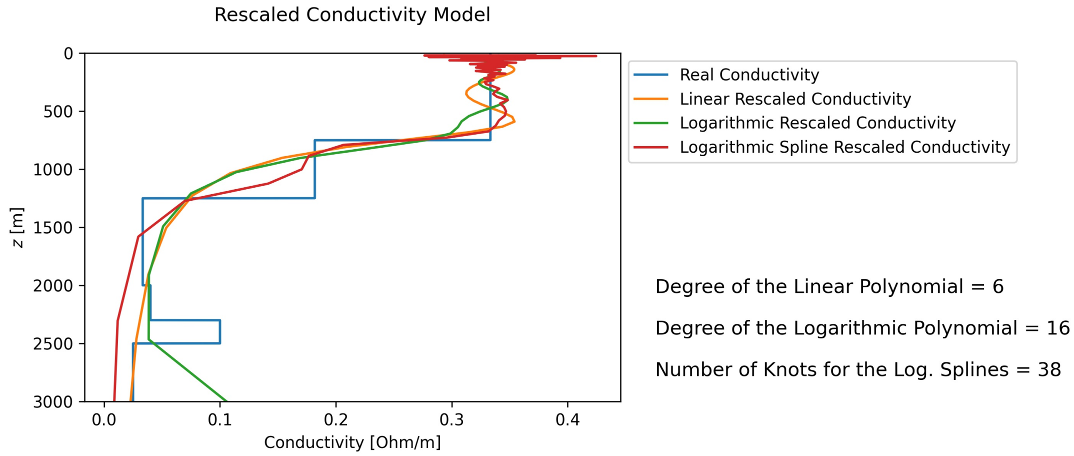

FIGURE 4.18: Rescaled conductivity models obtained by deriving the corrected cumulative conductivity models for the Delft case for the three different representations of the data. Similarly to the resistivity rescaled model.

Figure 4.20 and 4.21 show that for this case the target layer is too thin and it cannot be seen by the apparent measurements performed in the surface. For this reason the methodology was applied but for this second attempt the MT sensors were placed at a depth of 1500 [m].

The new resistivity model for the Delft case is shown in Figure 4.19.

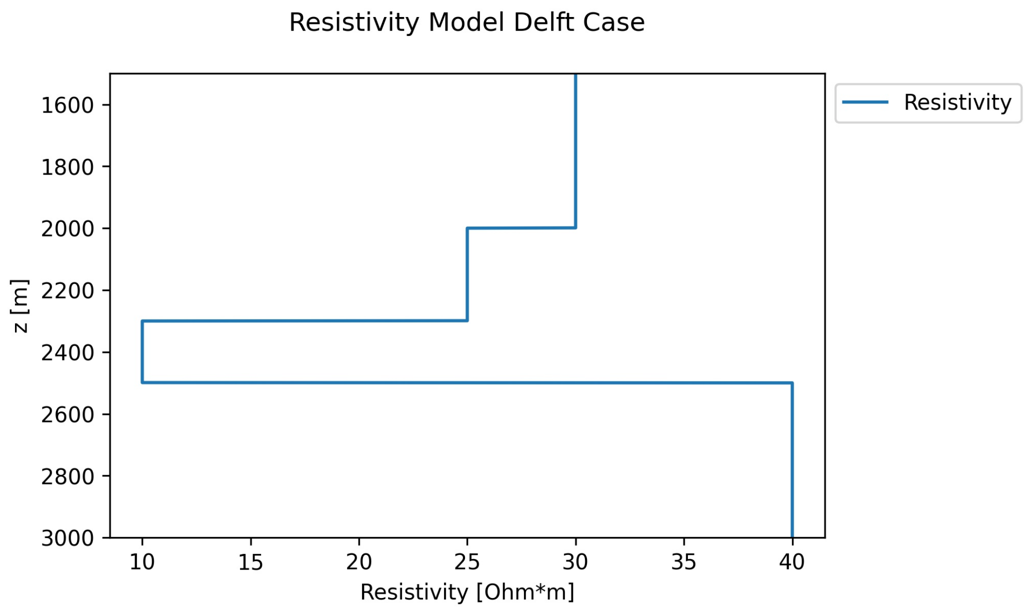

FIGURE 4.19: Updated Delft resistivity model. This model takes into consideration the movement of the sensors 1500 [m] in the subsurface.

Once the differences between apparent and local measurements were corrected for the resistivity model shown in Figure 4.19 a rescaled model was obtained by means of Equation 3.11 for each representation of the data. Figures **??** and **??**

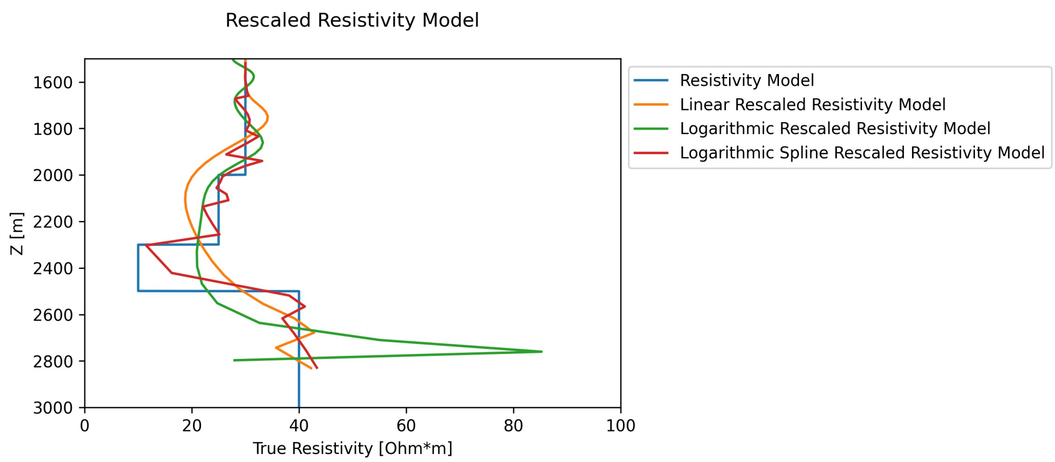

FIGURE 4.20: Rescaled resistivity models obtained by deriving the corrected cumulative resistivity models for the updated version of the Delft resistivity model for the three different representations of the data. The model obtained by the logarithmic spline corrected data was the one that resembles the geological settings of the subsurface the most.

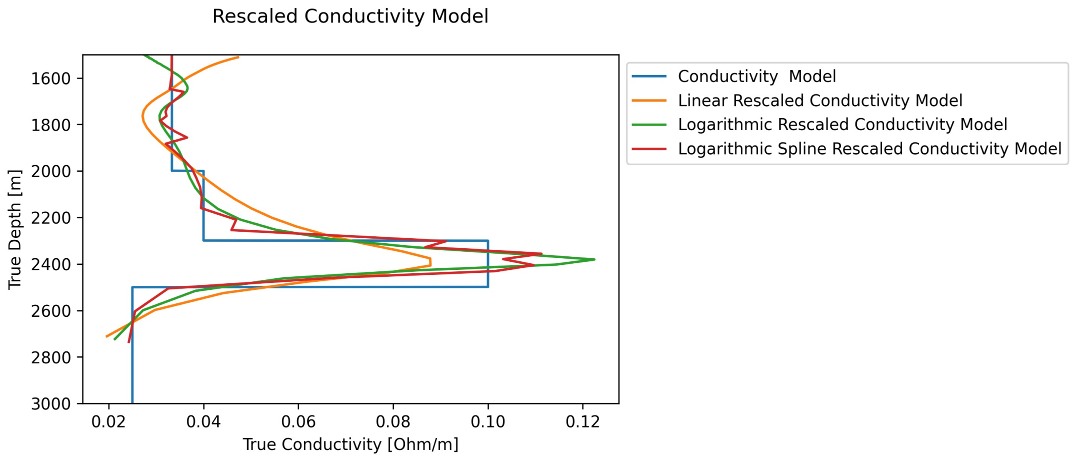

FIGURE 4.21: Rescaled conductivity models obtained by deriving the corrected cumulative resistivity models for the updated version of the Delft conductivity model for the three different representations of the data. The model obtained by the logarithmic spline corrected data was the one that resembles the geological settings of the subsurface the most.

The error between rescaled models was obtained to determine the quality of the approximations. Table 4.23 shows the total and average error between the resistivity model derived for each polynomial obtained for the updated Delft resistivity model.

TABLE 4.23: Total and average error comparison for each polynomial used in the rescaling process of the resistivity model.

Rescaled Model Total Error %		
Linear Polynomial	**Logarithmic Polynomial**	**Cubic Splines Polynomial**
1011	899	1302
Rescaled Model Average Error %		
Linear Polynomial	**Logarithmic Polynomial**	**Cubic Splines Polynomial**
15	13	20

For this case the polynomial obtained for the logarithmic representation of the data provided the best approximation.

4.4.1 Delft System Resistivity Variation

For this real case the resistivity present in the waterbearing zone has been monitored and the changes in the layer resistivity were registered. For this case is is known that the resistivity of the target layer increased by

TABLE 4.24: Resistivity perturbations registered for the Delft system.

Resistivity Perturbations		
Original Value	**Disturbed Value**	**Difference %**
10 [Ohm*m]	35 [Ohm*m]	350%

Considering this new resistivity tree rescaled models were obtained are are reported in Figure 4.22. Each figure display the results using the three polynomials obtained and in each figure is displayed the original layer model (blue line), the rescaled original model (dashed blue line), the disturbed model that is unknown (orange line) and the rescaled disturbed model retrieved (dashed orange line).

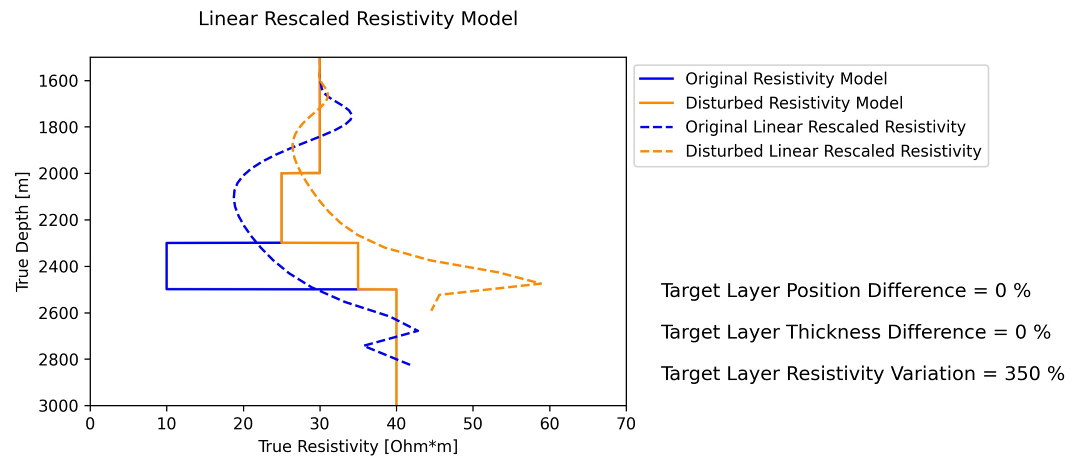

(a) Rescaled model for the Delft system with 350 % resistivity variation compared with the original model using the polynomial expression obtained without applying any change to the apparent data.

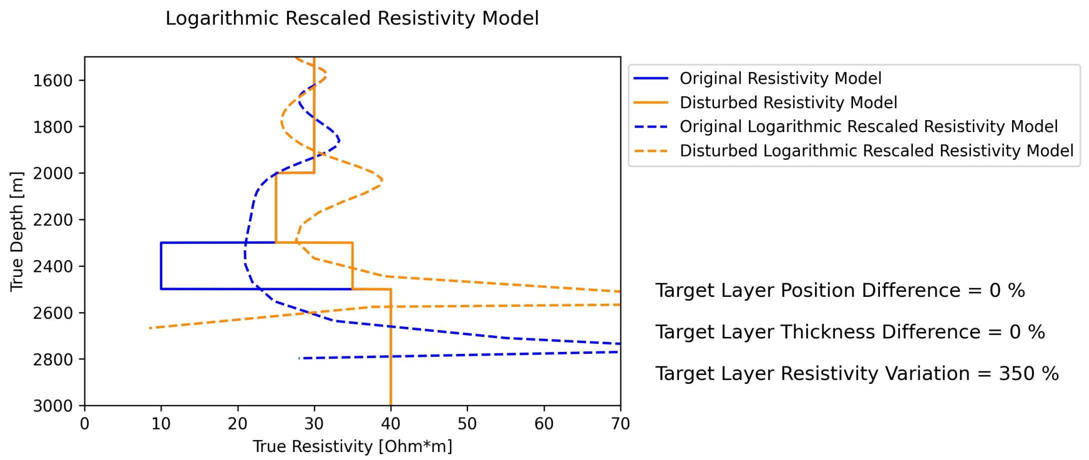

(b) Rescaled model for the Delft system with 350 % resistivity variation compared with the original model using the polynomial expression obtained for the logarithmic representation of the data.

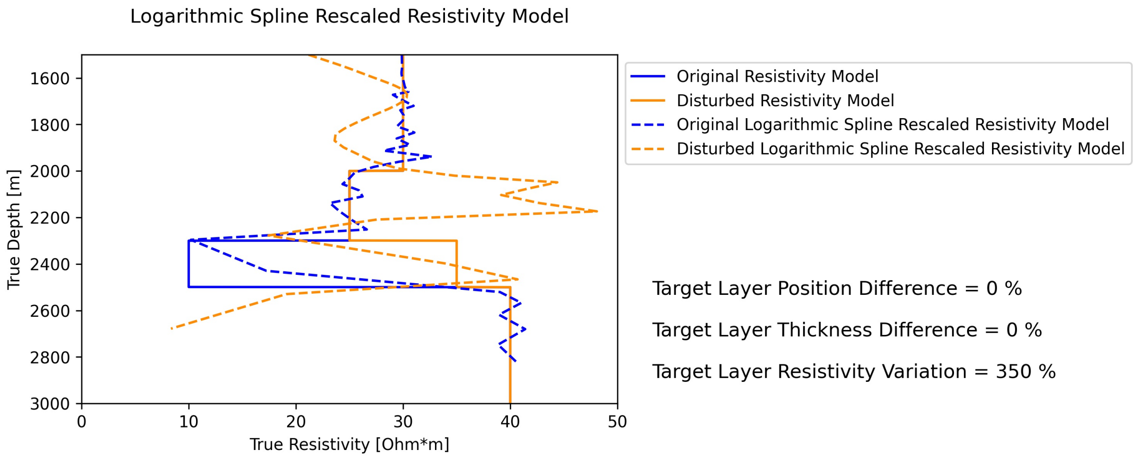

(c) Rescaled model for the Delft system with 350 % resistivity variation compared with the original model using the polynomial expression obtained by using cubic splines for the logarithmic representation of the data.

FIGURE 4.22: Comparison between the three rescaling process using different polynomials for a 350% variation in the resistivity of the target layer of the Delft system.

Table 4.25 shows the error comparison between the polynomials used to obtained the rescaled model for a resistivity variation of 350 % for the Delft system.

TABLE 4.25: Total and average error comparison for each polynomial used in the rescaling process for the 350% resistivity disturbed Delft model.

Rescaled Model Total Error %		
Linear Polynomial	**Logarithmic Polynomial**	**Cubic Splines Polynomial**
1845	1452	2003
Rescaled Model Average Error %		
Linear Polynomial	**Logarithmic Polynomial**	**Cubic Splines Polynomial**
30	23	33

Figure 4.22 shows that the proposed rescaling process is able to track the resistivity changes in the target layer due to the water injection. However, as seen in the previous tests the rescaled resistivity does not correspond to the actual change in resistivity. This over or under estimation in the resistivity value should be studied in the future to improve the rescaling technique.

As mentioned at the beginning of this chapter only the most representative results were included in this thesis. The following link contains a series of videos summarizing all the results obtained during the testing phase.

- `https://1drv.ms/u/s!AhbYaiuBV_Gqh_NQ91hU1HQQB2toOg?e=OmfaAH`

Chapter 5

Conclusions and Future Work

5.1 Conclusions

This work was performed to determine if it is possible to obtain a mathematical expression able to transform apparent measurements form a MT survey into electrical values that represent the geological settings present in the subsurface.

Starting from field measurements and assuming information from a exploratory well, the apparent resistivity measured by the MT survey at the surface is processed to obtain a first apparent depth-apparent electrical model. This model is compared to the local model obtained in the assumed exploratory well and the differences between models are obtained. To correct the differences between apparent and local measurements a polynomial regression is used to model and correct these differences and once the apparent resistivity is corrected a resistivity model is derived and is compared to the actual resistivity model of the subsurface.

However, for the polynomial expression to be of practical use it should be able to transform apparent measurements into local measurements from zones in which the geological settings are slightly different from the ones used to create this expression. The proposed method was tested different geological settings varying one of the following parameters.

- Resistivity of the target layer.
- Thickness of the target layer.
- Position of the target layer.

The variations of each parameter provided approximately 100 different models to test the applicability of the rescaling tool.

Based on the testing phase it can be concluded that the proposed rescaling process is able to track resistivity changes of the target layer for geological systems with high resistivity contrast as shown in Figures 4.1 and 4.2. In systems with a smoother resistivity contrast (Figures 4.10 and 4.11) the rescaling tool is still able to provide an approximate tracking of the resistivity variation, however as the contrast between layers diminishes the tracking capabilities of the method diminishes too.

For changes in the thickness of the target the proposed methodology is not able to provide a realistic rescaled geological model, in this case the rescaling process misinterpret thickness variations as resistivity variations. If the thickness of the target layer increases it is rescaled as a increase in the resistivity of the target layer and vice versa. This might be due to several factors that should be studied in the future.

For changes in the position of the target the proposed methodology presents a more complex behavior. In the case of a high resistivity contrast the rescaling tool can track the movement of the target layer as shown in Figures 4.5 and 4.6. Nonetheless, for a smooth resistivity contrast the proposed rescaling tool can track the movement of the target layer only if the layer is above its original position as shown in Figure 4.14, if the target layer is below its original position the rescaled model will misinterpret the change in position as a resistivity change as shown in Figure 4.15.

In monitoring scenario the proposed methodology was able to reflect the change in the resistivity of the formation as shown in the Figure 4.22, however, the rescaled geological model can be improved.

At the moment the method can be used to track resistivity changes in a target layer, as shown in Figures 4.1 ,4.2, 4.10, 4.11 and 4.22 providing a good first approximation resistivity model that can be used as a starting point for the interpretation of the geological settings present in the subsurface. This might be useful for tracking the movement of shallow plumes of contaminated water along a certain area or for tracking the movement of the salt water wedge near the coast.

Overall the proposed rescaling process can provide a first approximation that can help in the process of retrieving accurate geological models for fields of study in which only surface measurements can be used.

5.2 Future Work

For future work the proposed rescaling process should be studied more in detail, in this work it has been proved that the method can transform apparent measurement into a geological model that resembles the properties of the subsurface under certain conditions. For the immediate future more wells should be included, if more data is added the rescaling capabilities of the polynomials can increase.

Something else that should be tested is the regression technique applied to create the polynomials used to model the difference between apparent and local measurements. Other type of regressions might characterize the properties of the subsurface in much more detail providing a more accurate rescaling tool. Combining the results of different regression techniques might also improve the technique overall.

Additionally, combining data from other geophysical surveys might help to improve the retrieved geological model, including different geophysical prospecting methods into one rescaling process might provide a robust approach in which different geophysical prospecting methods complement each other.

Further research is needed to determine the actual limits of the proposed rescaling process, as a first step, the method seems promising especially for identifying resistivity variations in shallow targets. From now on different approaches can be taken to test the capabilities and limitations of the proposed rescaling method, but surely is something worthy of further research.

Bibliography

Chave, A. D. and Jones, A. G. (2012). *The magnetotelluric method: Theory and practice*. Cambridge University Press.

Comeau, M. (2015). *Electrical Resistivity Structure of the Altiplano-Puna Magma Body and Volcan Uturuncu from Magnetotelluric Data: University of Alberta*. PhD thesis, PhD thesis, 337 pp.

Florio, G. (2018). Mapping the depth to basement by iterative rescaling of gravity or magnetic data. *Journal of Geophysical Research: Solid Earth*, 123(10): 9101–9120.

Gómez-Treviño, E. (1996). Approximate depth averages of electrical conductivity from surface magnetotelluric data. *Geophysical Journal International*, 127(3): 762–772.

Gupta, R. K. (2019). *Numerical Methods: Fundamentals and Applications*. Cambridge University Press.

Loewenthal, D. and Landisman, M. (1973). Theory for magnetotelluric observations on the surface of a layered anisotropic half space. *Geophysical Journal International*, 35(1-3):195–214.

Martí i Castells, A. (2006). Magnetotelluric investigation of geoelectrical dimensionality and study of the central betic crustal structure, a.

Montgomery, D. C., Peck, E. A., and Vining, G. G. (2021). *Introduction to linear regression analysis*. John Wiley & Sons.

Moorkamp, M. (2017). Integrating electromagnetic data with other geophysical observations for enhanced imaging of the earth: a tutorial and review. *Surveys in Geophysics*, 38(5):935–962.

Nabighian, M. N. (1991). *Electromagnetic Methods in Applied Geophysics: Volume 2, Application, Parts A and B: Volume 2, Application, Parts A and B*. Society of Exploration Geophysicists.

Niblett, E. R. and Sayn-Wittgenstein, C. (1960). Variation of electrical conductivity with depth by the magneto-telluric method. *Geophysics*, 25(5):998–1008.

Pellerin, L. (2002). Applications of electrical and electromagnetic methods for environmental and geotechnical investigations. *Surveys in Geophysics*, 23(2):101–132.

Price, A. (1949). The induction of electric currents in non-uniform thin sheets and shells. *The Quarterly Journal of Mechanics and Applied Mathematics*, 2(3):283–310.

Rawlings, J. O., Pantula, S. G., and Dickey, D. A. (2001). *Applied regression analysis: a research tool*. Springer Science & Business Media.

Ren, Z. and Kalscheuer, T. (2020). Uncertainty and resolution analysis of 2D and 3 D inversion models computed from geophysical electromagnetic data. *Surveys in Geophysics*, 41(1):47–112.

Socco, L. V., Comina, C., and Khosro Anjom, F. (2017). Time-average velocity estimation through surface-wave analysis: Part 1—s-wave velocity. *Geophysics*, 82(3):U49–U59.

Spies, B. R. (1989). Depth of investigation in electromagnetic sounding methods. *Geophysics*, 54(7):872–888.

Swift Jr, C. M. (1988). Fundamentals of the electromagnetic method. *Electromagnetic Methods in Applied Geophysics*, 1:5–10.

Thiel, S. (2008). *Modelling and inversion of magnetotelluric data for 2-D and 3-D lithospheric structure, with application to obducted and subducted terranes*. PhD thesis.

Ueda, T., Mitsuhata, Y., Uchida, T., Marui, A., and Ohsawa, K. (2014). A new marine magnetotelluric measurement system in a shallow-water environment for hydrogeological study. *Journal of Applied Geophysics*, 100:23–31.

Unsworth, M. (2005). New developments in conventional hydrocarbon exploration with electromagnetic methods. *CSEG Recorder*, 30(4):34–38.

Van Huffel, S. and Vandewalle, J. (1991). *The total least squares problem: computational aspects and analysis*. SIAM.

Vozoff, K. (1991). The magnetotelluric method. In *Electromagnetic methods in applied geophysics: Volume 2, application, parts A and B*, pages 641–712. Society of exploration geophysicists.

Zhdanov, M. S., Wan, L., Gribenko, A., Čuma, M., Key, K., and Constable, S. (2011). Large-scale 3d inversion of marine magnetotelluric data: Case study from the gemini prospect, gulf of mexico. *Geophysics*, 76(1):F77–F87.